

SPRINGER BRIEFS IN MOLECULAR SCIENCE

Yujun Feng
Zonglin Chu
Cécile A. Dreiss

Smart Wormlike Micelles

Design,
Characteristics and
Applications



Springer

SpringerBriefs in Molecular Science

More information about this series at <http://www.springer.com/series/8898>

Yujun Feng · Zonglin Chu
Cécile A. Dreiss

Smart Wormlike Micelles

Design, Characteristics and Applications

 Springer

Yujun Feng
State Key Laboratory of Polymer
Materials Engineering
Polymer Research Institute
Sichuan University
Sichuan
China

Cécile A. Dreiss
Institute of Pharmaceutical Science
King's College London
London
UK

Zonglin Chu
Physical Chemistry Institute
University of Zürich
Zürich
Switzerland

ISSN 2191-5407
ISBN 978-3-662-45949-2
DOI 10.1007/978-3-662-45950-8

ISSN 2191-5415 (electronic)
ISBN 978-3-662-45950-8 (eBook)

Library of Congress Control Number: 2014957867

Springer Heidelberg New York Dordrecht London
© The Author(s) 2015

This work is subject to copyright. All rights are reserved by the Publisher, whether the whole or part of the material is concerned, specifically the rights of translation, reprinting, reuse of illustrations, recitation, broadcasting, reproduction on microfilms or in any other physical way, and transmission or information storage and retrieval, electronic adaptation, computer software, or by similar or dissimilar methodology now known or hereafter developed.

The use of general descriptive names, registered names, trademarks, service marks, etc. in this publication does not imply, even in the absence of a specific statement, that such names are exempt from the relevant protective laws and regulations and therefore free for general use.

The publisher, the authors and the editors are safe to assume that the advice and information in this book are believed to be true and accurate at the date of publication. Neither the publisher nor the authors or the editors give a warranty, express or implied, with respect to the material contained herein or for any errors or omissions that may have been made.

Printed on acid-free paper

Springer-Verlag GmbH Berlin Heidelberg is part of Springer Science+Business Media
(www.springer.com)

Preface

Can you imagine water being thickened as a highly viscoelastic gel upon dissolving just one small drop of detergent inside? Yes, it is possible, although not expected from aqueous solutions containing small solute molecules, such as the everyday detergents we use. Such a fascinating phenomenon results from the three-dimensional network built-up in solutions by so-called “wormlike micelles”: giant, flexible micelles which entangle like a dish of spaghettis, imparting fascinating elasticity to their solutions. Now imagine this elastic gel being illuminated by UV light, or heated up, or adding a drop of lemon and suddenly it reverts back to water? And this can be repeated, over many, many cycles? This is the world of “smart” wormlike micelles, which we describe in this book.

Wormlike micelles (also called rod-like micelles, thread-like micelles, cylindrical micelles, elongated micelles, giant micelles) are one type of morphologies that are spontaneously adopted by surfactant molecules in aqueous solution, conditional on a number of factors such as surfactant shape, concentration, and physicochemical parameters. These types of micelles exhibit strong viscosifying capacities and a rheological behavior similar to polymer solutions; however, unlike polymers, wormlike micelles are constantly breaking and reforming, in a dynamic equilibrium. Because of their unique microstructures and rheological response, wormlike micelles have found applications in personal care products, drag reduction, and most importantly in the oil upstream industry for oilwell stimulation. In the academic community, wormlike micelles are regarded as ideal models of “living” or “equilibrium” polymers, and research on these giant micelles has been burgeoning over the last three decades. Wormlike micelles represent a very active area of soft matter and have imparted new life to the traditional field of surfactants. Recently, the emergence of “smart” wormlike micelles represents a new avenue in the design of intelligent materials and holds great promise in terms of specialized applications.

A major scientific challenge of the past decade pertaining to the field of soft matter has been to craft “adaptable” materials, inspired by nature, which can dynamically alter their structure and functionality on demand, in response to triggers produced by environmental changes. Among these, “smart” surfactant

wormlike micelles are indeed a recent area of development, yet offer a myriad of possibilities, given the simplicity of the design, which relies on the spontaneous organization of small amphiphilic molecules. The “switching” on and off of micellar assemblies has now been reported using electrical, optical, thermal, or pH triggers and is now envisaged for multiple stimuli. The structural changes happening at the nanoscopic level, in turn, induce major changes in the macroscopic characteristics, affecting properties such as viscosity and elasticity, leading in some cases to an effective “sol/gel” transition. These new materials offer tremendous potential in a broad spectrum of applications.

Over the years, we have designed “Smart Wormlike Micelles” responsive to different stimuli, seeking applications in drug delivery, oil, and gas production, in which formulations are inherently subject to the impact of environmental factors such as pH, temperature, salinity, or the presence of hydrocarbons. The rise in interest in the field and its rapid development make this a propitious moment to bring together all the information that has been accumulating in this area over the last few years. We thought it would be timely to share our experience and summarize the latest developments with those involved in this area or simply interested in this topic. One of us contributed a comprehensive review on the general properties of wormlike micelles [1], and we three joined together last year to co-author a critical review on the state of the art of smart wormlike micelles [2]. Shortly after, Springer Editor June Tang became aware of our work and the newly-published review, and invited us to extend this review into a Springer Brief-style monograph. Thus we reorganized our review, rewrote, and updated some of its chapters into this Brief. In particular, the Chap. 5 has been completely rewritten based on our very recent work in this area.

One of our goals is to showcase cutting-edge formulation technologies and the attractive properties of smart wormlike micelles to a large audience, both scientists already active in the field and those interested to learn about it. In this monograph, we start in Chap. 1 by briefly introducing the basic properties of wormlike micelles, which have been well described in several comprehensive reviews. The following chapters are then organized according to the type of trigger: heat, light, pH, CO₂ in Chaps. 2–5. Chapter 6 gathers research on triggers that have received limited attention to date, such as redox potential, hydrocarbons, and also smart reverse micelles and the emerging field of multi-stimuli responsiveness. In all chapters describing individual triggers, the structure follows a logical sequence: the molecular structure of the surfactants and/or hydrotropes, the microstructures formed in aqueous solution, and the corresponding macroscopic behavior (mainly the rheological response). Finally, applications of these smart wormlike micelles (prospective and current) are discussed in Chap. 7, with a particular highlight on applications in the oil upstream industry.

While we have attempted to integrate a wide range of studies so as to present an up-to-date and comprehensive picture of smart wormlike micelles, some areas, in particular polymeric wormlike micelles have not been dealt with to a great extent, as our objective was to focus mainly on surfactant systems. The rapid development of polymeric wormlike micelles however leads us to ponder over the

two following open questions unsolved so far: Can the critical packing parameter theory be extended to predict the morphologies of polymeric micelles? If yes, how can we determine packing parameters, that is, the length and volume of the hydrophobic parts, the surface area of the hydrophilic portion, from the polymer architecture?

This monograph summarizes a large number of papers scattered across many scientific journals. We sincerely thank the authors whose results have been cited in this book, and thank Dr. Yongmin Zhang, whose Ph.D. thesis on CO₂-switchable wormlike micelles enabled us to considerably expand Chap. 5. We also would like to thank the editors, Heather Feng and June Tang from Springer for the invitation to write this book, for their patience in waiting for our manuscript, as well as their constant and kind reminders to push this monograph ahead. Finally, YF would like to thank the funding from National Natural Science Foundation of China (Grant No. 21173207, 21273223), Science and Technology Department of Sichuan Province (Grant No: 2010JQ0029, 2012NZ0006), and the start-up fund from Sichuan University.

Yujun Feng
Zonglin Chu
Cécile A. Dreiss

References

1. Dreiss CA (2007) Wormlike micelles: where do we stand? Recent developments, linear rheology and scattering techniques. *Soft Matter* 3:956–970
2. Chu Z, Dreiss CA, Feng Y (2013) Smart wormlike micelles. *Chem Soc Rev* 42:7174–7203

Contents

1 Basic Properties of Wormlike Micelles	1
References	4
2 Thermo-responsive Wormlike Micelles	7
2.1 Thermo-thickening WLMs	8
2.1.1 Thermo-thickening Non-ionic WLMs	8
2.1.2 Thermo-thickening Cationic WLMs	12
2.1.3 Thermo-thickening Hybrid WLMs	17
2.1.4 Thermo-thickening Zwitterionic WLMs	18
2.2 WLMs with Thermo-induced “Sol/Gel” Transition	20
References	25
3 Light-responsive Wormlike Micelles	29
3.1 Light-responsive WLMs Formed by a Surfactant in the Presence of a Light-responsive Additive	30
3.1.1 Monomerization/Dimerization of a Light-sensitive Additive ...	30
3.1.2 UV/Vis Isomerization of a Light-responder	31
3.2 Light-responsive WLMs Formed by a Photo-sensitive Surfactant ...	38
References	39
4 pH-Responsive Wormlike Micelles	41
4.1 pH-Responsive WLMs Based on Zwitterionic Surfactants	41
4.2 pH-Responsive WLMs Based on Cationic Surfactants in the Presence of an Acid	43
4.3 pH-Responsive WLMs Obtained from the Design of Surfactant Architecture	44
References	46
5 CO₂-Responsive Wormlike Micelles	49
5.1 CO ₂ -Switchable WLMs from Commodity Anionic Surfactants and an Amine Hydrotrope	50

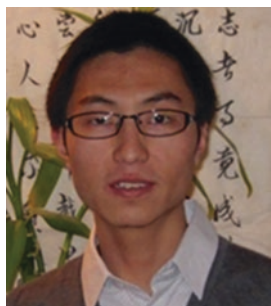
5.2	CO ₂ -Switchable WLMs Based on a C18-Tailed Polyamine	54
5.3	CO ₂ -Switchable WLMs Formed from a C22-Tailed Tertiary Amine	60
5.4	CO ₂ -Rupturing WLMs Formed from Sodium Erucate.	62
	References	64
6	Other Types of Smart Wormlike Micelles.	67
6.1	Redox-Responsive WLMs	67
6.2	Hydrocarbon-Responsive WLMs	69
6.3	Multi-stimuli-Responsive WLMs	71
6.4	Responsive Reverse WLMs	73
	References	75
7	Applications of Smart Wormlike Micelles	79
7.1	Biomedicine	80
7.2	Oil Upstream Industry	81
7.2.1	Hydrocarbon-responsive SWLMs Used as Clean Fracturing Fluids	81
7.2.2	pH-responsive SWLMs in Self-diverting Acidizing	82
7.2.3	Classes of Surfactants Used in SWLMs for Oilwell Stimulation.	83
7.2.4	WLMs for Enhanced Oil Recovery	84
7.3	Cleaning Processes	85
7.4	Electrorheological Fluids	85
7.5	Photo-rheological Fluids	86
7.6	Drag Reduction with Light-responsive WLMs	86
7.7	Templating	87
	References	88

About the Authors



Yujun Feng is currently Professor at the Polymer Research Institute and State Key Laboratory of Polymer Materials Engineering, Sichuan University. After earning his Ph.D. in Applied Chemistry from Southwest Petroleum University, China, in 1999, he moved to France to undertake his postdoctoral research at the Laboratoire de Physico-Chimie des Polymères, CNRS/ Université de Pau, and at the Institut Français du Pétrole (IFP), respectively. In 2004, he joined the Chengdu Institute of Organic Chemistry, Chinese Academy of Sciences, and has been acting as a team leader since

then. In September 2012, he relocated to Sichuan University, where he is focusing on smart soft materials, in particular stimuli-responsive surfactants and polymers. Professor Feng is now serving as an associate editor for the “Journal of Surfactants and Detergents” published by Springer.



Dr. Zonglin Chu obtained his Ph.D. in Applied Chemistry from the Chengdu Institute of Organic Chemistry, Chinese Academy of Sciences in 2011. After a year of postdoctoral research on multi-step organic synthesis at the Lab of Organic Chemistry, ETH Zürich, he is currently working on surfaces with special wettability in Prof. Dr. Stefan Seeger’s group in the Department of Chemistry, University of Zürich. His research interests lie at the interface of organic synthesis, colloid and interface science, hydrogels, smart materials, and functional surfaces.



Cécile A. Dreiss is Senior Lecturer at the Institute of Pharmaceutical Science, King's College London, UK. Her research focuses on understanding and exploiting self-assembly in soft matter, spanning colloidal, polymeric and biological systems, by establishing relationships between properties on the macro-scale (bulk behaviour or functionality) and the organization at the nanoscale. She uses neutron and X-ray scattering techniques extensively as well as rheology. Cécile graduated in Chemistry and Chemical Engineering (ENSIC, France). She received her Ph.D. from Imperial College London (chemical engineering) in

2003, after which she took up a 2-year postdoctoral position at the University of Bristol. She then moved back to London and was appointed as a Lecturer in September 2005.

Abbreviations

η	Shear viscosity
η_0	Zero-shear viscosity
τ_R	Relaxation time
C^*	Overlapping concentration
G'	Elastic or storage modulus
G''	Viscous or loss modulus
G_0	Plateau modulus
3,3'-Azo2Na	Sodium 3,3'-azobenzene dicarboxylate
5mS	5-methyl salicylic acid
AzoNa	Sodium (4-phenylazo-phenoxy)-acetate
AZTMA	4-butylazobenzene-4'-(oxyethyl)-trimethyl-ammonium bromide
C-11S	Cocamid monoethanolamine
C_{12} -azo- C_{12}	Sodium-2,2'-(diazene-1,2-diylbis (4,1-phenylene))didodecanoate
C_{12} DMAO	Dodecyldimethylamine oxide
C_{14} DMAO	Tetradecyldimethylamine oxide
C_{16} MIMBr	1-hexadecyl-3-methylimidazolium bromide
$C_{18}\Phi P_a E_b S$	Octadecylphenylalkoxysulfonate
$C_8 F_{17} EO_{10}$	Perfluoroalkyl sulfonamide ethoxylate
$C_8 OH$	<i>n</i> -octanol
ChEO _y	Polyoxyethylene cholesteryl ether
Cin ⁻	Cinnamate
C_n DMAO	Alkyldimethylamine oxide
C_n EO _m	Polyoxyethylene alkyl ether
Cryo-TEM	Cryogenic transmission electron microscopy
Ct	2,4,4'-trihydroxychalcone
CTA ⁺	Cetyltrimethylammonium
CTAB	Cetyltrimethylammonium bromide
CTAHNC	Hydroxynaphthalene-2-carboxylate
DLS	Dynamic light scattering

DPA	Decylphosphoric acid
DR	Drag reducing
EDAB	Erucyl dimethyl amidopropyl betaine
EDAS	3-(<i>N</i> -erucamidopropyl- <i>N,N</i> -dimethyl ammonium) propane sulfonate
EHAC	Erucyl bis-(hydroxyethyl)methylammonium chloride
ER	Electro-rheological
FC4-HC6	Sodium 1-[4-(nonafluorobutyl)phenyl]-1-oxo-2-octanesulfonate
FC6-HC2	Sodium 1-[4-(tridecafluorohexyl)phenyl]-1-oxo-2-butanesulfonate
FC6-HC4	Sodium 1-[4-(tridecafluorohexyl)phenyl]-1-oxo-2-hexanesulfonate
FF-TEM	Freeze-fracture transmission electron microscopy
FTMA	(11-ferrocenylundecyl) trimethyl-ammonium bromide
HC6-HC4	Sodium 1-(4-hexylphenyl)-1-oxo-2-hexane-sulfonate
HNC ⁻	3-hydroxynaphthalene-2-carboxylate
HOOC-CTAB	ω -carboxyl cetyltrimethyl-ammonium bromide
HR-TEM	High-resolution transmission electron microscopy
HSal	Salicylic acid
Me ₂ PE-C32-Me ₂ PE	Dotriacotane-1,32-diyl-bis[2(demethyl-ammonio)ethylphosphate]
ML	Monolaurin
MP	Monopalmitin
NaCin	Sodium cinnamate
NaOA	Sodium oleate
NaOE	Sodium erucate
NaSal	Sodium salicylate
ODPTA	Octadecyl dipropylene triamine
OMCA	Ortho-methoxycinnamic acid
PCA	Paracoumaric acid
PDAS	3-(<i>N</i> -palmitamidopropyl- <i>N,N</i> -dimethyl ammonium) propane Sulfonate
<i>p</i> DoAO	<i>p</i> -dodecyloxybenzyl dimethylamine oxide
PEG	Polyoxyethylene
PhyEO _x	Polyoxyethylene phytosteryl ether
PR	Photo-rheological
RWLMs	Reverse wormlike micelles
SANS	Small-angle neutron scattering
SAXS	Small X-ray scattering
SDC	Deoxycholate
SDS	Sodium dodecyl sulfate
SEM	Scanning electron microscopy
SLS	Static light scattering

SWLMs	Smart wormlike micelles
TMHM	Tetramethylammoniumhydrogen-2-dodecyl malonate
UC ₂₂ AMPM	<i>N</i> -erucamidopropyl- <i>N,N</i> -dimethylamine
UV	Ultraviolet
VES	Viscoelastic surfactants
Vis	Visible
WLMs	Wormlike micelles

Chapter 1

Basic Properties of Wormlike Micelles

Abstract Surfactants are probably the most fascinating family of small amphiphilic molecules, not only because of their everyday use in our life, but also because of their attractive macroscopic properties—all of which result from their versatile self-assembly properties and microstructures. In this chapter, we recall the basic properties of surfactant assemblies, in particular, the classical “critical packing parameter” theory which is widely used to predict aggregate morphology, and retrace the historical development of wormlike micelles (WLMs), and the unique characteristics that WLMs possess, as well as generic models used to describe them. Finally, we state the motivation and the organization of this monograph.

Keywords Surfactant · Self-assembly · Critical packing parameter · Wormlike micelles · Stimuli-responsive · Viscoelastic surfactant

As typical amphiphilic compounds, surfactants, composed of a hydrophilic head-group and a hydrophobic tail, spontaneously self-assemble into a multitude of micellar microstructures when dissolved in water. The micellar shape can be predicted to some extent by the concept of the “critical packing” parameter proposed by Israelachvili and co-workers [1]

$$P = v/a_0l_c \quad (1.1)$$

where v is the volume of the hydrophobic portion of the molecule, a_0 is the optimal surface group area occupied by one surfactant headgroup at the micelle–water interface, and l_c is the critical length of the hydrophobic tail, effectively the maximum extent to which the chain is stretched under the specific conditions imposed by molecular structure and environmental factors.

Figure 1.1 represents the array of possible morphologies adopted by surfactant self-assemblies according to different values of the “critical packing parameter”: $P < 1/3$, spherical/spheroidal micelles; $1/3 < P < 1/2$, rodlike or wormlike micelles (WLMs); $1/2 < P < 1$, vesicles; $P \sim 1$, bilayers; and $P > 1$, reverse micelles.

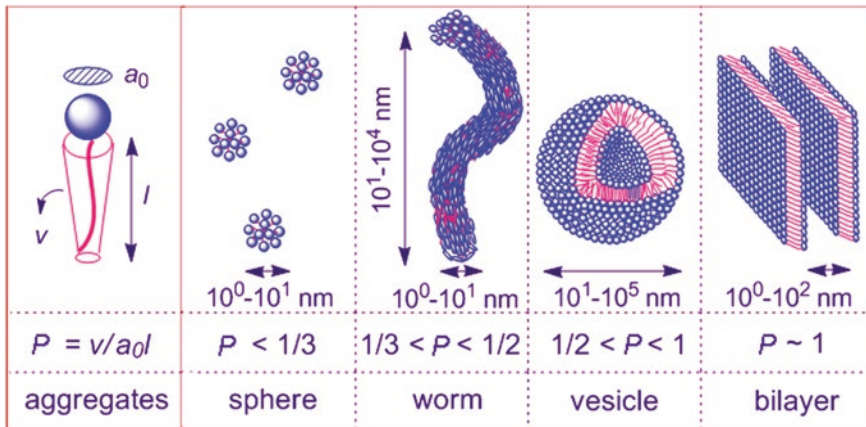


Fig. 1.1 Schematic illustration of the relationship between the packing parameter P and the morphology of self-assembled surfactant aggregates. Redrawn based on Ref. [1]

Amongst the various types of supramolecular self-assemblies, the very long cylindrical and flexible WLMs have gained considerable interest from both theoreticians and experimentalists because of their peculiar micellar structure and remarkable rheological response [2]. When micelles grow into worms, the aggregates show many similarities with polymers: in particular, they entangle with each other above the critical overlapping concentration (C^*) to form a transient network, imparting interesting viscoelastic properties and nonlinear rheology characteristics. However, unlike polymers, WLMs are constantly breaking and reforming in a dynamic equilibrium; for this reason, they are also referred to as “living” or “equilibrium” polymers [3]. As such, WLMs have found applications and offer great potential in numerous technological and industrial fields including drag reduction [4], personal and home care products, but the most successful stories come from the upstream oil industry where they have been used in clean fracturing fluids [5] and acid diversion [6] during oil well stimulation, which are discussed in Chap. 7.

Although the concept of packing parameter to predict the formation of rod-like micelles was only proposed in 1976, the discovery of WLMs dates back to the early 1950s, when Debye and Anacker [7] found by light scattering that the addition of potassium bromide caused a size increase and morphological transition of colloidal aggregates of hexadecyltrimethyl ammonium bromide (HTAB), from spherical to rodlike micelles. A few years later, Nash [8] mapped out viscoelastic regions of HTAB solutions with various naphthalene derivatives. In 1976, Gravsholt [9] observed that salicylate or chlorobenzoate counterions could efficiently promote uniaxial growth of surfactant micelles, and attributed viscoelasticity of these solutions to entanglements and reptation, just as in polymer solutions. In the early 1980s, the traditional terminologies of “rodlike micelles” and “elongated micelles” were replaced, and the terms “giant micelles” and “WLMs” were coined by Porte et al. [10] and Ikeda [11], respectively, because some of the

micelles observed by electron microscopy appeared as threadlike and tortuous filaments or worms [12]. At the same period, Candau et al. [13, 14] demonstrated a clear crossover between dilute and semi-dilute regimes and scaling laws as a function of the concentration, two features that were known from polymers. Thus, several epithets such as elongated, rodlike, threadlike, wormlike, and even polymer-like or “spaghetti-like” [15] have been applied to refer to these micelles. The latest but more widely used term, “WLMs”, is used throughout this monograph.

To date, WLMs have been mainly formed by mixing a surfactant (mostly cationic) and a low molecular weight hydrotrope [16] (or primer [15]) that screen the electrostatic repulsions between the surfactant charged headgroups, but more recent studies have shown that both long-chain zwitterionic [17, 18] and non-ionic [19] surfactants can form WLMs without the introduction of hydrotropes.

Although the theory, design, rheology, microstructure, and practical applications of WLMs have been thoroughly reviewed by Rehage and Hoffmann [20], Dan and Safran [21], Ezrahi et al. [22], Lerouge and Berret [2], Berret [23], Dreiss [16], Candau and Oda [24], Palazzo [15], amongst others, the main concepts of interest are briefly introduced here, as they are important to the understanding of WLM behaviour, and often referred to in the following chapters of this monograph.

According to Cates’ model [25], two dynamic regimes are considered, depending on the relative values of two characteristic relaxation times: the reptation time, τ_{rep} , corresponding to the curvilinear diffusion of a chain along a tube generated by the entanglements from the other chains, and the breaking time, τ_{b} , corresponding to the mean time required for a chain of mean length to break into two pieces:

If $\tau_{\text{b}} \ll \tau_{\text{rep}}$, the long-time behaviour of the stress relaxation is a single exponential decay with the relaxation time τ_{R} given by

$$\tau_{\text{R}} = (\tau_{\text{b}} \tau_{\text{rep}})^{1/2} \quad (1.2)$$

Correspondingly, the behaviour of the solution is described by the Maxwell equations:

$$G'(\omega) = \frac{\omega^2 \tau_{\text{R}}^2}{1 + \omega^2 \tau_{\text{R}}^2} G_0 \quad (1.3)$$

$$G''(\omega) = \frac{\omega \tau_{\text{R}}}{1 + \omega^2 \tau_{\text{R}}^2} G_0 \quad (1.4)$$

where G' , G'' , and G_0 are the storage, loss, and plateau modulus, respectively.

If $\tau_{\text{b}} > \tau_{\text{rep}}$, on timescales comparable to τ_{b} , the so-called living polymer chains behave as ordinary “dead” polymers, as they are dominated by reptation.

Apart from the dynamic properties, another characteristic nature of WLMs is their scaling behaviour. In the dilute regime, the viscosity (η) increases linearly with increasing volume fraction of the surfactant (ϕ) following Einstein’s viscosity equation [26]

$$\eta = \eta_s(1 + 2.5\phi) \quad (1.5)$$

In the semi-dilute regime instead, both steady zero-shear viscosity (η_0) and dynamic rheological parameters (G_0 and τ_R) follow a scaling law with theoretical scaling exponents 3.5, 2.25, and 1.25, respectively [23].

The crafting of intelligent materials that dynamically alter their structures and properties on demand or in response to environmental changes, and particularly those that can be switched between an “on” and “off” state, have been a major scientific focus of the past decade [27]. Supramolecular assemblies are ubiquitous in nature and provide an endless source of inspiration to design smart materials with bespoke functionalities and responsiveness. Similar to smart polymers, smart wormlike micelles (SWLMs), namely WLMs that can sense a signal in their environment and respond to it by displaying a relatively large physical or chemical change, have recently emerged as a new type of “smart” materials. Generally, the “responsiveness” of WLMs relies on a change in surfactant packing and thus micellar morphology: both micellar elongation and entanglement, resulting in an enhancement of viscoelasticity, or, inversely, surfactant disassembly leading to the loss of viscous and elastic characteristics, thus providing an effective “sol/gel” transition. Traditional triggers such as pH [28], heat [29], light [30], and redox potential [31] have all been explored as stimuli to impart a responsive behaviour to WLMs. To avoid by-product accumulation in solution, gas-switchable WLMs using CO_2 as a trigger have also been recently developed [32].

The aim of this monograph was to present the state of the art of SWLMs. We will review and discuss selected examples of SWLM systems to illustrate how the microscopic structures, and thus the concomitant macroscopic response, can be tuned via different external stimuli. These examples open the door to a range of potential applications, which will also be discussed. The following Chaps. 2–6 are organized according to the type of stimulus used to manipulate the response of the SWLMs: temperature, UV/Vis light, pH, CO_2 , redox, hydrocarbon, and combined stimuli. In Chap. 7, potential applications of SWLMs are discussed. Finally, a brief overview of the current state and future challenges are presented to conclude this review.

References

1. Israelachvili JN, Mitchell DJ, Ninham BW (1976) Theory of self-assembly of hydrocarbon amphiphiles into micelles and bilayers. *J Chem Soc Faraday Trans II* 72:1525–1568
2. Lerouge S, Berret J-F (2010) Shear-induced transitions and instabilities in surfactant wormlike micelles. *Adv Polym Sci* 230:1–71
3. Cates ME (1988) Dynamics of living polymers and flexible surfactant micelles: scaling laws for dilution. *J Phys France* 49:1593–1600
4. Zakin JL, Bewersdorff HW (1998) Surfactant drag reduction. *Rev Chem Eng* 14:253–320
5. Kefi S, Lee J, Pope TL, Sullivan P, Nelson E, Hernandez AN, Olsen T, Parlar M, Powers B, Roy A, Wilson A, Twynam A (2004) Expanding applications for viscoelastic surfactants. *Oilfield Rev* 16:10–23

6. Al-Anzi E, Al-Mutawa M, Al-Habib N, Al-Mumen A, Nasr-El-Din H, Alvarado O, Brady M, Davies S, Fredd C, Fu D, Lungwitz B, Chang F, Huidobro E, Jemmali M, Samuel M, Sandhu D (2003) Positive reactions in carbonate reservoir stimulation. *Oilfield Rev* 15:28–45
7. Debye P, Anacker E (1951) Micelle shape from dissymmetry measurements. *J Phys Chem* 55:644–655
8. Nash T (1958) The interaction of some naphthalene derivatives with a cationic soap below the critical micelle concentration. *J Colloid Sci* 13:134–139
9. Gravsholt S (1976) Viscoelasticity in highly dilute aqueous solutions of pure cationic detergents. *J Colloid Interface Sci* 57:575–577
10. Porte G, Poggi Y, Appell J, Maret G (1984) Large micelles in concentrated solutions. The second critical micellar concentration. *J Phys Chem* 88:5713–5720
11. Ikeda S (1984) Sphere-rod transition of surfactant micelles and size distribution of rodlike micelles. *J Phys Chem* 88:2144–2149
12. Imae T, Kamiya R, Ikeda S (1984) Electron microscopic observation of rod-like micelles of dimethyloleylamine oxide regenerated from its aqueous solutions. *J Colloid Interface Sci* 99:300–301
13. Candau S, Hirsch E, Zana R (1985) Light scattering investigations of the behavior of semidilute aqueous micellar solutions of cetyltrimethylammonium bromide: analogy with semidilute polymer solutions. *J Colloid Interface Sci* 105:521–528
14. Candau S, Hirsch E, Zana R, Adam M (1988) Network properties of semidilute KBr solutions of cetyltrimethyl ammonium bromide. *J Colloid Interface Sci* 122:430–440
15. Palazzo G (2013) Wormlike reverse micelles. *Soft Matter* 9:10668–10677
16. Dreiss CA (2007) Wormlike micelles: where do we stand? Recent developments, linear rheology and scattering techniques. *Soft Matter* 3:956–970
17. Chu Z, Feng Y, Su X, Han Y (2010) Wormlike micelles and solution properties of a C22-tailed amidosulfobetaine surfactant. *Langmuir* 26:7783–7791
18. Zhang Y, Luo Y, Wang Y, Zhang J, Feng Y (2013) Single-component wormlike micellar system formed by a carboxylbetaine surfactant with C22 saturated tail. *Colloid Surf A-Physicochem Eng Asp* 436:71–79
19. Wang J, Wang J, Wang B, Guo S, Feng Y (2013) Synthesis and aqueous solution properties of polyoxyethylene surfactants with ultra-long unsaturated hydrophobic chains. *J Disp Sci Technol* 34:504–510
20. Rehage H, Hoffmann H (1991) Viscoelastic surfactant solutions: model systems for rheological research. *Mol Phys* 74:933–973
21. Dan N, Safran SA (2006) Junctions and end-caps in self-assembled non-ionic cylindrical micelles. *J Colloid Interface Sci* 123:323–331
22. Ezrahi S, Tuval E, Aserin A (2006) Properties, main applications and perspectives of worm micelles. *Adv Colloid Interface Sci* 128–130:77–102
23. Berret J-F (2006) Rheology of wormlike micelles: equilibrium properties and shear banding transitions. In: Weiss RG, Terech P (eds) *Molecular gels: materials with self-assembled fibrillar networks*. Springer, Dordrecht, pp 667–720
24. Candau SJ, Oda R (2001) Linear viscoelasticity of salt-free wormlike micellar solutions. *Colloid Surf A-Physicochem Eng Asp* 183–185:5–14
25. Cates ME (1987) Reptation of living polymers: dynamics of entangled polymers in the presence of reversible chain-scission reactions. *Macromolecules* 20:2289–2296
26. Hoffmann H (2003) Viscoelastic surfactant solutions. In: Esumi K, Ueno M (eds) *Structure-performance relationships in surfactants*. *Surfactants Sci Ser* 112. Marcel Dekker, New York, pp 433–483
27. Cohen Stuart MA, Huck WTS, Genzer J, Müller M, Ober C, Stamm M, Sukhorukov GB, Szleifer I, Tsukruk VV, Urban M, Winnik F, Zauscher S, Luzinov I, Minko S (2010) Emerging applications of stimuli-responsive polymer materials. *Nat Mater* 9:101–113
28. Lin Y, Han X, Huang J, Fu H, Yu C (2009) A facile route to design pH-responsive viscoelastic wormlike micelles: smart use of hydrotropes. *J Colloid Interface Sci* 330:449–455

29. Kalur GC, Frounfelder BD, Cipriano BH, Norman AI, Raghavan SR (2005) Viscosity increase with temperature in cationic surfactant solutions due to the growth of wormlike micelles. *Langmuir* 21:10998–11004
30. Sakai H, Orihara Y, Kodashima H, Matsumura A, Ohkubo T, Tsuchiya K, Abe M (2005) Photo-induced reversible change of fluid viscosity. *J Am Chem Soc* 127:13454–13455
31. Tsuchiya K, Orihara Y, Kondo Y, Yoshino N, Ohkubo T, Sakai H, Abe M (2004) Control of viscoelasticity using redox reaction. *J Am Chem Soc* 126:12282–12283
32. Zhang Y, Feng Y, Wang J, He S, Guo Z, Chu Z, Dreiss C (2013) CO₂-switchable wormlike micelles. *Chem Commun* 49:4902–4904

Chapter 2

Thermo-responsive Wormlike Micelles

Abstract This chapter summarizes findings on the simplest trigger applied to wormlike micellar: temperature. Thermo-thinning systems are not discussed since a viscosity decrease with temperature is a rather general characteristic of most systems. Instead, the unique thermo-viscosifying behaviour displayed by some WLMs and the possibility of imparting a pseudo “sol/gel” transition in specific systems are extensively addressed. These two types of systems show a transition from either a low-viscosity fluid or a viscoelastic solution to a gel-like state by tuning the temperature. The thermo-thickening behaviour and the underlying mechanisms of various types of thermo-thickening wormlike micellar systems (non-ionic, cationic, anionic, and zwitterionic) are discussed in terms of molecular structure–property relationships.

Keywords Thermo-responsive · Thermo-thickening · Thermo-viscosifying · Wormlike micelles · Sol/gel transition · Surfactant gel

This chapter deals with the simplest possible trigger, which is temperature. Stimuli responsiveness can be defined as a physicochemical change resulting from a small external variation in environmental conditions. From this point of view, one may regard both thermo-thinning (i.e. a viscosity decrease with temperature) and thermo-thickening (i.e. a viscosity increase with temperature) fluids as examples of temperature responsiveness. Generally, however, the micellar contour length decays exponentially with increasing temperature, which in turn leads to an exponential decrease in zero-shear viscosity η_0 , following an Arrhenius law [1]:

$$\eta_0 = G_0 A e^{E_a/RT} \quad (2.1)$$

where A is a pre-exponential factor, T is the absolute temperature, E_a is the flow activation energy, and R is the gas constant. Thermo-thinning is therefore a general characteristic of WLMs and for this reason will not be discussed here. Instead, we will focus in this chapter on the unique thermo-viscosifying behaviour displayed by some WLMs [2–10] (Sect. 2.1) and the possibility of imparting a pseudo

“sol/gel” transition in some systems, with a transition from either a low-viscosity fluid or a viscoelastic solution to a gel-like sample [11–13] by playing on the temperature (Sect. 2.2). It is worth noting from the start that thermo-viscosifying WLMs do not necessarily show a thermo-thickening response over the whole temperature range. Instead, a maximum value is usually present in the curve of η_0 as a function of temperature; therefore, a thermo-thickening response can be obtained at low temperatures while a thermo-thinning behaviour at high temperatures, separated by a critical temperature.

2.1 Thermo-thickening WLMs

Thermo-thickening WLMs have been reported for all types of surfactants: non-ionic, cationic, anionic, and zwitterionic. Their thermo-thickening behaviour and the underlying mechanisms are discussed in the following sections, which are organized according to the nature of the surfactant.

2.1.1 Thermo-thickening Non-ionic WLMs

Polyoxyethylene (PEG) is widely used as a responder to thermal stimulus, since the hydration of the oxyethylene unit is dramatically affected by temperature [14]: the hydration of PEG is weakened upon increasing the temperature, and thus, its solubility decreases. As a result, its corresponding aqueous solutions exhibit an upper miscibility gap with a lower critical solution point, usually referred to as a cloud point [15]. The biocompatibility of PEG is well known, and it has been approved for oral, subcutaneous, intramuscular, and intravenous injections into human bodies for biomedical applications [16]. Its unique thermo-responsiveness has been exploited to develop thermally responsive polymers [17–20], hydrogels [16, 21–23], molecular brushes [24], nanoparticles [25], nanofibres [26], and other thermally responsive materials [27]. In recent years, PEG has also been used to construct WLMs utilizing PEG-based non-ionic surfactants (Fig. 2.1), such as polyoxyethylene phytosteryl ether (PhyEO_x, Fig. 2.1a) [14, 28], polyoxyethylene cholesteryl ether (ChEO_y, Fig. 2.1b) [29, 30], polyoxyethylene alkyl ether (C_nEO_m, Fig. 2.1c) [31–34], and perfluoroalkyl sulphonamide ethoxylate (C₈F₁₇EO₁₀, Fig. 2.1d) [35]. Similar to PEG-based macromolecules, these non-ionic wormlike micellar systems also display thermo-viscosifying behaviour [8, 14, 28, 30–34].

In a study on mixed non-ionic WLMs formed by PhyEO₃₀ and C₁₂EO₃ in aqueous solutions, a maximum η_0 was observed by Abe et al. [14] as a function of temperature, for a surfactant concentration of 5 wt% and mixing fraction (X , expressed as the weight fraction of C₁₂EO₃) of 0.36. As exhibited in Fig. 2.2a, upon increasing the temperature from 15 to 30 °C, η_0 rises by more than one order of magnitude; upon a further increase in temperature, η_0 decreases monotonically.

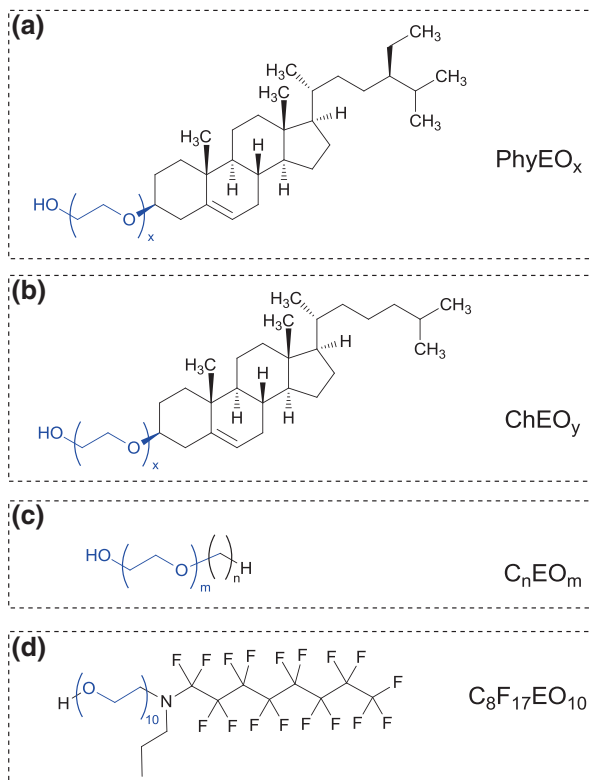


Fig. 2.1 Structures of some amphiphiles involved in thermo-sensitive WLM formation and bearing polyoxyethylene headgroups: **a** PhyEO_x , **b** ChEO_y , **c** C_nEO_m and **d** $\text{C}_8\text{F}_{17}\text{EO}_{10}$

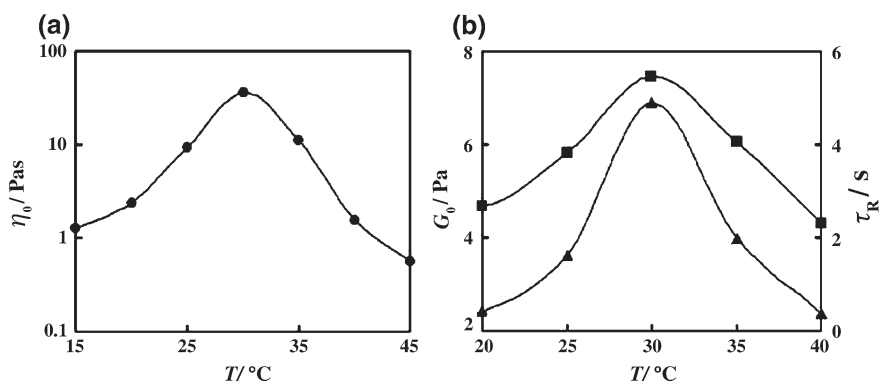


Fig. 2.2 Variation of the zero-shear viscosity η_0 (a) and plateau modulus G_0 and relaxation time τ_R (b) as a function of temperature (T) for 5 wt% “ $\text{PhyEO}_{30}/\text{C}_{12}\text{EO}_3$ ” system at $X = 0.36$. Adapted with permission from Ref. [14]. Copyright (2009) American Chemical Society

Dynamic rheological experiments also demonstrated the thermo-viscosifying and thermo-thinning effects below and above 30 °C, respectively; that is, maximum values of G_0 and τ_R are present at 30 °C (Fig. 2.2b). From small-angle X-ray scattering (SAXS) measurements, micellar size, in terms of the maximum dimension of the aggregates (D_{\max}), was seen to grow when increasing the temperature from 15 to 30 °C and then decrease at higher temperatures. The authors suggested that the thermo-viscosifying response below 30 °C could be understood in terms of the decrease in interfacial curvature of the aggregates due to the progressive dehydration of the PEG headgroups. Replacing $C_{12}EO_3$ with monoglycerides such as monolaurin (ML) and monopalmitin (MP), the same group [30] again observed a thermo-thickening in the rheological response. For 10 wt% PhyEO₃₀/ML solutions, when the mixing fraction X —expressed in weight fraction of ML (or MP for the other system)—ranged from 0.21 to 0.29, a gradual increase, followed by a decrease of the η_0 versus T curve, was clearly observed. The behaviour of 10 wt% “PhyEO₃₀/MP” was essentially similar, with the only exception that the viscosity growth was detected at higher temperatures, due to the longer hydrophobic chain of MP. The existence of a maximum was attributed to a temperature-induced micellar growth, followed by micellar branching. The interfacial curvature of the aggregates decreases with increasing temperature due to the progressive dehydration of the PEG headgroup and thus favours micellar growth; however, upon further increasing the temperature, intermicellar junctions are formed, and these connections can slide along the worms’ bodies, releasing the stress and thus resulting in a decrease of the viscosity, as speculated by the authors [30]. This “branching” has been widely documented in the WLMs literature, in general to explain the presence of a viscosity maximum as a function of salt or cosurfactant in mixed surfactant systems [36].

Very recently, the same authors [30] extended their work to the polyoxyethylene cholesteryl ether (ChEO₂₀) wormlike micellar system, using cocamide monoethanolamine (C-11S) as a cosurfactant. For WLMs composed of 10 wt% ChEO₂₀ and 5.7 wt% C-11S, rheological measurements performed over a wide range of temperatures revealed changes in viscosity of various orders of magnitude upon small increases in the temperature. Ahmed and Aramaki [31] investigated the effect of PEG chain length on the temperature sensitivity of ChEO _{x} WLMs, using ChEO₁₅ and ChEO₃₀ as a model surfactant and $C_{12}EO_3$ as a cosurfactant. Again, the rheological properties of the worms were found to be highly sensitive to temperature, but largely dependent on the hydrophilic size of the surfactant: the ChEO₃₀ systems are less temperature sensitive than the ChEO₁₅ worm systems; that is, the increase of the PEG chain length reduces the thermo-sensitivity of the worms.

Aramaki et al. [8] also investigated the thermo-viscosifying effect of the non-ionic WLMs formed by $C_{14}EO_3$ and Tween 80 in aqueous media. Upon increasing the temperature, the viscosity increased promptly. The authors suggested that one-dimensional micellar growth is enhanced at high temperature since the molecular cross-sectional area at the hydrophile–lipophile interface decreases gradually because of the dehydration of the polyoxyethylene chains, causing a reduction

in the spontaneous curvature and an increase in the end-cap energy. Constantin et al. [32] investigated the thermo-thickening mechanism of WLMs with the sole use of $C_{12}EO_6$ as a model amphiphile, in the absence of any additives. For $C_{12}EO_6$ concentrations between 5 and 35 wt%, it was found that the viscosity first increased with temperature and then decreased after reaching a maximum. The thermo-viscosifying temperature ranged from 0 to ~ 40 °C, depending on the surfactant concentration. Compared with $C_{12}EO_6$ WLMs, the thermo-viscosifying range of $C_{12}EO_8$ WLMs was shifted to higher temperatures [32], implying that an increase in PEG chain length can be used to tune the critical responsive temperature, in agreement with the findings by Ahmed and Aramaki discussed above [31]. Utilizing Cryo-TEM observation and light scattering techniques, Talmon et al. [33] examined the temperature sensitivity of WLMs formed by a similar polyoxyethylene alkyl ether, $C_{12}EO_5$. As shown in Fig. 2.3a, the coexistence of spheroidal (arrowheads) and rather short (<50 nm) threadlike micelles (arrows) was observed at 8 °C. Upon increasing the temperature to 18 °C (Fig. 2.3b), longer flexible cylindrical micelles with contour lengths ranging between 50 and 100 nm were formed and a small number of threefold junctions or branching points (small arrows) were also observed. The micelles became much longer (>100 nm) and the density of the threefold junctions higher (large arrows) with a further increase in temperature to 29 °C (Fig. 2.3c). From static light scattering (SLS) measurements, the Rayleigh ratio was found to increase with temperature at a constant surfactant concentration, reflecting temperature-induced micellar growth.

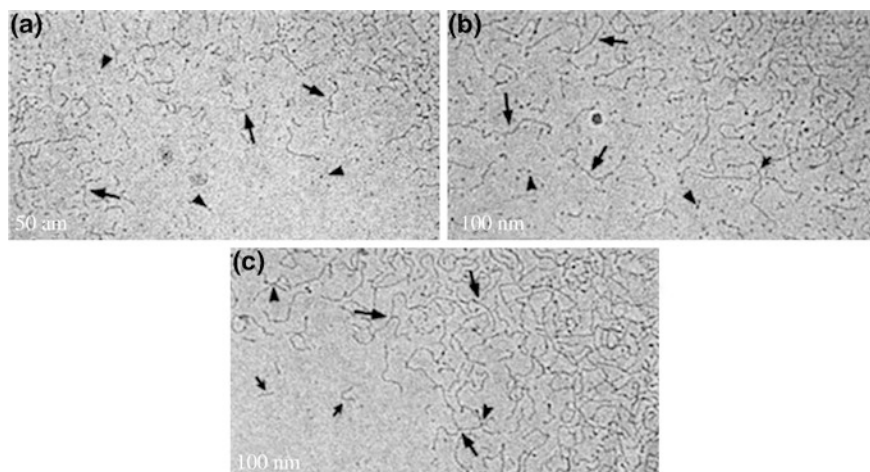


Fig. 2.3 Cryo-TEM images of a 0.5 wt% aqueous $C_{12}E_5$ solution at three different temperatures. At 8 °C (a), spheroidal (arrowheads) and rather short (<50 nm) wormlike micelles (arrows) coexist. At 18 °C (b), the coexistence of spheroidal (arrowheads) and cylindrical micelles (arrows) is again identified, but the worms are longer (50–100 nm) and threefold junctions (small arrow) are present. At 29 °C (c), the worms are much longer (>100 nm), and the density of the threefold junctions (larger arrows) is higher. Adapted with permission from Ref. [33]. Copyright (2000) American Chemical Society

In addition to the above non-ionic thermo-thickening WLM systems, WLMs formed by the hybrid non-ionic surfactant perfluoroalkyl sulphonamide ethoxylate ($C_8F_{17}EO_{10}$) were also found to display a thermo-thickening behaviour [35]. In this novel system, a thermo-viscosifying behaviour was detected at surfactant concentration as low as 1 wt%. Viscosity increased monotonously up to a critical temperature of ca. 35 °C, referred to as $T_{\eta, \max}$, followed by a gradual decrease and ultimately phase separation. SAXS experiments revealed a gradual micellar growth until a slight “lamellar-like” structural pattern was observed at 45 °C. The authors speculated that this transition from WLMs to lamellar phase was probably related to the formation of micellar branching points. As the increase in temperature normally decreases the curvature, it is not yet clearly understood how a structural transition from WLMs to lamellar-like structures with a very low interfacial curvature could take place.

To summarize, non-ionic WLMs composed of PEG hydrophilic blocks have been shown to display thermo-viscosifying properties, since micellar growth (which leads to increased entanglements and longer relaxation processes) is favoured by heating due to the dehydration of the polyoxyethylene blocks [37, 38]. It is worth noting that heat-induced micellar growth (generally from globular micelles to short rods) has been widely reported for other than PEG-derived surfactants [34, 39–41]; however, viscoelasticity was not studied because the rods were not long enough to form a three-dimensional network.

2.1.2 Thermo-thickening Cationic WLMs

Since the early studies on rodlike or WLMs carried out by Debye and Anacker [42], and Nash [43], WLMs based on cationic surfactants have been extensively investigated [44–49]. However, cationic wormlike micelles with thermo-thickening rheological response have scarcely been reported. As summarized in Fig. 2.4, thermo-thickening behaviour in cationic WLMs has been found for cetyltrimethylammonium 3-hydroxynaphthalene-2-carboxylate (CTAHNC, Fig. 2.4a) [2, 7, 9, 50, 51], erucyl bis-(hydroxyethyl)methylammonium chloride (EHAC, Fig. 2.4b) [3] or CTAB (Fig. 2.4c, d) [4, 52] in the presence of strongly hydrophobic organic compounds: 3-hydroxynaphthalene-2-carboxylate (HNC^- , Fig. 2.4b) [3], 5-methyl salicylic acid (5mS, Fig. 2.4c) [4] or *n*-octanol (C_8OH , Fig. 2.4d) [52]. The corresponding thermo-thickening mechanism is usually ascribed to a micellar shape transition upon heating.

The first known example of thermo-thickening cationic WLMs was reported for aqueous solutions of the surfactant CTAHNC (Fig. 2.4a) by Manohar et al. [2]. CTAHNC was simply prepared by mixing CTAB and sodium 3-hydroxynaphthalene-2-carboxylate (SHNC), followed by removal of the inorganic counterions (Na^+ and Br^-) through a solvent extraction technique using methyl isobutyl ketone [7, 9] and then further purifying via recrystallization from a mixture of benzene, petroleum ether [9]. At concentrations higher than 3 wt% at room temperature, the samples were turbid and solidlike, consisting of lamellar dispersions,

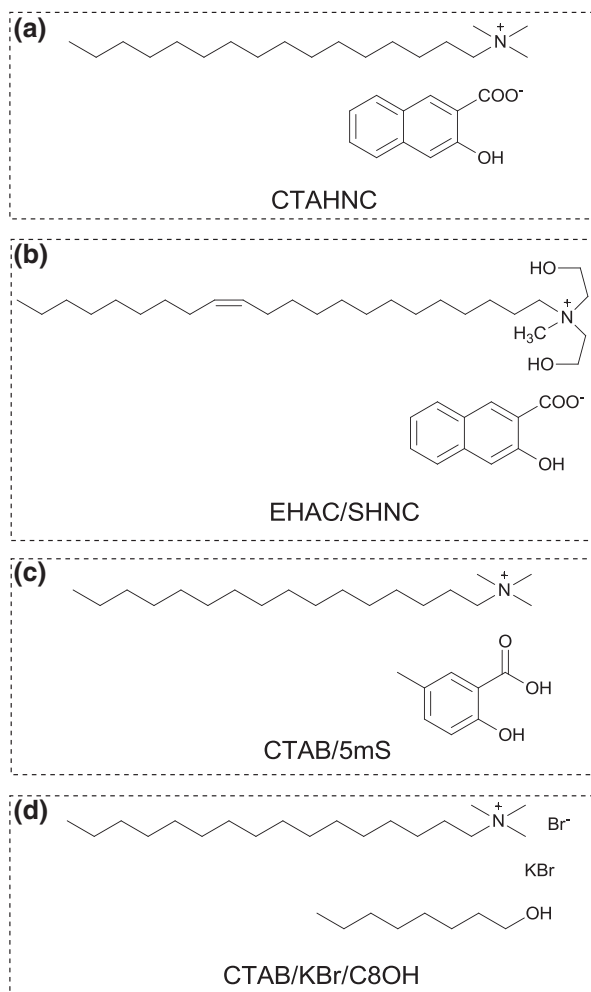


Fig. 2.4 Structures of thermo-thickening cationic WLMs reported in the literature: CTAHNC (a), EHAC/SHNC (b), CTAB/5mS (c), and CTAB/KBr/C8OH (d)

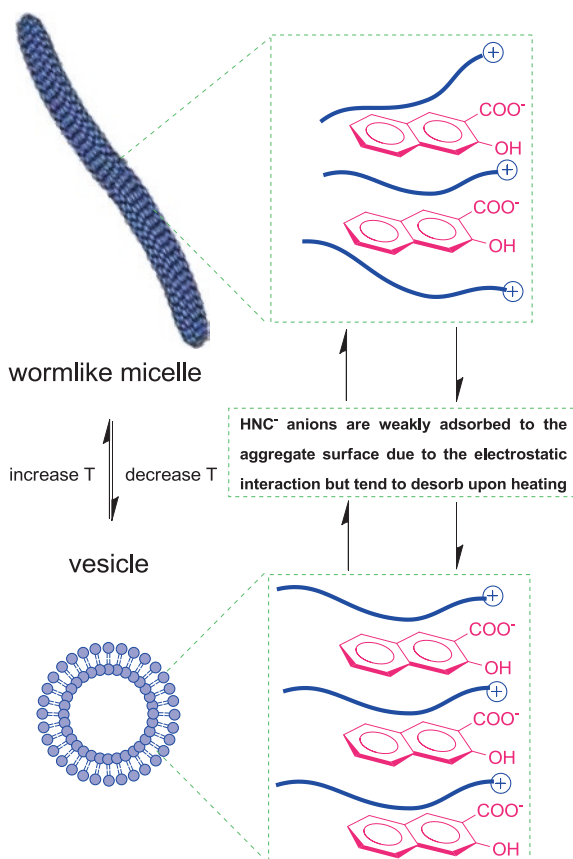
as demonstrated by polarized light microscopy [2]. Upon heating to well-defined temperatures, these samples turned into optically clear, strongly viscoelastic fluids, presumably consisting of long flexible WLMs. At 0.6 % (m/v), a CTAHNC solution also showed a turbid-to-clear transition, similar to the one observed at higher concentrations, accompanied by a viscosity increase by two orders of magnitude, as the solution became clear. However, the corresponding micellar transition was different from the concentrated samples. In the dilute regime, a vesicle-to-worm transition was detected by Cryo-TEM.

Soon after, Candau et al. [7] investigated the same micellar system, 0.6 wt% CTAHNC, at temperatures ranging from 30 to 70 °C. At temperatures up to 40 °C,

a low-viscosity vesicular solution phase was present, as demonstrated by rheology and optical microscopy. However, upon increasing the temperature to ~ 50 °C or higher, highly elongated WLMs were formed, as suggested by rheological measurements. Rheological and optical experiments performed on mixed systems of 12 mM CTAHNC and small amounts of CTAB (≤ 2 mM) also revealed a vesicle-to-worm transition upon heating [7]. SANS experiments performed by Mendes et al. [50] on the same solutions confirmed a phase transition from vesicles at 37 °C to WLMs at 55 °C. Differential scanning calorimetry (DSC) measurements on CTAHNC solutions carried out by Hoffmann et al. [51] showed a transition peak at 46 °C, independent of CTAHNC concentration, reflecting a transition within the lamellar phase at 46 °C due to the melting of the vesicle surface. Conductivity of the solution showed a jump at about the same temperature, implying the release of ions from the melting surface of the vesicles and implying a loss of surface-adsorbed HNC^- and their concomitant increase in the bulk water phase.

A possible mechanism for the vesicle-to-worm transition is schematically illustrated in Fig. 2.5 [52]. Vesicles are formed at low temperatures, because of the presence of an equimolar amount of HNC^- anions adsorbed at the aggregate

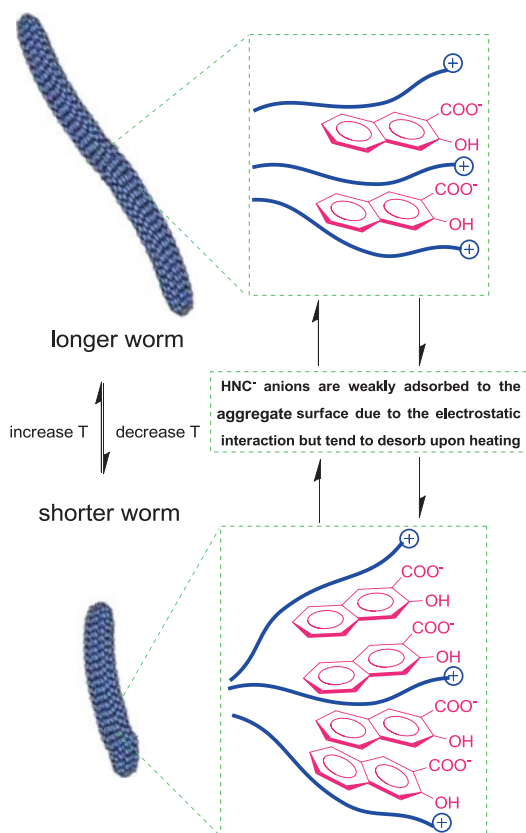
Fig. 2.5 Mechanism of the vesicle-to-worm transition in the CTASHNC system. Reproduced from Ref. [52] with permission from The Royal Society of Chemistry



surface due to weak physical electrostatic forces. Upon heating, however, some of the HNC^- anions at the aggregate/water interface are transferred into the bulk as the weak physical adsorption is hindered by heating. This desorption changes the molecular geometry and hence reduces the interfacial curvature of the aggregates, inducing a transition from vesicles to WLMs. More details about the vesicle-to-worm transition of the CTAHNC systems can be found in the review by Narayanan et al. [9].

By simply mixing EHAC and SHNC without removing NaBr side product, Raghavan et al. [3] recently developed another type of thermo-viscosifying WLM system (Fig. 2.4b). A typical example of their experimental results on “40 mM EHAC/360 mM SHNC” is shown in Fig. 2.6 [52]. The sample is a low-viscosity, waterlike Newtonian fluid at 25 °C. However, upon gradual heating up to 45 °C, the viscosity increases steadily, while the fluid maintains its Newtonian behaviour. Upon raising the temperature further, the viscosity still increases continuously, but a shear-thinning response at high shear rates is observed for temperatures above 60 °C. When varying SHNC concentration, in some cases, the viscosity of the sample reaches a maximum at a critical temperature, beyond which it then

Fig. 2.6 Mechanism of the rod-to-worm transition in the EHAC/SHNC system. Adapted with permission from Ref. [52]. Copyright (2013) Royal Society of Chemistry



decreases. The onset and magnitude of the viscosity increase, as well as the peak temperature, can all be altered by varying SHNC concentration. SANS data confirmed an increase in contour length of the micelles with temperature, at the origin of the thermo-thickening behaviour. The heat-induced increase in contour length was attributed to a temperature-dependent counterion binding at the micelle/water interface (Fig. 2.6). This is different from the case of CTAHNC since an excess of SHNC is present in such solutions. HNC^- anions are strongly hydrophobic, and the HNC^- ions in excess stay near the micelle/water interface, resulting in a higher interfacial curvature, thereby forming shorter rods at lower temperature. Upon heating, some of the HNC^- anions at the micelle/water interface shift to the bulk [3] as the weak physical adsorption forces are overcome, similar to the case of CTASHNC. However, in contrast to the former system, desorption reduces the interfacial curvature, thus favouring the growth of the worms.

Following this study, the same group developed another thermo-viscosifying WLM system (Fig. 2.4c) [4], based on the simple mixing of CTAB with the hydrotrope 5mS. A transition from a bluish, low-viscosity liquid around 48 °C to a colourless, perceptibly viscous and flow-birefringent fluid at about 54 °C was detected over a range of concentrations. A typical study of optical density at 500 nm and η_0 as a function of temperature for a sample containing 12.5 mM CTAB and 20 mM 5mS suggested a micellar transition from vesicle to worm upon heating, and this interpretation was further confirmed by SANS. It is worth noting that the transition is temperature switchable; that is, vesicles that are disrupted into worms upon heating can be re-formed upon cooling. Both the transition temperature and the magnitude of the viscosity increase could be finely-tuned by varying sample composition. The mechanism responsible for the vesicle-to-worm transition upon heating was attributed to a temperature-dependent counterion binding at the micelle/water interface, similar to the CTAHNC system discussed above.

Sreejith et al. [53] investigated the mixture of CTAB and C_8OH in the presence of KBr (Fig. 2.4d) and observed a thermally-induced response for $\text{C}_8\text{OH}/\text{CTAB}$ molar ratios above ~ 0.25 . Based on rheological measurements, dynamic light scattering (DLS) analysis, and Cryo-TEM observation, the authors ascribed the thermo-response to a vesicle-to-worm transition. At low temperatures, a sufficient amount of C_8OH molecules were expected to be inserted between CTAB molecules to promote vesicle formation. However, upon increasing the temperature, Br^- ions were released into the bulk water, favouring the increase of the interfacial curvature and thus a transition to WLMs.

Thermo-thickening cationic WLMs have thus been prepared with long-chain cationic surfactants in the presence of strongly hydrophobic hydrotropes. The underlying thermo-thickening mechanism is usually attributed to a modification of the micellar architecture, caused by a change in the interfacial curvature prompted by a depletion of the hydrotropes at the micelle/water interface at high temperature.

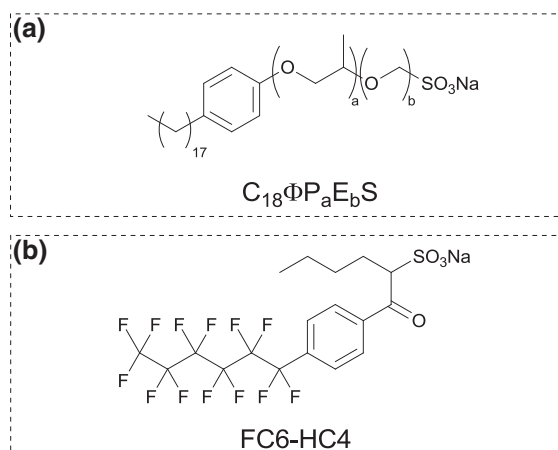
2.1.3 Thermo-thickening Hybrid WLMs

Pioneering studies on anionic thermo-thickening viscoelastic surfactants can be tracked back to 1988 [10], though no verification was made by Cryo-TEM observation at that time. Similar to PEG-derived non-ionic surfactants described above, the PEG-derived anionic surfactant octadecylphenylalkoxysulphonate ($C_{18}\phi P_5E_{11}S$, Fig. 2.7a) also shows a thermo-viscosifying behaviour, due to the presence of PEG units that are thermally responsive. For example, 10 mM $C_{18}\phi P_5E_{11}S$ solution is a waterlike Newtonian fluid composed of globular micelles at temperatures below $\sim 45^\circ\text{C}$ and becomes a shear-thinning fluid composed of WLMs at high temperatures. The mechanisms underlying the thermo-responsive behaviour of $C_{18}\phi P_5E_{11}S$ WLMs, however, are similar to the PEG-based non-ionic surfactants discussed in Sect. 2.1.1, i.e. a dehydration of PEG chains, inducing micellar growth and a subsequent viscosity increase.

Apart from this particular example, no other common anionic WLMs have been found to show a thermo-thickening rheological response; however, some specific anionic surfactants with a hybrid structure, such as sodium 1-[4-(tridecafluorohexyl)phenyl]-1-oxo-2-hexanesulphonate (FC6-HC4, Fig. 2.7b) [5, 6], have been shown to possess such an unusual behaviour.

Yoshino et al. [54] synthesized the fluoro-hybrid anionic surfactant FC6-HC4 by reacting 1-[4-(perfluoroalkyl)phenyl]-1-alkanones with a sulphur trioxide/1,4-dioxane complex in 1,2-dichloroethane, followed by neutralization with aqueous sodium hydroxide, and then investigated its rheological behaviour as a function of temperature [6, 54]. A thermo-thickening response was detected for concentrations ranging from 7 to 15 wt%; the viscosity peak and corresponding temperature could be tuned by varying surfactant concentration [6]. Since thermo-viscosifying was not observed for monohydrocarbon chain surfactants, such as 1-pentanesulphonic

Fig. 2.7 Structures of hybrid anionic surfactants showing a thermo-thickening rheological response



acid sodium salt and SDS, or monofluorocarbon chain-type surfactants such as perfluoroheptanoate, or neither fluoro-hybrid-type surfactants such as sodium 1-[4-(tridecafluorohexyl)phenyl]-1-oxo-2-butanedisulphonate (FC6–HC2), sodium 1-[4-(nonafluorobutyl)phenyl]-1-oxo-2-octadisulphonate (FC4–HC6), and its double hydrocarbon chain counterpart, sodium 1-(4-hexylphenyl)-1-oxo-2-hexadisulphonate (HC6–HC4), the authors assigned the unique thermo-responsive behaviour of FC6–HC4 micellar solutions to its peculiar chemical structure, i.e. a hybrid fluorocarbon/hydrocarbon double chain, with six carbon atoms in the fluorocarbon chain and four carbon atoms in the hydrocarbon chain [5, 6, 55]. Cryo-TEM measurements [56] were later undertaken, in combination with rheology, digital light microscopy, and self-diffusion NMR. Cryo-TEM revealed a heat-induced micellar transition from mainly short rodlike micelles at 20 °C to very large multilamellar vesicles at temperatures at 30 and 40 °C, and to a disordered lamellar phase at 50 °C and above [56]. Although the structure of the assemblies present at the temperature of 36 °C, i.e. where the viscosity showed a maximum—could not be elucidated by Cryo-TEM (due to an on-the-grid transformation during specimen preparation), rheology and self-diffusion NMR experiments indicated the presence around 40 °C of assemblies that are larger than those present at lower (mainly short rodlike micelles) and higher temperatures (a disordered multiconnected lamellar phase), which could explain the thermo-responsive behaviour [56].

2.1.4 Thermo-thickening Zwitterionic WLMs

Despite being very gentle on the human skin and more environmentally friendly because of their neutral charge, zwitterionic surfactant WLMs have been scarcely reported [11, 57–61] compared to non-ionic, cationic, and anionic surfactants. To the best of our knowledge, only one type of thermo-thickening zwitterionic WLMs has been reported, which was recently developed by Chu and Feng using a synthesized sulphobetaine amphiphile, 3-(*N*-palmitamidopropyl-*N,N*-dimethyl ammonium) propane sulphonate (PDAS, Fig. 2.10d) [57].

The steady-state rheological behaviour of 1.0 M PDAS solution in the presence of 0.5 M NaCl is shown in Fig. 2.8. The shear viscosity of the sample (Fig. 2.8a) at 30 °C remains constant at 0.05 Pa s, regardless of shear rate, typical of Newtonian flow behaviour. Such low viscosity in surfactant solutions is usually attributed to the presence of globular micelles or short rodlike micelles (Fig. 2.9a). However, upon increasing the temperature to 40 °C, the same solution becomes shear thinning, which is well acknowledged as the evidence of WLMs becoming aligned in the flow field (Fig. 2.9b). The high viscosity of this solution could be switched on and off by altering the temperature. As exhibited in Fig. 2.9b, the apparent viscosity at a shear rate of 10 s^{-1} (η_{10}) stays constant at 0.05 Pa s and 30 °C; however, when increasing the temperature from 30 to 40 °C, η_{10} increases 200-fold because of the thermal stimulus. Dynamic rheology also revealed an interesting thermo-switchable transition, which is discussed in the next section.

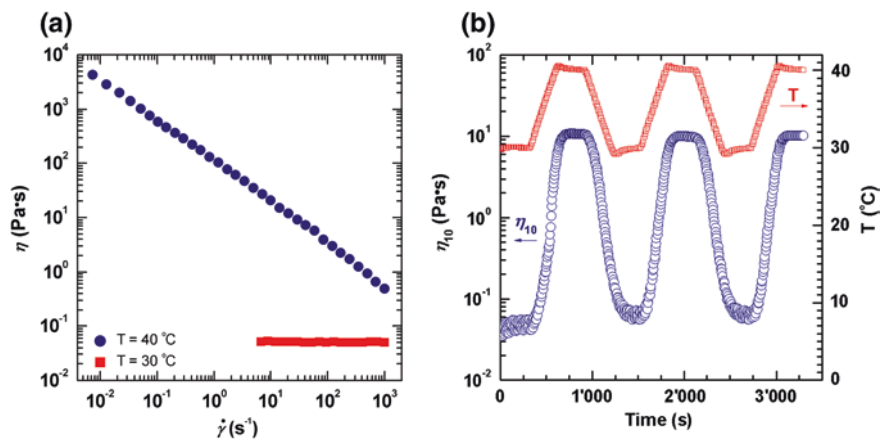
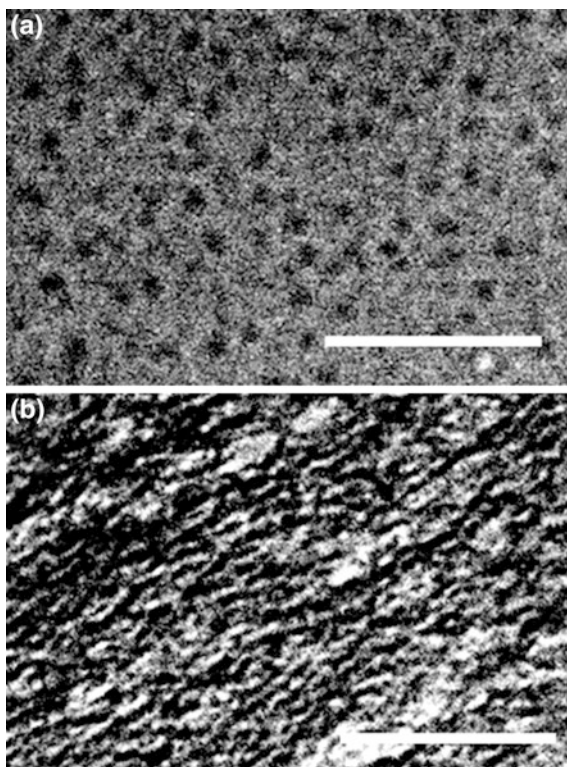


Fig. 2.8 Thermal stimuli response of the PDAS/NaCl solution: shear viscosity η as a function of shear rate $\dot{\gamma}$ (a) and thermo-reversible viscosity at shear rate of 10 s⁻¹, η_{10} (b). Reproduced from Ref. [57] with permission from The Royal Society of Chemistry

Fig. 2.9 Cryo-TEM observations of the 30 °C (a) and 40 °C (b) PDAS/NaCl solutions. Bars are 100 nm. Reproduced from Ref. [57] with permission from The Royal Society of Chemistry



2.2 WLMs with Thermo-induced “Sol/Gel” Transition

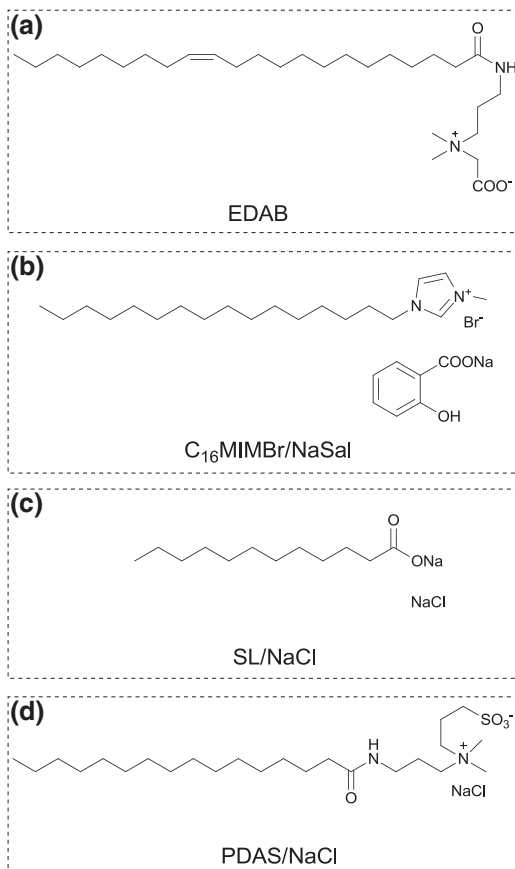
The typical rheological behaviour of WLM solutions follows the Maxwell model; namely, it displays a combination of viscous and elastic behaviour with a single relaxation time. However, a number of WLM systems have been reported which depart from this typical behaviour and are considerably stiffer, with very high values of G' and G'' , showing very little dependence on shear frequency, thereby making them similar to gels. As such, they offer considerable potential for biomedical applications, in particular tissue engineering [62], if stimulus responsiveness can be imparted to them. In tissue repair, hydrogels are used as scaffolds, either combined with the patients' own cells or using the body as a bioreactor; injectable in situ gelling materials reactive to a range of stimuli are of interest, in particular responsiveness to temperature, in order to trigger gelation upon contact with the body. While the vast majority of thermally responsive gelators reported to date are polymers or peptides, surfactant gels based on the reversible formation and entanglement of long flexible wormlike micelles show considerable promise [11, 57, 59, 63].

We begin the discussion with a very brief account of gels and so-called surfactant gels. A gel is usually loosely identified on the basis of its ability to withstand its own weight under gravity in an inverted vial; more rigorously, in dynamic rheology, its elastic modulus G' is always higher than its viscous G'' , and both are independent of shear frequency [64]. The strict definition of a “gel” has historically always been a topic of contention; the term is widely misused in the literature to describe a material that is “gel-like” but does not satisfy the strict rheological definition [64, 65]. The term “surfactant gel” has been applied to WLM networks in several reviews [63, 64], and we use it here to describe WLM systems showing a rheological behaviour characterized by $G' > G''$ and largely independent of frequency over a very wide range.

A detailed rheological investigation of such a surfactant gel was carried out by Chu et al. [58] on 3-(*N*-erucamidopropyl-*N,N*-dimethyl ammonium) propane sulphonate (EDAS) as a model system. Their results revealed a finite η_0 , and that G' and G'' should cross over at a very low shear frequency, not accessible; thereby, “surfactant gels” are strongly solidlike viscoelastic fluids with a finite η_0 and ultra-long τ_R rather than a “real” gel with infinite η_0 and τ_R . Based on these definitions, we can now discuss examples of thermo-induced “sol/gel” transitions in WLM systems reported in the literature (Fig. 2.9).

Raghavan et al. [11] investigated the “sol/gel” transition of WLMs formed by EDAB (Fig. 2.10a). At temperatures below 40 °C, concentrated EDAB solutions (for instance 50 and 100 mM) were strongly gel-like with G' exceeding G'' over the entire experimental frequency range (10^{-2} – 10^1 rad s⁻¹), both of which were slight functions of shear frequency, which made these samples similar to elastic gels. However, one cannot exclude that G' and G'' may cross over at a frequency much lower than the experimentally accessible range, for instance, 10^{-3} rad s⁻¹ or even lower. In any case, the relaxation time τ_R should be very long: at least 10^3 s from a simple estimate of $1/\tau_R$. Cryo-TEM and SANS revealed the presence of WLMs in

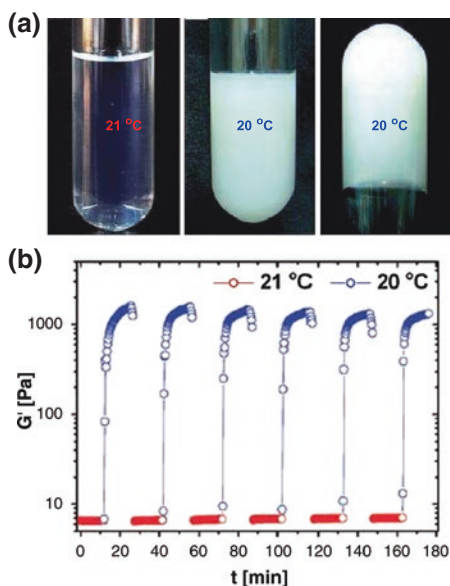
Fig. 2.10 Thermo-responsive WLM systems reported in the literatures: EDAB (a), C₁₆MIMBr/NaSal (b), SL/NaCl (c), and PDAS/NaCl (d)



these concentrated EDAB solutions. Upon increasing the temperature to 60 °C and above, the EDAB gels became Maxwellian with much shorter τ_R , about 300 and 40 s for 50 mM EDAB at 60 and 70 °C, and 100 and 15 s for 100 mM EDAB at 65 and 75 °C, respectively. The ultra-long τ_R of concentrated EDAB samples at low temperatures was ascribed to its extremely long breaking time, possibly linked to its ultra-long C22 hydrophobic tail. Later, work on another C22-tailed zwitterionic surfactant EDAS by Chu and Feng [57] was also consistent with this speculation. Therefore, the “sol/gel” transition mechanism for EDAB WLMs is the decrease of τ_R upon increasing the temperature. Interestingly, the “sol/gel” transition of EDAB is unusual since the plateau modulus G_0 before and after the transition is almost the same.

Huang et al. [12] reported a novel thermo-responsive WLM gel (Fig. 2.11b) with a narrow temperature “window” based on a mixture of 1-hexadecyl-3-methylimidazolium bromide (C₁₆MIMBr) and sodium salicylate (NaSal). Figure 2.11a depicts the visual appearance of the “sol/gel” transition of “40 mM C₁₆MIMBr/28 mM NaSal” WLM solution. At 21 °C, the sample is transparent and shows low viscosity. Upon decreasing the temperature to 20 °C, it instantaneously becomes

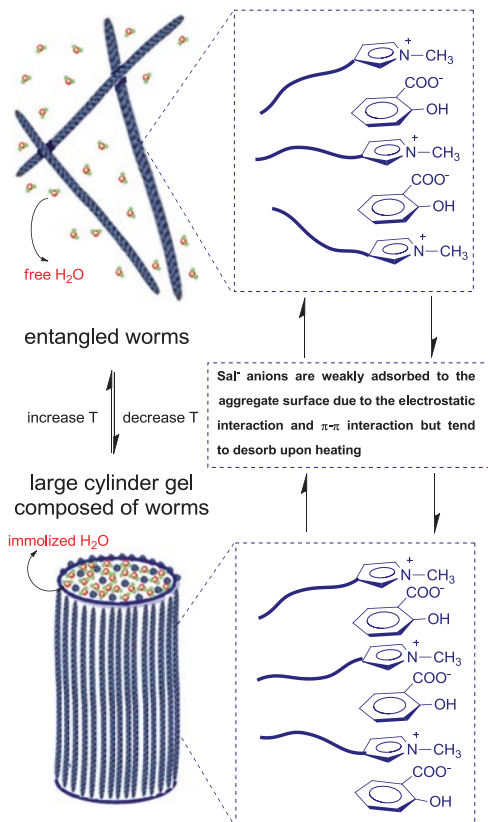
Fig. 2.11 The thermo-responsive “sol/gel” transition of the $C_{16}MIMBr/NaSal$ WLM system. Adapted from Ref. [12] with permission from The Royal Society of Chemistry



opalescent and can be turned upside down without flowing. This suggests a sol/gel transition upon cooling, which was further confirmed by dynamic rheology. As shown in Fig. 2.11b, the sol-to-gel transition is reversible, which means that a fluid and a gel can always be obtained by increasing and decreasing the temperature between 21 and 20 °C. In contrast to the case of EDAB WLMs described above, in which no detectable change in G_0 occurred between the “sol” and “gel” states, G' in the $C_{16}MIMBr/NaSal$ system showed an abrupt jump of over two orders of magnitude, before and after the transition. Scanning electron microscopy (SEM) at 20 °C revealed the presence of a network of large cylindrical structures with diameters ranging from 1 to 2 μm , responsible for the formation of the hydrogel, since large amounts of water could be immobilized. Similarly, a previous work on another thermo-responsive gel formed by sodium laurate (SL, Fig. 2.10c) in the presence of NaCl, reported by Hao et al. [13], revealed the presence of a network of fibres composed of bundles of parallel WLMs, as assessed by high-resolution transmission electron microscopy (HR-TEM). In both systems [12, 13], the large cylinders were hypothesized to originate from the crystallization of WLMs, since the physical interaction between surfactant headgroups and added salt was modified upon cooling.

A possible mechanism for this type of thermo-responsive gels, taking the $C_{16}MIMBr/NaSal$ system as an example, is illustrated schematically in Fig. 2.12. At 21 °C and above, the Sal^- anions are adsorbed at the micelle/water interface due to a combination of the following three physical interactions: the hydrophobic effect of the benzene ring, the electrostatic interaction between the ammonium cations and Sal^- anions, and the $\pi-\pi$ interaction between the benzene ring and the imidazolium ring. However, upon cooling to 20 °C and below, more Sal^- are

Fig. 2.12 Mechanism of the “sol/gel” transition in the C_{16} MIMBr/NaSal WLM system. Adapted from Ref. [52] with the permission from The Royal Society of Chemistry



adsorbed at the interface since the physical interactions are slightly strengthened, which slightly increases the interfacial curvature, inducing the fusion of the WLMs and thereby the formation of large cylinders composed of WLMs [12].

All the above WLM gels exhibit a common characteristic of gelation upon cooling. Instead, the thermo-switchable gel based on PDAS (Fig. 2.10d) shows the remarkable characteristic of gelation upon heating [57]. As discussed above, concentrated PDAS solutions showed a thermo-thickening behaviour in steady-state rheology. Dynamic rheology measurements (Fig. 2.13a) show a clear viscous response for a 1.0 M PDAS solution in the presence of 0.5 M NaCl at 30 °C, with a characteristic G' much lower than G'' over the entire shear frequency range. Upon heating to 40 °C, both G' and G'' increase by several orders of magnitude, and the rheological response becomes elastic, with G' exceeding G'' for all shear frequencies measured. The gelling process could be reversed by cooling, which enables one to switch the gel between an “on” and “off” state simply by heating and cooling, respectively (Fig. 2.13b). As schematically illustrated in Fig. 2.14, the mechanism of the switchable gelation was ascribed to the strengthened “salting-out” effect at increased temperature. At lower temperatures (ca. 30 °C), the “salting-out”

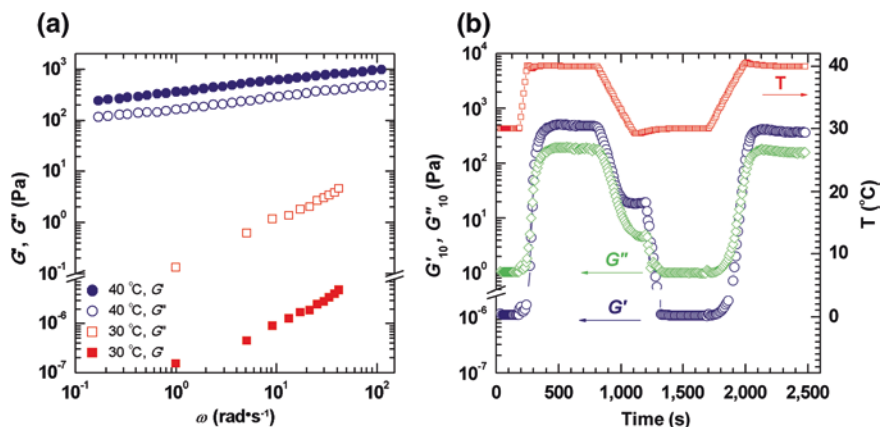


Fig. 2.13 Thermal response of the PDAS/NaCl solution: elastic (G') and viscous (G'') modulus as a function of oscillatory shear frequency ω (a) and thermo-reversible gelling processes (b). Reproduced from Ref. [57] with permission from The Royal Society of Chemistry

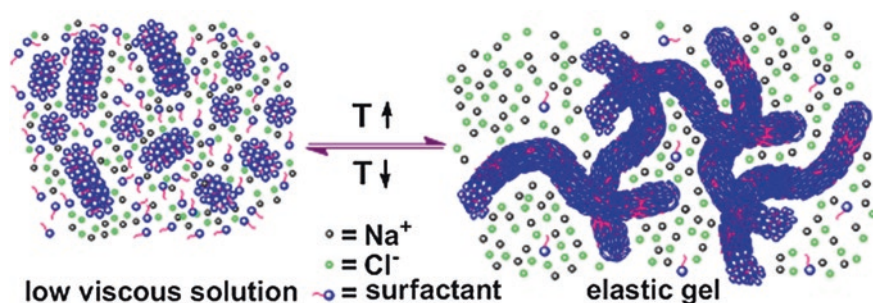


Fig. 2.14 Schematic illustration of the switchable gelation mechanism. Reproduced from Ref. [57] with permission from The Royal Society of Chemistry

effect of PDAS caused by the added salt is weaker, and thus, more PDAS molecules are present as monomers. However, upon increasing the temperature to 40 °C, the “salting-out” effect becomes stronger, and thus, the solubility of the hydrophobic moieties of PDAS tail worsens, enhancing micellization and the growth of the micelles from short rods into entangled long worms. The micellar structures immobilize the water, thereby resulting in the formation of a hydrogel. Upon decreasing back the temperature to its initial value, the entangled worms are lost due to the transfer of amphiphiles from the micellar phase to the bulk, and the self-assembly structures as well as the rheological properties revert back to the initial state.

Some WLM systems have thus proven to be effective thermo-switchable gelators and could therefore find interesting applications, offering generally, over traditional gelators, facile synthesis, simple mechanisms of gelation, and cost-effectiveness.

References

1. Candau SJ, Hirsch E, Zana R, Delsanti M (1989) Rheological properties of semidilute and concentrated aqueous solutions of cetyltrimethylammonium bromide in the presence of potassium bromide. *Langmuir* 5:1225–1229
2. Salkar RA, Hassan PA, Samant SD, Valaulikar BS, Kumar VV, Kern F, Candau SJ, Manohar C (1996) A thermally reversible vesicle to micelle transition driven by a surface solid–fluid transition. *Chem Commun* 10:1223–1224
3. Kalur GC, Frounfelker BD, Cipriano BH, Norman AI, Raghavan SR (2005) Viscosity increase with temperature in cationic surfactant solutions due to the growth of wormlike micelles. *Langmuir* 21:10998–11004
4. Davies TS, Ketner AM, Raghavan SR (2006) Self-assembly of surfactant vesicles that transform into viscoelastic wormlike micelles upon heating. *J Am Chem Soc* 128:6669–6675
5. Abe M, Tobita K, Sakai H, Kamogawa K, Momozawa N, Kondo Y, Yoshino N (2000) Thermoresponsive viscoelasticity of concentrated solutions with a fluorinated hybrid surfactant. *Colloid Surf A-Physicochem Eng Asp* 167:47–60
6. Tobita K, Sakai H, Kondo Y, Yoshino N, Kamogawa K, Momozawa N, Abe M (1998) Temperature-induced critical phenomenon of hybrid surfactant as revealed by viscosity measurements. *Langmuir* 14:4753–4757
7. Hassan PA, Valaulikar BS, Manohar C, Kern F, Bourdieu L, Candau SJ (1996) Vesicle to micelle transition: rheological investigations. *Langmuir* 12:4350–4357
8. Varade D, Ushiyama K, Shrestha LK, Aramaki K (2007) Wormlike micelles in Tween-80/ C_mEO_3 mixed nonionic surfactant systems in aqueous media. *J Colloid Interface Sci* 312:489–497
9. Narayanan J, Mendes E, Manohar C (2002) Vesicle to micelle transition driven by surface solid–fluid transition. *Int J Mod Phys B* 16:375–382
10. Greenhill-Hooper MJ, O'Sullivan TP, Wheeler PA (1988) The aggregation behavior of octadecylphenylalkoxysulfonates: I. Temperature-dependence of the solution behavior. *J Colloid Interface Sci* 124:77–87
11. Kumar R, Kalur GC, Ziserman L, Danino D, Raghavan SR (2007) Wormlike micelles of a C22-tailed zwitterionic betaine surfactant: from viscoelastic solutions to elastic gels. *Langmuir* 23:12849–12856
12. Lin Y, Qiao Y, Yan Y, Huang J (2009) Thermo-responsive viscoelastic wormlike micelle to elastic hydrogel transition in dual-component systems. *Soft Matter* 5:3047–3053
13. Yuan Z, Lu W, Liu W, Hao J (2008) Gel phase originating from molecular quasi-crystallization and nanofiber growth of sodium laurate-water system. *Soft Matter* 4:1639–1644
14. Sharma SC, Shrestha LK, Tsuchiya K, Sakai K, Sakai H, Abe M (2009) Viscoelastic wormlike micelles of long polyoxyethylene chain phytosterol with lipophilic nonionic surfactant in aqueous solution. *J Phys Chem B* 113:3043–3050
15. Strunk H, Lang P, Findenegg GH (1994) Clustering of micelles in aqueous solutions of tetraoxyethylene-*N*-octyl ether (C(8)E(4)) as monitored by static and dynamic light-scattering. *J Phys Chem* 98:11557–11562
16. Moon HJ, Ko DY, Park MH, Joo MK, Jeong B (2012) Temperature-responsive compounds as in situ gelling biomedical materials. *Chem Soc Rev* 41:4860–4883
17. Lee H, Pietrasik J, Sheiko SS, Matyjaszewski K (2010) Stimuli-responsive molecular brushes. *Prog Polym Sci* 35:24–44
18. Lutz J-F, Akdemir O, Hoth A (2006) Point by point comparison of two thermosensitive polymers exhibiting a similar LCST: is the age of poly(NIPAM) over? *J Am Chem Soc* 128:13046–13047
19. Lutz J-F, Hoth A (2006) Preparation of ideal PEG analogues with a tunable thermosensitivity by controlled radical copolymerization of 2-(2-methoxyethoxy)ethyl methacrylate and oligo(ethylene glycol) methacrylate. *Macromolecules* 39:893–896

20. Munoz-Bonilla A, Fernandez-Garcia M, Haddleton DM (2007) Synthesis and aqueous solution properties of stimuli-responsive triblock copolymers. *Soft Matter* 3:725–731
21. Yin XC, Stover DH (2003) Hydrogel microspheres formed by complex coacervation of partially MPEG-grafted poly(styrene-alt-maleic anhydride) with PDADMAC and cross-linking with polyamines. *Macromolecules* 36:8773–8779
22. Lutz J-F, Weichenhan K, Akdemir O, Hoth A (2007) About the phase transitions in aqueous solutions of thermoresponsive copolymers and hydrogels based on 2-(2-methoxyethoxy)ethyl methacrylate and oligo(ethylene glycol) methacrylate. *Macromolecules* 40:2503–2508
23. Hwang MJ, Suh JM, Bae YH, Kim SW, Jeong B (2005) Caprolactonic poloxamer analog: PEG-PCL-PEG. *Biomacromolecules* 6:885–890
24. Yamamoto S, Pietrasik J, Matyjaszewski K (2007) ATRP synthesis of thermally responsive molecular brushes from oligo(ethylene oxide) methacrylates. *Macromolecules* 40:9348–9353
25. Otsuka H, Nagasaki Y, Kataoka K (2003) PEGylated nanoparticles for biological and pharmaceutical applications. *Adv Drug Deliv Rev* 55:403–419
26. Moon K-S, Kim H-J, Lee E, Lee M (2007) Self-assembly of T-Shaped aromatic amphiphiles into stimulus-responsive nanofibers. *Angew Chem Int Ed* 46:6807–6810
27. Kim J-K, Lee E, Kim M-C, Sim E, Lee M (2009) Reversible transformation of helical coils and straight rods in cylindrical assembly of elliptical macrocycles. *J Am Chem Soc* 131:17768–17770
28. Sharma SC, Shrestha LK, Sakai K, Sakai H, Abe M (2010) Viscoelastic solution of long polyoxyethylene chain phytosterol/monoglyceride/water systems. *Colloid Polym Sci* 288:405–414
29. Afifi H, Karlsson G, Heenan RK, Dreiss CA (2011) Solubilization of oils or addition of monoglycerides drives the formation of wormlike micelles with an elliptical cross-section in cholesterol-based surfactants: a study by rheology, SANS, and Cryo-TEM. *Langmuir* 27:7480–7492
30. Shrestha RG, Sakai K, Sakai H, Abe M (2011) Rheological properties of polyoxyethylene cholesteryl ether wormlike micelles in aqueous system. *J Phys Chem B* 115:2937–2946
31. Ahmed T, Aramaki K (2009) Temperature sensitivity of wormlike micelles in poly(oxyethylene) surfactant solution: importance of hydrophobic-group size. *J Colloid Interface Sci* 336:335–344
32. Constantin D, Freyssingeas É, Paliarne J-F, Oswald P (2003) Structural transition in the isotropic phase of the C₁₂EO₆/H₂O lyotropic mixture: a rheological investigation. *Langmuir* 19:2554–2559
33. Bernheim-Groswasser A, Wachtel E, Talmon Y (2000) Micellar growth, network formation, and criticality in aqueous solutions of the nonionic surfactant C₁₂E₅. *Langmuir* 16:4131–4140
34. Bulut S, Hamit J, Olsson U, Kato T (2008) On the concentration-induced growth of nonionic wormlike micelles. *Eur Phys J E: Soft Matter Biol Phys* 27:261–273
35. Acharya DA, Sharma SJ, Rodriguez-Abreu C, Aramaki K (2006) Viscoelastic micellar solutions in nonionic fluorinated surfactant systems. *J Phys Chem B* 110:20224–20234
36. Dreiss CA (2007) Wormlike micelles: where do we stand? Recent developments, linear rheology and scattering techniques. *Soft Matter* 3:956–970
37. Johansson H, Karlstrom G, Tjerneld F (1993) Experimental and theoretical study of phase separation on aqueous solutions of clouding polymers and carboxylic acids. *Macromolecules* 26:4478–4483
38. Zhang KW, Karlstrom G, Lindman B (1994) Ternary aqueous mixture of a non-ionic polymer with a surfactant or a 2nd polymer—a theoretical and experimental investigations of the phase behavior. *J Phys Chem* 98:4411–4421
39. Wennerström H, Lindman B (1979) Micelles—physical chemistry of surfactant association. *Phys Rep—Rev Sec Phys Lett* 52:1–86
40. Lindmann B, Wennerström H (1991) Nonionic micelles grow with increasing temperature. *J Phys Chem* 95:6053–6054
41. Corti M, Minero C, Degiorgio V (1984) Cloud point transition in non-ionic micellar solutions. *J Phys Chem* 88:309–317

42. Debye P, Anacker E (1951) Micelle shape from dissymmetry measurements. *J Phys Chem* 55:644–655
43. Nash T (1958) The interaction of some naphthalene derivatives with a cationic soap below the critical micelle concentration. *J Colloid Sci* 13:134–139
44. Raghavan SR, Kaler EW (2001) Highly viscoelastic wormlike micellar solutions formed by cationic surfactants with long unsaturated tails. *Langmuir* 17:300–306
45. Gravsholt S (1976) Viscoelasticity in highly dilute aqueous solutions of pure cationic detergents. *J Colloid Interface Sci* 57:575–577
46. Porte G, Appell J, Poggi Y (1980) Experimental investigations on the flexibility of elongated cetylpyridinium bromide micelles. *J Phys Chem* 84:3105–3110
47. Imae T, Kamiya R, Ikeda S (1985) Formation of spherical and rodlike micelles of cetyltrimethylammonium bromide in aqueous NaBr solutions. *J Colloid Interface Sci* 108:215–225
48. Rehage H, Hoffmann H (1988) Rheological properties of viscoelastic surfactant systems. *J Phys Chem* 92:4712–4719
49. Li J, Zhao W, Zheng L (2012) Spontaneous formation of vesicles by *N*-dodecyl-*N*-methylpyrrolidinium bromide (C₁₂MPB) ionic liquid and sodium dodecyl sulfate (SDS) in aqueous solution. *Colloid Surf A-Physicochem Eng Asp* 396:16–21
50. Mendes E, Oda R, Manohar C, Narayanan J (1998) A small-angle neutron scattering study of a shear-induced vesicle to micelle transition in surfactant mixtures. *J Phys Chem B* 102:338–343
51. Horbaschek K, Hoffmann H, Thunig C (1998) Formation and properties of lamellar phases in systems of cationic surfactants and hydroxy-naphthoate. *J Colloid Interface Sci* 206:439–456
52. Chu Z, Dreiss CA, Feng Y (2013) Smart wormlike micelles. *Chem Soc Rev* 42:7174–7203
53. Sreejith L, Parathakkat S, Nair SM, Kumar S, Varma G, Hassan PA, Talmon Y (2011) Octanol-triggered self-assemblies of the CTAB/KBr system: a microstructural study. *J Phys Chem B* 115:464–470
54. Yoshino N, Hamano K, Omiya Y, Kondo Y, Ito A, Abe M (1995) Synthesis of hybrid anionic surfactants containing fluorocarbon and hydrocarbon chains. *Langmuir* 11:466–469
55. Tobita K, Sakai H, Kondo Y, Yoshino N, Iwahashi M, Momozawa N, Abe M (1997) Thermoresponsive viscoelasticity of sodium 1-oxo-1-[4-(tridecafluorohexyl)phenyl]-2-hexanesulfonate aqueous solutions. *Langmuir* 13:5054–5055
56. Danino D, Weihs D, Zana R, Orädd G, Lindblom G, Abe M, Talmon Y (2003) Microstructures in the aqueous solutions of a hybrid anionic fluorocarbon/hydrocarbon surfactant. *J Colloid Interface Sci* 259:382–390
57. Chu Z, Feng Y (2011) Thermo-switchable surfactant gel. *Chem Commun* 47:7191–7193
58. Chu Z, Feng Y, Su X, Han Y (2010) Wormlike micelles and solution properties of a C22-tailed amidosulfobetaine surfactant. *Langmuir* 26:7783–7791
59. Chu Z, Feng Y (2010) Amidosulfobetaine surfactant gels with shear banding transitions. *Soft Matter* 6:6065–6067
60. Chu Z, Feng Y, Sun H, Li Z, Song X, Han Y, Wang H (2011) Aging mechanism of unsaturated long-chain amidosulfobetaine worm fluids at high temperature. *Soft Matter* 7:4485–4489
61. Fisher P, Rehage H, Grüning B (2002) Linear flow properties of dimer acid betaine solutions with and without changed ionic strength. *J Phys Chem B* 106:11041–11046
62. Lee KY, Mooney DJ (2001) Hydrogels for tissue engineering. *Chem Rev* 101:1869–1879
63. Trickett K, Eastoe J (2008) Surfactant-based gels. *Adv Colloid Interface Sci* 144:66–74
64. Raghavan SR (2009) Distinct character of surfactant gels: a smooth progression from micelles to fibrillar networks. *Langmuir* 25:8382–8385
65. Kavanagh GM, Ross-Murphy SB (1998) Rheological characterisation of polymer gels. *Prog Polym Sci* 23:533–562

Chapter 3

Light-responsive Wormlike Micelles

Abstract UV/Vis light as a trigger displays a set of advantages over other types of stimuli in terms of its “clean” character, low cost, and precise spatial localization, and for these reasons it has been widely exploited in the development of smart materials. Light-responsive wormlike micelles take advantage of light-induced *cis*–*trans* isomerization or dimerization of light-sensitive surfactants or additives containing a suitable chromophore. These changes alter the packing of surfactant molecules in the aggregates and drive micellar transitions between wormlike micelles and other structures, thus tuning the viscoelasticity. This chapter summarizes two types of strategies in manipulating light-sensitive wormlike micelles—either to incorporate light-sensitive additives into classical existing wormlike micellar solutions or to directly introduce light-sensitive functional moieties on the surfactant molecules. In both cases, the worms self-assemble or disassemble upon alternate UV/Vis light irradiation.

Keywords Photo-switchable • Light-responsive • Wormlike micelles • Azobenzene • *Cis*–*trans* isomerization • Photo-rheology

UV/Vis light as a trigger displays a set of benefits over other types of stimuli and thus has been widely exploited in the development of smart materials [1–4]. Light as a stimulus is relevant to many biological processes, in which optical signals are recorded and transduced as sophisticated biochemical events. In addition, in contrast to redox reagents, pH, stress, or salinity, light is an elegant and non-invasive trigger and can be operated in a clean environment, thus avoiding changes in the composition or thermodynamic conditions. It is a cheap and readily available trigger as a mild energy source. Finally, better than ultrasound and electricity, light can be directed at a precise spatial location; this is particularly valuable in nanoscience and nanotechnology and for medical applications.

Light has been used as a trigger by exploiting dimerization, *cis*–*trans* isomerization, photo-scission, polymerization, or polarity changes in a range of systems [3]. However, quite obviously, not all reported light-sensitive surfactants

can be used for the construction of light-responsive WLMs. The development of light-responsive WLMs dates back to the early 1980s [5], though the term was coined very recently [6]. In general, light-responsive WLMs reported to date take advantage of light-induced *cis-trans* isomerization or dimerization of light-sensitive surfactants or additives containing a suitable chromophore. Clearly, these changes alter the packing of surfactant molecules in the aggregates and drive micellar transitions between WLMs and other structures, thus tuning the viscoelasticity. In terms of manipulating the systems, two types of strategies can be distinguished to formulate light-sensitive WLMs: one is to incorporate light-sensitive additives into existing WLMs solutions; the other is to directly introduce light-sensitive functional moieties on the surfactant molecules. In both cases, the worms self-assemble or disassemble upon alternate UV/Vis light irradiation.

3.1 Light-responsive WLMs Formed by a Surfactant in the Presence of a Light-responsive Additive

3.1.1 Monomerization/Dimerization of a Light-sensitive Additive

Wolff et al. [5] pioneered UV/Vis stimuli-responsive WLMs based on the classic surfactant cetyltrimethylammonium bromide (CTAB) in the presence of 9-methylantracene. Tunable viscosity was first achieved via photo-illumination, which was attributed to the photo-reversible dimerization of 9-methylantracene. 9-methylantracene was efficient in inducing the growth of CTAB WLMs and thereby enhancing the viscosity of the solution; however, 9-methylantracene monomers were dimerized upon photo-irradiating with a wavelength over 300 nm. Compared with their monomers, the dimers were less efficient in inducing the formation of WLMs because of unfavourable geometry. As a consequence, the WLMs became much shorter, resulting in a decrease in viscosity. When re-irradiating at a wavelength of 249 nm, the viscosity could be recovered.

Thereafter, the authors expanded their work on switchable viscosity to a wide range of 9-alkyl-substituted non-polar anthracene derivatives [7]. Viscosity enhancement (from ca. 1 mPa s to less than 10 mPa s) was evidenced when small amounts of non-polar anthracene derivatives was added to pure concentrated CTAB (250 mM) solutions, following the order: methyl < *n*-propyl < *n*-butyl. After UV irradiation, a slight decrease in viscosity was observed for 9-butylantracene and 9-pentylantracene, but not documented for the other systems. Further work showed that the presence of 2,2,2-trifluoro-1-(9-anthryl)-ethanol would also induce the formation of CTAB rodlike micelles, and in situ photo-dimerization of this photo-responsive solubilizate leads to reduced elasticity caused by a decrease in micelle size [8].

Recently, the same group further compared the rheological response of tetramethylammoniumhydrogen-2-dodecyl malonate (TMHM) solutions in the absence and presence of monomeric and photo-dimerized acridizinium bromide as solubilizers [9]. WLMs were present in pure TMHM solutions, as confirmed by rheological experiments. However, upon adding acridizinium bromide, the viscoelasticity of the initial TMHM WLMs solution decreased significantly because the acridizinium cations adsorbed strongly at the negatively charged TMHM head-groups and changed the overall charge of the micellar surface, and thus affected their aggregation behaviour. Interestingly, upon UV irradiation, the viscosity was increased again because the photo-dimers of acridizinium cations were released from the micellar surface, possibly because of the steric restrictions or strong solvation by water.

The authors further developed systems with photo-switchable viscosity by introducing coumarin derivatives into the aqueous solutions of Triton X-100 and CTAB [10]. They found that coumarins generally increased the viscosity, but the extent of the increase was specific: alkyl chains of medium length showed the largest effect. In situ photo-dimerization of the coumarins led to a further rise in the viscosity for short alkyl substituents, but to a drop in the viscosity for long alkyl substituents.

3.1.2 UV/Vis Isomerization of a Light-responder

Azobenzene is a commonly used UV/Vis responder and has been used to design light-responsive WLMs simply by adding it to otherwise light-insensitive WLM solutions (Fig. 3.1) [1, 11, 12].

Abe et al. [11] prepared a light-responsive WLM system based on CTAB and an azobenzene-modified cationic surfactant, 4-butylazobenzene-4'-(oxyethyl)-trimethylammonium bromide (AZTMA), in the presence of NaSal. The introduction of a small amount (10 mM) of *trans*-AZTMA to pre-formed “50 mM CTAB/50 mM NaSal” WLMs solutions increased the zero-shear viscosity (η_0) from 60 to 100 Pa s, while the storage (G') and loss (G'') moduli as a function of shear frequency conserved their Maxwell behaviour, which is a typical characteristic of WLMs. However, UV light irradiation for 2 h led to a decrease of η_0 by 4 orders of magnitude (to 0.1 Pa s) and a loss of the plateau region in G' over the frequency range measured. In addition, the changes were reversible, by alternating UV and visible light irradiation. This “switch” can be explained by the reversible *trans*-*cis* photo-isomerization of AZTMA (Fig. 3.1a), which drives changes in the geometrical structure and thus the interfacial properties. While *trans*-AZTMA was easily incorporated into WLMs of CTAB and NaSal, due to the linear structure of its hydrophobic tail, the bulky structure of *cis*-AZTMA disrupted the spontaneous packing into long cylindrical aggregates, thus disrupting the entanglement and leading to a drop in viscoelasticity.

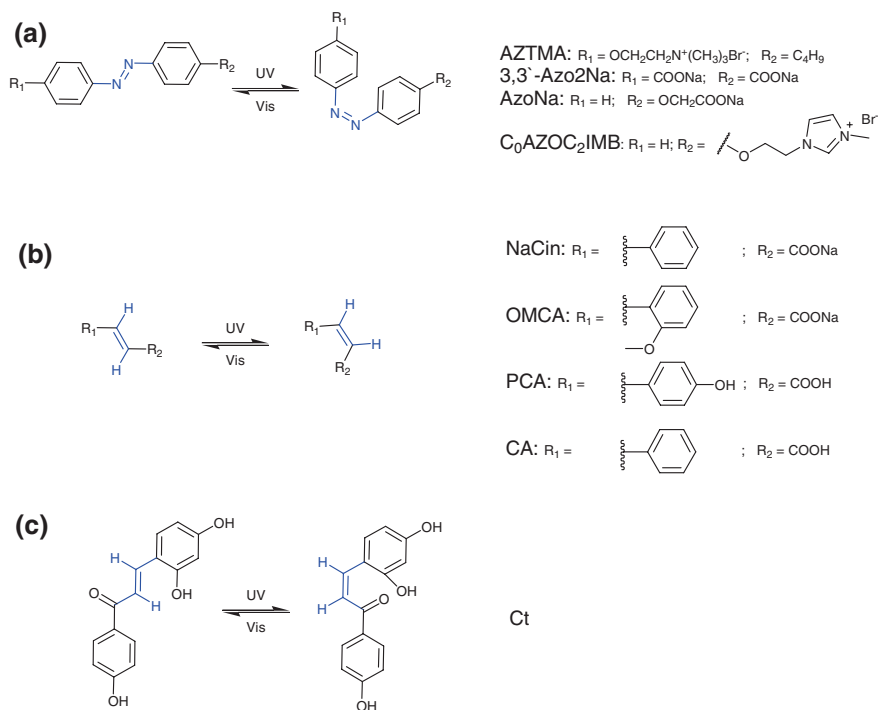


Fig. 3.1 UV/Vis responders and their isomerization used to prepare light-responsive WLMs

Subsequently, the same group [12] further investigated the photo-chemical control of viscoelasticity using sodium 3,3'-azobenzene dicarboxylate (3,3'-Azo2Na, Fig. 3.1a) for molecularly switching CTAB/NaSal WLMs. When an equimolar solution was irradiated by UV light, the 3,3'-Azo2Na exhibited a *trans*–*cis* photoisomerization. In stark contrast to the reduction in viscosity observed in the previous CTAB/NaSal/AZTMA system, η_0 was seen to increase nearly sevenfold, compared to its initial state. The authors explained this contrasting behaviour as follows: the molecular size of 3,3'-Azo2Na is not as large as that of AZTMA, and the conformation change in the CTAB/NaSal/3,3'-Azo2Na system following photo-isomerization is not sufficient to cause the collapse of WLMs. In the case of the *trans*-form, both the anionic salicylate ions and 3,3'-Azo2Na form a complex with cationic CTAB through electrostatic attraction. However, this capacity to form a complex is reduced when the *trans*-to-*cis* transformation occurs, because *cis*-3,3'-Azo2Na has a bent structure that leads to steric exclusion. As a result, some of the 3,3'-Azo2Na molecules exit from the WLMs and are replaced with NaSal, which therefore promotes WLM elongation and their entanglement, leading to a reinforcement of the viscoelastic properties.

Huang and co-workers [1] created photo-modulated multi-state and multi-scale molecular assemblies by incorporating a binary-state molecular switch, sodium (4-phenylazo-phenoxy)-acetate (AzoNa, Fig. 3.1a), into CTAB solutions.

Depending on the UV irradiation duration, the *trans/cis* isomerization state of the azobenzene group could be tuned to generate multi-state transitions to either WLMs, vesicles, planar lamellae, cylindrical micelles, or small spherical micelles, leading to significant changes in solution properties at the macroscopic scale. By exposing to UV or visible light, the multi-state and multi-scale molecular self-assemblies could be reversibly controlled. The authors proposed that light-triggered structural changes in the dipole moment and geometry of the azobenzene group, which in turn imparted a significant effect on the critical packing parameter of the surfactant, were responsible for the peculiar properties of this system.

Similarly, Zheng et al. [13] prepared a UV-induced self-assembly based on *N*-methyl-*N*-cetylpyrrolidinium bromide (C16MPBr) and sodium (4-phenylazo-phenoxy)-acetate (AzoNa) through facile mixing of C16MPBr and *trans*-AzoNa in water. Li and co-workers [14] reported a new class of light-responsive viscoelastic fluids based on sodium oleate in the presence of a cationic azobenzene dye, 1-[2-(4-phenylazo-phenoxy)-ethyl]-3-methylimidazolium bromide (C₀AZOC₂IMB, Fig. 3.1a). These binary systems are gel-like fluids at certain concentration ratios, owing to the formation of WLMs. The viscosity of these fluids can be controlled reversibly by light due to photo-isomerization between the *trans* and *cis* configuration. Evidence for the structural transition is provided by UV-Vis spectroscopy, rheology, ¹H NMR and cryo-TEM measurements. Takashi et al. [15] reported an unusual viscoelasticity behaviour in aqueous solutions consisting of CTAB and an anionic photo-responsive amphiphile, sodium [4-(4-butylphenylazo)phenoxy]acetate (C4AzoNa). When C4AzoNa molecules were *trans*-isomers, spheroidal micelles were formed, whose viscosity was low. Irradiation of such a solution by UV light yielded a highly viscous gel consisting of wormlike micelles due to *trans*-to-*cis* transition of C4AzoNa. The drastic change in surfactant solution viscosity was attributed to the formation and disruption of wormlike micelles. The geometrical structural transformation of the azobenzene groups in the C4AzoNa molecules of the CTAB/C4AzoNa mixture would lead to a change in the critical packing parameter of the mixture, thereby inducing the morphological transformation of the aggregates from spheroidal micelles to WLMs.

To simplify and step up from the ternary systems, Abe and co-authors [16] proposed a photo-switchable system based on CTAB and sodium cinnamate (NaCin, Fig. 3.1b). They started from a “50 mM CTAB/50 mM NaCin” solution with η_0 of 66.0 Pa s and a typical viscoelastic response. Upon exposure to UV light with prolonged duration, G' and G'' gradually shifted towards higher frequencies, and finally the sample changed into a low-viscosity (2.1×10^{-3} Pa s) Newtonian liquid with a purely viscous response over the entire range of frequencies. This drastic change suggested that irradiation triggers a transition from entangled WLMs to smaller molecular aggregates, which could be ascribed to the photo-isomerization of NaCin molecules from *trans*-to-*cis*. Moreover, the environment of NaCin molecules examined by ¹H NMR before and after UV irradiation indicated that in its *cis* form, the carboxylic acid moiety of NaCin is in a more hydrophilic environment and thereby binds to the micellar interface less efficiently than its *trans*-isomer. The authors invoked a two-contemporaneous mechanism to explain the

viscosity change upon UV irradiation: the photo-isomerization of NaCin molecules solubilized within CTAB micelles induces the formation of the bulky *cis* generated and a subsequent increase in the distance between the polar CTA⁺ groups, and some of the UV irradiation-induced *cis*-Cin⁻ ions move further from the micellar surface, resulting in a transformation of WLMs to non-entangled rod-like or small spherical micelles. It is worth pointing out that the drawback of this system is a rather long reaction time (15–20 h) to reach the photo-stationary state.

While work on light-responsive WLMs in Abe's group [11, 12, 16] focused on the application of various UV/Vis responders to CTAB WLMs, Raghavan and co-workers achieved a photo-responsive rheological behaviour by concentrating on the commercially available photo-isomerizable ortho-methoxycinnamic acid (OMCA, Fig. 3.1b) combined with different surfactants. In particular, they reported two photo-rheological (PR) fluids, a photo-thinning [17] and a photo-thickening [18], both of which are based on the UV irradiation of *trans*-OMCA to its *cis* form. The former [17] is composed of *trans*-OMCA (neutralized by excessive NaOH) and CTAB, while the latter [18] also comprises *trans*-OMCA (neutralized by buffering to a mixture of equimolar of Na₂CO₃ and NaHCO₃ with pH = 10) but with a C22-tailed zwitterionic surfactant, erucyl dimethyl amidopropyl betaine (EDAB). The evolution of η_0 before and after UV irradiation for the former and the latter systems is presented in Fig. 3.2a, b, respectively. CTAB/*trans*-OMCA solutions in the correct ratio are strongly viscoelastic because of the presence of entangled networks of WLMs [17]. However, upon UV irradiation, the samples are converted into a low-viscosity, Newtonian fluid, and a drop in η_0 of more than 4 orders of magnitude is observed for a "60 mM CTAB/40 mM OMCA" solution (Fig. 3.2a). Structural information for the "5 mM CTAB/5 mM OMCA" sample before and after UV illumination obtained from small-angle neutron scattering (SANS) measurements shows a drastic decrease in micellar length from about 3,000 to 40 Å. Both the rheology and SANS reveal a microstructural transition from entangled WLMs to unentangled short rods. Instead, the EDAB/*trans*-OMCA solutions exhibit an opposite trend upon UV irradiation, namely, a substantial increase in viscosity (Fig. 3.2b) [18]. Specifically, the "50 mM CTAB/130 mM *trans*-OMCA" sample is a water like liquid with a viscosity close to that of water (1 mPa s). However, upon irradiating *trans*-OMCA into its *cis* form with UV light, the initial solution becomes a strongly viscoelastic fluid, with a substantial increase in η_0 (more than 10,000-fold). SANS measurements demonstrated that the microstructural basis for the photo-thickening involves light-induced WLMs growth. In both systems, the viscosity can be tuned through the composition of the mixture, as well as the duration of the photo-irradiation. This ingenious approach circumvents the need of specialized organic synthesis and can be readily replicated with inexpensive chemicals. In principle, the photo-isomerisation from *trans*-OMCA to *cis*-OMCA should be reversible; however, because the absorbance of the *cis* isomer is lower than that of the *trans* over most of the UV and Vis wavelength ranges, the change in viscosity was found to be irreversible [17].

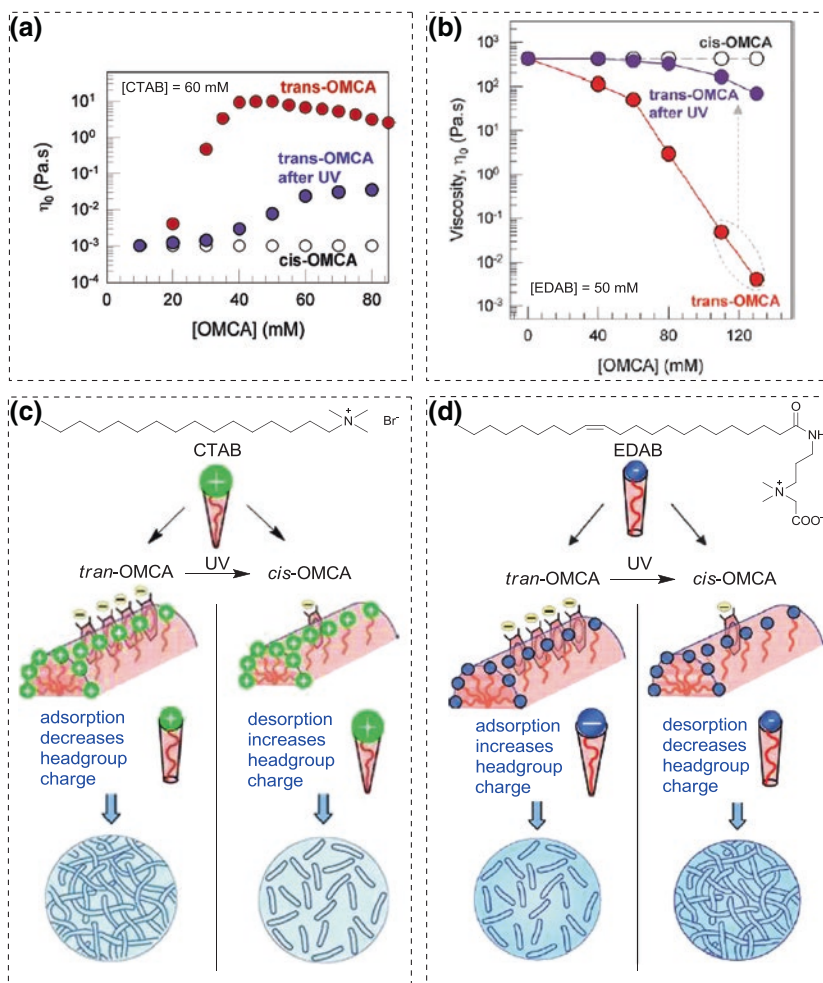


Fig. 3.2 Viscosity change upon UV irradiation (**a**, **b**) and the corresponding responsive mechanism (**c**, **d**) for photo-thinning WLMs based on “CTAB/OMCA” (**a**, **c**) and photo-thickening WLMs based on “EDAB/OMCA” (**b**, **d**). **a**, **c** Reprinted and adapted with permission from Ref. [17], respectively. Copyright (2007) American Chemical Society. **b**, **d** Reproduced and adapted from Ref. [18], respectively, by permission of The Royal Society of Chemistry

Since the two photo-responsive WLM systems are based on the same light-responder, an obvious question then is why their responsive behaviours show these opposite trends? To answer this question, one should take into account not only the photo-isomerisation of OMCA but also the different characteristics of the amphiphiles. In both cases, the key parameter controlling micellar growth is the critical packing parameter, which is dominated by the adsorption/desorption of OMC^- ions at the micellar interface. Compared to *trans*-OMCA, *cis*-OMCA binds to the micellar interface less effectively due to its unfavourable geometry

and higher hydrophilicity [17, 18]. Therefore, after UV irradiation, more OMC^- ions desorb from the micellar interface and join the bulk aqueous phase. Desorption occurs in both WLM systems, but why does it lead to a reverse effect on micellar growth? This can probably be attributed to the different characteristics of CTAB and EDAB. CTAB is a cationic surfactant and is well known to self-organize into WLMs upon the addition of various aromatic carboxylates and sulfonates, but cannot form WLMs without additives [19]. Instead, EDAB is a neutral zwitterionic surfactant and can form WLMs without any additive (Fig. 3.2b, $[\text{OMCA}] = 0 \text{ mM}$) [18]. Therefore, the photo-thinning and photo-thickening behaviours for the CTAB/OMCA and EDAB/OMCA systems can be explained based on the schematics of Fig. 3.2c, d, respectively. At the molecular level, *trans*- OMC^- binds to CTAB micellar interface effectively, decreasing the positive charge on the micellar surface and thereby the effective headgroup size. The “effective” geometry thus changes from a cone to a truncated cone shape, and hence the critical parameter becomes favourable to the formation of long, flexible WLMs that can form a three-dimensional network and impart viscoelasticity to the solution (Fig. 3.2c). Upon UV irradiation, *trans*- OMC^- is isomerized into *cis*- OMC^- and comes out of the micellar aggregates. The “effective” geometry changes into the “additive-free” cone shape, corresponding to the case of CTAB in the absence of additive. Accordingly, only short rods are formed and the viscoelasticity lost. *Trans*- OMC^- also binds to EDAB micelles more effectively than its *cis* isomer, but the binding increases the negative charge on the micellar interface headgroups (as confirmed by *zeta*-potential monitoring) and thereby the effective headgroup size. The “effective” geometry of the surfactant thus changes from a truncated cone to a cone shape (Fig. 3.2d). As a result, spheres or short cylinders are formed. When *trans*- OMC^- is photo-isomerized into *cis*- OMC^- , the latter desorbs from the micelles. The micellar surface charge decreases, and the molecular geometry changes into an “additive-free” truncated cone shape, similar to the case of EDAB in the absence of additive. Correspondingly, the micelles grow into long flexible WLMs, enhancing the viscoelasticity remarkably.

In order to improve the poor heat-transfer capabilities of conventional WLMs used in drag reduction, Zakin, Raghavan, and co-workers [6] developed light-responsive WLMs composed of the cationic surfactant ethoquad O/12 PG (EO_{12}) [a mixture of oleyl bis(2-hydroxyethyl)methyl ammonium chlorides (75 wt%) and propylene glycol (25 wt%)] and the sodium salt of *trans*-OMCA. Initially, these fluids contained numerous WLMs and, consequently, were strongly viscoelastic. Upon exposure to UV light, OMCA was photo-isomerized from its *trans*-to-*cis* configuration, causing a reduction in micellar size, as confirmed by Cryo-TEM, leading to a significant reduction in viscosity and viscoelasticity of the solution. Unfortunately, as for the other OMCA systems discussed above, the fluids are not photo-reversible.

Savelli et al. [20] examined the effect of surfactant structure on photo-sensitive fluids consisting of CTAB and *trans*-OMCA in a basic environment. The *trans*-to-*cis* photo-isomerization of *trans*-OMCA by UV light modified the molecular packing, reducing the length of the WLMs and thus inducing a reduction in viscosity,

following the mechanism exposed above. Examining the role of the counterion and the effect of headgroup size on this phenomenon, they concluded that “soft” counterions such as Br^- were the most favourable to the formation of WLMs, since the hydrophobic interaction rather than the electrostatic effect was the driving force in the association of *trans*-OMC $^-$ into micellar aggregates. They also found that the nature of the surfactant’s counterion influenced the response to UV light stimulus. Although all the $\text{CTA}^+\text{X}^-/\textit{trans}$ -OMCA systems were photo-sensitive, in the case of $(\text{CTA})_2^+\text{SO}_4^{2-}$ -based systems, a drastic decrease in viscosity and loss of the crossover point between G' and G'' was observed. When replacing the inorganic counterion X^- with OMC $^-$, the UV light response was even more effective. Interestingly, the substitution of the three methyl groups connected to the ammonium headgroup with three ethyl ones led to a large reduction in viscosity, because the increase of the headgroup size seemed to prevent the intercalation of the *trans*-OMC $^-$ -anions.

Hao’s team [4] developed a photo-responsive aqueous fluid system based on 150 mM tetradecyldimethylamine oxide (C_{14}DMAO) in the presence of 60 mM *trans*-paracoumaric acid (PCA). After 60 min of UV light irradiation, the *trans*-PCA turned into *cis*-PCA (Fig. 3.1b), inducing the bilayers vesicles to turn into WLMs, as verified by cryo-TEM observation. Macroscopically, both the oscillatory and Cole–Cole curves displayed a typical Maxwell model at low shear frequency, in agreement with the presence of WLMs.

Zheng et al. [21] created a photo-responsive fluid composed of 50 mM of an imidazolium-type surfactant 1-hexadecyl-3-methylimidazolium bromide and 50 mM of a commonly photo-sensitive aromatic compound *trans*-cinnamic acid (*trans*-CA, Fig. 3.1b) in aqueous solution. The binary system showed a viscoelastic response due to the formation of WLMs. After 100 min of UV irradiation, however, the CA molecules exhibited molecular photo-isomerization from *trans*- to *cis*-, which resulted in a change of WLMs into spherical micelles accompanied with drop in η_0 from 1.5 to 0.04 Pa s.

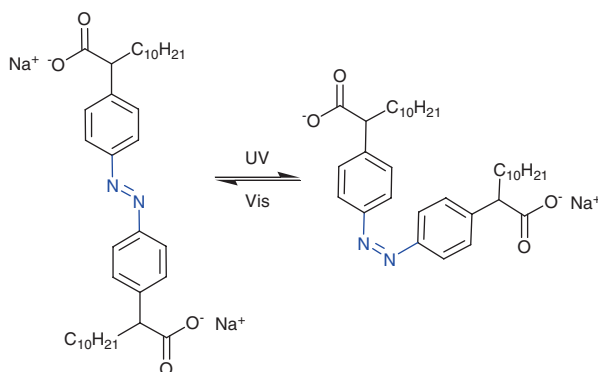


Fig. 3.3 Surfactant C_{12} -azo- C_{12} and its *trans/cis* isomerization regulated by UV/Vis irradiation

Scheven and co-workers [22] employed a multi-state photo-active compound, 2,4,4'-trihydroxychalcone (Ct, Fig. 3.1c), to impart photo-rheological properties to aqueous solutions of weakly entangled WLMs formed by CTAB in the presence of salicylic acid (HSal). Significantly, a very small amount of Ct ($[Ct]/[CTAB] = 1\%$) could give rise to a reversible photo-chromic and photo-rheological response of CTAB/HSal solutions, in the poorly entangled regime where viscoelastic properties depended strongly on the concentration of the intercalant. The presence of Ct led to a multiequilibrium system, involving several chemical species interconvertible by light and pH, and its UV-induced *trans-cis* isomerization indirectly caused changes in micellar morphology, which consequently affected the viscoelastic response of the micellar fluid. The observed photo-rheological phenomena were reversible by thermal relaxation, at a rate that can be tuned by adjusting the acidity of the solution. Light and thermal relaxation processes drove the transfer of the photo-sensitive compound Ct between CTAB WLMs and the bulk, respectively. The most remarkable feature of this light-sensitive system was that photo-chromism provided a direct visualization of the micellar state the fluid was in. In the initial absence of light, the sample appeared as lightly yellowish, and the corresponding steady shear viscosity at 0.5 s^{-1} is 7 Pa s . After 10 min of UV irradiation or sunlight illumination, the colour of the sample changed to a strong dark-orange, indicating the transformation of Ct to the flavylum cation AH^+ . Correspondingly, the viscosity dropped by a factor of 2 over the course of a few minutes. The dark-state viscosity could recover after removing illumination, but the time needed to reach equilibrium viscosity was as long as 40 min.

3.2 Light-responsive WLMs Formed by a Photo-sensitive Surfactant

Although some of the photo-chromic compounds described above are commercially available, the formulations of the above multi-component systems are quite complex. Thus, achieving the same effects in single-component systems is desirable. Nevertheless, this objective appears to be quite challenging since very few such systems have been reported so far.

To our knowledge, only Zhao and co-workers [23] have managed to develop a single-component light-responsive WLM system. They introduced an azobenzene group into the spacer of a gemini surfactant, sodium-2,2'-(diazene-1,2-diylbis(4,1-phenylene))-didodecanoate (C_{12} -azo- C_{12} , Fig. 3.3). A 60 mM aqueous solution of this surfactant produced a very viscous transparent fluid of orange colour, with η_0 as high as 734 Pa s , in conformity with the densely entangled networks observed by FF-TEM. This high viscosity can be attributed to the presence of the rigid azo-spacer, which kept the two hydrophobic tails apart, resulting in a “pseudo-volume” between them. This increased the packing parameter p , and thus favoured the formation of WLMs. Upon UV irradiation for 3 h, the *trans*-azobenzene group converted to the *cis* form, substantially reducing the distance between the two

ionic headgroups, and therefore breaking down the entangled network into small and discrete micelles. As a result, η_0 dropped by 5 orders of magnitude to ca. 0.007 Pa s. The viscosity recovered its original value upon irradiation with light for 2 h and for several cycles without any decay.

Light-responsive WLMs have been developed by either incorporating light-sensitive additives existing WLMs solutions or directly introducing light-sensitive functional moieties into surfactant molecules. The worms are constructed and destructed upon alternate UV/Vis light irradiation, which take advantage of dimerization, *cis*–*trans* isomerization, photo-scission, polymerization, or polarity changes of light-sensitive molecules.

References

1. Lin Y, Cheng X, Qiao Y, Yu C, Li Z, Yan Y, Huang J (2010) Creation of photo-modulated multi-state and multi-scale molecular assemblies via binary-state molecular switch. *Soft Matter* 6:902–908
2. Willerich I, Gröhn F (2010) Photoswitchable nanoassemblies by electrostatic self-assembly. *Angew Chem Int Ed* 49:8104–8108
3. Eastoe J, Vesperinas A (2005) Self-assembly of light-sensitive surfactants. *Soft Matter* 1:338–347
4. Wang D, Dong R, Long P, Hao J (2011) Photo-induced phase transition from multilamellar vesicles to wormlike micelles. *Soft Matter* 7:10713–10719
5. Müller N, Wolff T, von Büнау G (1984) Light-induced viscosity changes of aqueous solutions containing 9-substituted anthracenes solubilized in cetyltrimethylammonium micelles. *J Photochem* 24:37–43
6. Shi HF, Wang Y, Fang B, Talmon Y, Ge W, Raghavan SR, Zakin JL (2011) Light-responsive threadlike micelles as drag reducing fluids with enhanced heat-transfer capabilities. *Langmuir* 27:5806–5813
7. Wolff T, Emming C-S, Suck TA, von Büнау G (1989) Photorheological effects in micellar solutions containing anthracene-derivatives: a rheological and static low-angle light scattering study. *J Phys Chem* 93:4894–4898
8. Wolff T, Kerperin KJ (1993) Influence of solubilized 2,2,2-trifluoro-1-(9-anthryl)-ethanol and its photodimerization on viscoelasticity in dilute aqueous cetyltrimethylammonium bromide solutions. *J Colloid Interface Sci* 157:185–195
9. Lehnberger C, Wolff T (1999) Photorheological effects in aqueous micellar tetramethylammoniumhydrogen-2-dodecyl malonate via photodimerization of acridizinium bromide. *J Colloid Interface Sci* 213:187–192
10. Yu XL, Wolff T (2003) Rheological and photorheological effects of 6-alkyl coumarins in aqueous micellar solutions. *Langmuir* 19:9672–9679
11. Sakai H, Orihara Y, Kodashima H, Matsumura A, Ohkubo T, Tsuchiya K, Abe M (2005) Photoinduced reversible change of fluid viscosity. *J Am Chem Soc* 127:13454–13455
12. Matsumura A, Sakai K, Sakai H, Abe M (2011) Photoinduced increase in surfactant solution viscosity using azobenzene dicarboxylate for molecular switching. *J Oleo Sci* 60:203–207
13. Yan H, Long Y, Song K, Tung C-H, Zheng L (2014) Photo-induced transformation from wormlike to spherical micelles based on pyrrolidinium ionic liquids. *Soft Matter* 10:115–121
14. Lu Y, Zhou T, Fan Q, Dong J, Li X (2013) Light-responsive viscoelastic fluids based on anionic wormlike micelles. *J Colloid Interface Sci* 412:107–111
15. Takahashi Y, Yamamoto Y, Hata S, Kondo Y (2013) Unusual viscoelasticity behaviour in aqueous solutions containing a photoresponsive amphiphile. *J Colloid Interface Sci* 407:370–374

16. Sakai H, Taki S, Tsuchiya K, Matsumura A, Sakai K, Abe M (2012) Photochemical control of viscosity using sodium cinnamate as a photoswitchable molecule. *Chem Lett* 41:247–248
17. Ketner AM, Kumar R, Davies TS, Elder PW, Raghavan SR (2007) A simple class of photorheological fluids: surfactant solutions with viscosity tunable by light. *J Am Chem Soc* 129:1553–1559
18. Kumar R, Raghavan SR (2009) Photogelling fluids based on light-activated growth of zwitterionic wormlike micelles. *Soft Matter* 5:797–803
19. Dreiss CA (2007) Wormlike micelles: where do we stand? Recent developments, linear rheology and scattering techniques. *Soft Matter* 3:956–970
20. Baglioni P, Braccalenti E, Carretti E, Germani R, Goracci L, Savelli G, Tiecco M (2009) Surfactant-based photorheological fluids: effect of the surfactant structure. *Langmuir* 25:5467–5475
21. Li J, Zhao M, Zhou H, Gao H, Zheng L (2012) Photo-induced transformation of wormlike micelles to spherical micelles in aqueous solution. *Soft Matter* 8:7858–7864
22. Pereira M, Leal CR, Parola AJ, Scheven UM (2010) Reversible photorheology in solutions of cetyltrimethylammonium bromide, salicylic acid, and trans-2,4,4'-trihydroxychalcone. *Langmuir* 26:16715–16721
23. Song BL, Hu YF, Zhao JX (2009) A single-component photo-responsive fluid based on a gemini surfactant with an azobenzene spacer. *J Colloid Interface Sci* 333:820–822

Chapter 4

pH-Responsive Wormlike Micelles

Abstract pH has been known for a long time and frequently used as a facile, inexpensive trigger to control molecular assemblies and thereby the bulk properties of the corresponding solutions. pH-responsive WLMs have been developed not only based on commercially available surfactants in the presence of hydrotropes, but also through the design of surfactant mixture composition and surfactant architecture. This chapter introduces pH-responsive wormlike micellar systems fabricated through the introduction of hydrotropes to conventional surfactant-based wormlike micellar systems, in appropriate mixtures of surfactants, or by modifying the surfactant molecular architecture with pH-sensitive functional groups, either the hydrophilic head or the hydrophobic tail. It is worth pointing out that a disadvantage of this trigger is that the cyclic addition of acid and base may deteriorate the repeated use of the wormlike micellar systems.

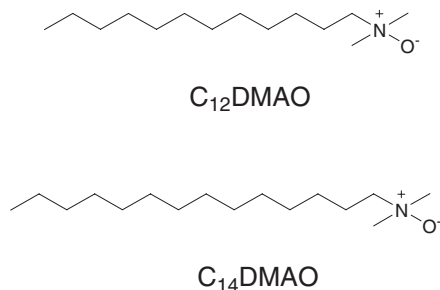
Keywords pH-responsive WLMs · pH-switchable WLMs · Wormlike micelles · Viscoelasticity · Acid/base

In contrast to redox and light triggers, pH has been known for a long time and frequently used as an easy to use and economical trigger to control molecular assemblies and hence the bulk properties of their solutions [1–17]. pH-responsive WLMs have been developed not only based on commercially available surfactants such as zwitterionic alkyldimethylamine oxide (C_n DMAO) [2–6] and cationic CTAB in the presence of hydrotropes [7–10], but also through the design of surfactant mixture composition [11, 12] and surfactant architecture [13–17].

4.1 pH-Responsive WLMs Based on Zwitterionic Surfactants

As typical zwitterionic surfactants, alkyldimethylamine oxides, C_n DMAO (Fig. 4.1), carry no net charge at neutral pH and thereby the repulsion between surfactant headgroups is very weak. They spontaneously self-organize into long,

Fig. 4.1 pH-responsive zwitterionic WLM systems, C_n DMAO



flexible wormlike micelles without the help of any additives because of the weak repulsion between the headgroups [18–20]. However, at a pH below a critical value, the isoelectric point, they become positively charged. Changes in pH induce significant modifications to their self-assembly, allowing a facile manipulation of the micellar architectures, and hence of the bulk properties [2–6]. As extensively documented [21–27], near the point of half-ionization ($\alpha = 0.5$, where α is the degree of ionization), dodecyltrimethylamine oxide (C_{12} DMAO) exhibits a characteristic maximum in micellar size and weight [21–24], subsequently in bulk viscosity [25], and a minimum in the critical micellar concentration (CMC) [24, 26] and surface tension at the CMC [26, 27].

Rathman and Christian [28] observed that infrared spectra in the half-ionization state reveal a disappearance of the $-\text{CH}_2-$ and $-\text{CNO}$ bending bands and a minimum in the frequency of the C–H stretching band. This indicates the formation of hydrogen bonds between protonated and unprotonated C_{12} DMAO molecules, which attain a maximum, while the number of unprotonated molecules equal the protonated ones [24, 29, 30]. The strong intermolecular attraction induces the formation of hydrogen-bonded dimers with a reduction in effective headgroup area per micellized surfactant [5]. Just like gemini surfactants, the dimers favour a low surface curvature, and consequently the formation of long WLMs [23, 29, 31]. As a result, a transition from spheres to longer worms is achieved when α approaches 0.5 [26, 29].

Similar to C_{12} DMAO, the ionization of C_{14} DMAO [3] also has a remarkable effect on the micellar length and thereby the viscoelasticity. It was observed that η_0 reached a maximum at the half-ionized state ($\alpha = 0.5$) because of double-tailed monomer formation, two orders of magnitude higher than that of the non-ionic ($\alpha = 0$) and cationic species ($\alpha = 1$). Later, the reversible transition of oleyldimethylamine oxide micellar solution from WLMs to vesicles was achieved by increasing the pH (and thereby the degree of protonation) [8]. More precisely, a micelle-to-vesicle conversion took place in the following sequence: growth of worms ($\alpha < 0.2$), fused networks ($\alpha = 0.3$), coexistence of worms and vesicles ($\alpha = 0.4$), and coexistence of vesicles and lamellae ($\alpha = 0.5$) [4].

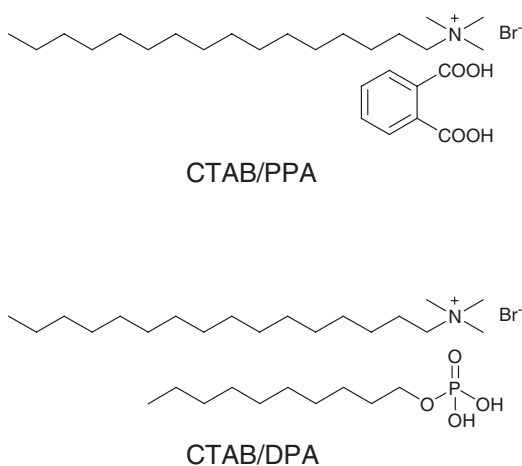
Besides the pH-responsive WLMs formed by commercially available alkyldimethylamine oxide, tailor-made *p*-dodecyloxybenzyltrimethylamine oxide

(*pDoAO*) [6] was also reported to show pH responsiveness in terms of micellar length and hence viscoelasticity. Similarly, pH-responsive micellar aggregates were developed by Ghosh et al. [12] using the amino acid-based zwitterionic surfactant *N*-(*n*-dodecyl-2-aminoethanoyl)-glycine ($C_{12}Gly$) in the presence of the anionic surfactant SDS. Fluorescence depolarization in combination with DLS, TEM, and fluorescence showed a transition between vesicles, spheres, and branched worms, as the pH or the surfactant composition was altered.

4.2 pH-Responsive WLMs Based on Cationic Surfactants in the Presence of an Acid

pH-Responsive WLMs can also be fabricated through the introduction of hydrotropes to cationic surfactant systems [7–10] (Fig. 4.2). Using CTAB as an amphiphile and potassium phthalic acid as a responder, a simple and effective strategy to prepare pH-responsive WLMs was developed by Huang and co-workers [7]. The fluid can be switched between gel-like and water-like states within a narrow pH range. Experimental results revealed a microstructural transition from long worms to short rods upon increasing the pH from 3.90 to 5.35. Based on the combination study by means of NMR, UV/Vis, and fluorescence anisotropy, the authors proposed that the pH responsiveness originated from the decreased binding ability of the hydrotrope to the surfactant as the pH increased, which affected the interfacial curvature, thus resulting in the formation of short rodlike micelles. This facile way of preparing pH-responsive WLMs can also be applied to other cationic surfactants and a variety of other hydrotropes have been reported by the same authors and other research groups [8–10].

Fig. 4.2 pH-responsive cationic WLM systems based on CTAB in the presence of an acid



Simply varying surfactant composition in appropriate mixtures represents another facile strategy towards pH-responsive WLMs [11, 12]. Lin et al. [11] developed pH-regulated surfactant self-assemblies by mixing CTAB and decylphosphoric acid (DPA) at a 1:1 molar ratio. Upon increasing the pH, the 1:1 cationic/anionic pair turned into a 1:2 cationic/anionic pair, which showed a weaker aggregating ability due to the steric effect and the larger hydration effect. Consequently, the self-assembled organization could be effectively tailored between spheres, worms, vesicles, and lamellar structures, thereby in turn controlling the viscoelasticity of the solution.

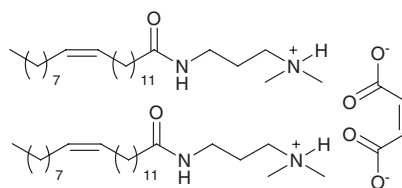
4.3 pH-Responsive WLMs Obtained from the Design of Surfactant Architecture

The design of new chemical structures, for instance, by introducing a pH-sensitive tertiary amine group to either surfactant headgroup [1, 13–15] or alkyl tail [16, 17] (Fig. 4.3), can also serve as a method to fabricate pH-responsive WLMs [1, 13–17]. In the latter case, the surfactant is regarded as a “bolaform” surfactant since it has a hydrophilic group in both terminals.

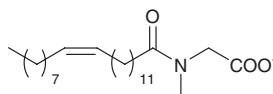
Chu and Feng [1, 13] developed a pH-switchable WLM system by using the neutralized surfactant from the insoluble long-chain tertiary amine *N*-erucamidopropyl-*N,N*-dimethylamine (UC22AMPM) and added maleic acid with a 2:1 molar ratio (named EAMA, Figs. 4.3 and 4.4). It was found that the solution exhibited a reversible Newtonian-to-viscoelastic transition with an increase in η_0 of five orders of magnitude when altering the pH from 6.20 to 7.29, which could be ascribed to the partial unprotonation of the quaternary ammonium headgroup. Correspondingly, the micellar aggregate showed a structural transformation from wormlike micelles to spheres. Upon further increasing the pH above ~ 9.80 , the thickening agent UC22AMPM precipitated from the bulk solution, allowing an easy recycling of the material [13]. Compared with its counterpart formed by replacing the maleic acid with a monoacid, for example hydrochloric acid, the EAMA system in its “on” state showed a much higher η_0 because of its peculiar “gemini-like” chemical structure [13]. In brief, these pH-switchable WLMs enable a facile, cost-effective, and remarkable control of the viscoelasticity of the solution, as well as the recycling of the thickening agent UC22AMPM, by simply altering the pH above 9.80.

The sugar-based (reduced glucose) gemini surfactant GS3 was also proven to show pH responsiveness [14, 15]. Specifically, a vesicle-to-worm transition was observed within a narrow pH region from 6.0 to 5.6 and a worm-to-sphere transformation at even lower pH. In the vesicular pH region (pH > 6.0), the vesicles are positively charged at pH < 7.0 with a good colloidal stability [14]. However, close to pH 7.0, the vesicles become unstable and rapidly flocculate and eventually sediment out of the solution. It was suggested that the micellization was driven by increased electrostatic repulsions caused by the protonation of the tertiary amine group. The nature of the sugar and spacer was found to have little influence on this process [15].

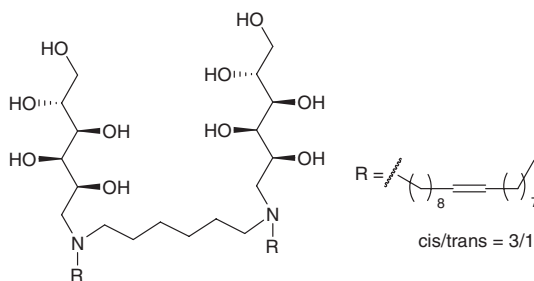
Fig. 4.3 pH-responsive WLM systems obtained through the design of specific surfactant architectures



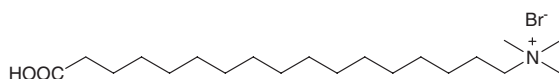
EAMA



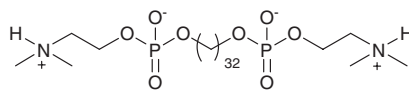
EMAA



GS3



HOOC-CTAB

Me₂PE-C32-Me₂PE

Yang et al. [32] synthesized a C22-tailed sarcosinate anionic surfactant, 2-(*N*-erucacyl-*N*-methyl amido) acetate (EMAA) and observed that its solutions display a pH-controllable transition from micelles to vesicles. In rheological experiments, when increasing the pH from 6.43 to 7.36, η_0 showed a substantial increase from 3.8 to 222.5 Pa s.

Apart from introducing a pH-responder to a conventional surfactant hydrophilic headgroup, pH-responsive WLMs can also be crafted by substituting the

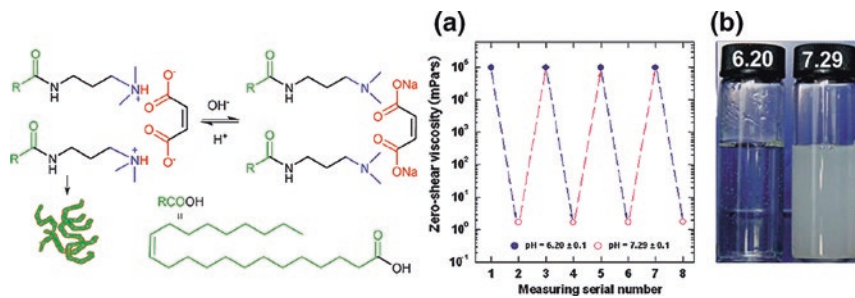


Fig. 4.4 pH-switchable WLM systems obtained from the “pseudo-gemini” structure formed by N-erucamidopropyl-N,N-dimethylamine (UC22AMPM) and added maleic acid with a 2:1 adapted from Ref. [1] by permission of The Royal Society of Chemistry

ω -position of the hydrophobic tail with a pH-sensitive group [16, 17]. Jaeger et al. [16] synthesized and investigated a bolaform surfactant, ω -carboxyl hexadecyltrimethylammonium bromide (HOOC-CTAB), and found that it formed ribbons at pH 6.8, rods at pH 2.2, and worms at pH 11.5.

Recently, the pH-responsive behaviour of another bolaamphiphile, dotriacotane-1,32-diyl-bis[2-(demethylammonio)ethyl]phosphate (Me₂PE-C32-Me₂PE), was reported by Graf et al. [17]. It was observed that the protonation of the headgroups depended on the pH and influenced the self-organized structures. At low pH, the headgroups were zwitterionic and stable WLMs hydrogels were formed, whereas, at high pH, the headgroups were negatively charged and the length of the worms diminished as did the stability of the gel networks.

pH-responsive WLMs can be fabricated through a number of strategies, including by utilizing commercially available zwitterionic alkyldimethylamine oxides, cationic surfactants in the presence of different hydrotropes, tuning surfactant composition in well-designed mixtures, as well as through bespoke modification of surfactant structure. However, it is worth noting that by-products (for instance NaCl) may be accumulated in the system during the repeated addition of acid and base, which will eventually affect the reversibility of the process.

References

1. Chu Z, Feng Y (2010) pH-switchable wormlike micelles. *Chem Commun* 46:9028–9030
2. Kawasaki H, Souda M, Tanaka S, Nemoto N, Karlsson G, Almgren M, Maeda H (2002) Reversible vesicle formation by changing pH. *J Phys Chem B* 106:1524–1527
3. Maeda H, Yamamoto A, Souda M, Kawasaki H, Hossain KS, Nemoto N, Almgren M (2001) Effects of protonation on the viscoelastic properties of tetradecyldimethylamine oxide micelles. *J Phys Chem B* 105:5411–5418
4. Maeda H, Tanaka S, Ono Y, Miyahara M, Kawasaki H, Nemoto N, Almgren M (2006) Reversible micelle-vesicle conversion of oleyldimethylamine oxide by pH changes. *J Phys Chem B* 110:12451–12458

5. Majhi PR, Dubin PL, Feng X, Guo X (2004) Coexistence of spheres and rods in micellar solution of dodecyltrimethylamine oxide. *J Phys Chem B* 108:5980–5988
6. Brinchi L, Germani R, Profio PD, Marte L, Savelli G, Oda R, Berti D (2010) Viscoelastic solutions formed by worm-like micelles of amine oxide surfactant. *J Colloid Interface Sci* 346:100–106
7. Lin Y, Han X, Huang J, Fu H, Yu C (2009) A facile route to design pH-responsive viscoelastic wormlike micelles: smart use of hydrotropes. *J Colloid Interface Sci* 330:449–455
8. Yan H, Zhao M, Zheng L (2011) A hydrogel formed by cetylpyrrolidinium bromide and sodium salicylate. *Colloid Surf A-Physicochem Eng Asp* 392:205–212
9. Verma G, Aswal VK, Hassan P (2009) pH-responsive self-assembly in an aqueous mixture of surfactant and hydrophobic amino acid mimic. *Soft Matter* 5:2919–2927
10. Ali M, Jha M, Das SK, Saha SK (2009) Hydrogen-bond-induced microstructural transition of ionic micelles in the presence of neutral naphthols: pH dependent morphology and location of surface activity. *J Phys Chem B* 113:15563–15571
11. Lin Y, Han X, Cheng X, Huang J, Liang D, Yu C (2008) pH-regulated molecular self-assemblies in a cationic–anionic surfactant system: from a “1-2” surfactant pair to a “1-1” surfactant pair. *Langmuir* 24:13918–13924
12. Ghosh S, Khatua D, Dey J (2011) Interaction between zwitterionic and anionic surfactants: spontaneous formation of zwitterionic vesicles. *Langmuir* 27:5184–5192
13. Smart fluids: switchable viscosity. NPG Asia Mater research highlight (2011). doi:[10.1038/asiamat.2011.29](https://doi.org/10.1038/asiamat.2011.29)
14. Johnsson M, Wagenaar A, Engberts JBFN (2003) Sugar-based gemini surfactant with a vesicle-to-micelle transition at acidic pH and a reversible vesicle flocculation near neutral pH. *J Am Chem Soc* 125:757–760
15. Johnsson M, Wagenaar A, Stuart MCA, Engberts JBFN (2003) Sugar-based gemini surfactants with pH-dependent aggregation behavior: vesicle-to-micelle transition, critical micelle concentration, and vesicle surface charge reversal. *Langmuir* 19:4609–4618
16. Jaeger DA, Li G, Subotkowski W, Carron KT (1997) Fibers and other aggregates of omega-substituted surfactants. *Langmuir* 13:5563–5569
17. Graf G, Drescher S, Meister A, Dobner B, Blume A (2011) Self-assembled bolaamphiphile fibers have intermediate properties between crystalline nanofibers and wormlike micelles: formation of viscoelastic hydrogels switchable by changes in pH and salinity. *J Phys Chem B* 115:10478–10487
18. Hoffmann H (1994) Viscoelastic surfactant solutions. In: Herb CA, Prud’homme RK (eds) *Structure and flow of surfactant solution*. ACS Symp Ser 578. American Chemical Society, Washington, DC, pp 2–31
19. Hashimoto K, Imae T (1991) Rheological properties of aqueous solutions of alkyl-dimethylamine and oleyldimethylamine oxides—spinnability and viscoelasticity. *Langmuir* 7:1734–1741
20. Ono Y, Shikata T (2005) Dielectric behavior of aqueous micellar solutions of betaine-type surfactants. *J Phys Chem B* 109:7412–7419
21. Ikeda S, Tsunoda M, Maeda H (1979) Effects of ionization on micelles size of dimethyldodecylamine oxide. *J Colloid Interface Sci* 70:448–455
22. Herrmann KW (1962) Nonionic–cationic micellar properties of dimethyldodecylamine oxide. *J Phys Chem* 66:295–300
23. Kaimoto H, Shoho K, Sasaki S, Maeda H (1994) Aggregation numbers of dodecyltrimethylamine oxide micelles in salt-solutions. *J Phys Chem* 98:10243–10248
24. Maeda H (1996) Dodecyltrimethylamine oxide micelles: stability, aggregation number and titration properties. *Colloid Surf A-Physicochem Eng Asp* 109:263–271
25. Chang DL, Rosano HL (1984) Interaction of long-chain dimethylamine oxide with sodium dodecyl sulfate in water. In: Rosen MJ (ed) *Structure-performance relationships in surfactants*. ACS Symp Ser 253. American Chemical Society, Washington, DC, pp 129–140
26. Maeda H, Kakehashi R (2000) Effects of protonation on the thermodynamic properties of alkyl dimethylamine oxides. *Adv Colloid Interface Sci* 88:275–293

27. Maeda H, Muroi S, Ishii M, Kakehashi R, Kaimoto H, Nakahara T, Motomoura K (1995) Effects of ionization on the critical micelle concentration and the surface excess of dodecyltrimethylamine oxide in salt solutions. *J Colloid Interface Sci* 175:497–505
28. Rathman JF, Christian SD (1990) Determination of surfactant activities in micellar solutions of dimethyldodecylamine oxide. *Langmuir* 6:391–395
29. Zhang H, Dubin PL, Kaplan JI (1991) Potentiometric and dynamic light scattering studies of micelles of dimethyldodecylamine oxide. *Langmuir* 7:2103–2107
30. Mille M (1981) Effect of nearest neighbor interactions on surface titrations. *J Colloid Interface Sci* 81:169–179
31. Imae T, Hayashi N (1993) Electrophoretic light scattering of alkyldimethylamine and oleyldimethylamine oxide micelles. *Langmuir* 9:3385–3388
32. Yao R, Qian J, Li H, Yasin A, Xie Y, Yang H (2014) Synthesis and high-performance of a new sarcosinate anionic surfactant with a long unsaturated tail. *RSC Adv* 4:2865–2872

Chapter 5

CO₂-Responsive Wormlike Micelles

Abstract Despite its extensive use, pH as a trigger has several drawbacks including the need of stoichiometric quantities of acid and base, the accumulation of by-products, and costly disposal. In this context, the weak acid gas, CO₂, represents an interesting alternative because it is inexpensive, relatively benign, and can be easily removed, thus is free of contamination. In addition, CO₂ can be completely removed by streaming an inert gas into the solution and/or mild heating, which allows the CO₂-reactive functional groups to resort to their initial forms. Presented in this chapter are four classes of CO₂-responsive wormlike micellar systems, three of which are based on amines, either located on the hydrotrope molecules or on the skeleton of long-chain surfactants. Carboxylate-based anionic wormlike micelles are also sensitive to CO₂, but the pre-formed wormlike micelles are ruptured by the presence of CO₂ and thus the macroscopic viscosity drops. The “CO₂/air” switchable system based on a C22-tailed tertiary amine is particularly attractive for practical applications because it provides a cost-effective, environment-friendly, and low-energy way to regulate the viscoelasticity in aqueous media simply by bubbling CO₂ or air at ambient temperature, without the need of heat or the use of an inert gas such as N₂ or Ar.

Keywords CO₂-responsive • CO₂-switchable • Wormlike micelles • Long-chain amine • “Clean” trigger

Despite its extensive use, pH as a trigger has several drawbacks, as described in Chap. 4, because acids or bases must be used in stoichiometric quantities and build up in the system after each cycle. In addition, their production and disposal are environmentally and economically costly [1]. A desirable alternative should be inexpensive, relatively benign, and easily removed so that the reverse state could be achieved by trigger removal rather than the addition of another trigger. In this context, the free, clean CO₂ resource represents an ideal candidate, since the function of CO₂ as a trigger is essentially similar to that of pH but is more easily removed and essentially free of contamination, with the production of bicarbonate

salts in water, thus potentially providing better properties to the “smart” system. CO₂ can be completely removed by streaming an inert gas into the solution and/or mild heating, which allows the CO₂-reactive functional groups to resort to their initial forms. This robust switchability implies that the CO₂ switch “on” and “off” cycles can be repeated many times without accumulation of the by-products [2]. Furthermore, CO₂ is an endogenous non-toxic metabolite (dissolved CO₂ in plasma is normally about 1.2 mM [3]) in cells and has good biocompatibility and membrane permeability [4], thus presenting great potential for applications in biotherapy [5–8].

Over the last decade, CO₂ has played an increasingly active role in the fabrication of switchable surfactants [9, 10], solutes [11], polymers [5–8, 12–14], ionic liquids [15–18], organogels [19, 20], as well as nanohybrids [21], following on from the pioneering work of Jessop team on CO₂-switchable solvents in 2005 [22]. The common feature of all of these CO₂-sensitive compounds is that they possess at least one basic group—principally amidine [6, 9, 13, 17, 21, 23], guanidine [10, 23], or amine [5, 7, 12, 24]—to react with CO₂ in the presence of water. Among these organobases, guanidine is relatively less used because of its “superbase” character which makes the “switching off” difficult after reaction with CO₂ [10]. Although their basicity is weaker than that of guanidine, amidine-containing compounds are usually difficult to be synthesized and prone to hydrolytic instability [25, 26]. Instead, as mild, stable, and readily available organobases, amines are the most commonly used CO₂-switchable functional groups. Generally, their protonated products, especially those generated from the reaction of tertiary amines with CO₂ in a wet or aqueous environment, are unstable and easily release CO₂ to return to the original state, even at room temperature.

Based on these considerations, three strategies are presented in this chapter for the design of CO₂-switchable WLMs originating from amine-based compounds, as well as a long-chain carboxylate anionic surfactant.

5.1 CO₂-Switchable WLMs from Commodity Anionic Surfactants and an Amine Hydrotrope

As stated in Sect. 4.3, we have observed pH-switchable behaviour from the wormlike micellar system composed of a C22-tailed tertiary amine, *N*-erucamidopropyl-*N,N*-dimethylamine (UC22AMPM), and maleic acid at a 2:1 molar ratio [27]. When maleic acid is added into UC22AMPM aqueous solution, the latter is protonated to form quaternary ammonium ions, two of which interact electrostatically with one maleic di-acid molecule, forming a “pseudo” ultra-long-chain “gemini” surfactant. The so-formed “pseudo-gemini” self-assemble into long wormlike arrays and then entangle with each other into a transient network, which is responsible for the remarkably enhanced solid-like behaviour.

A natural further development of this concept would be to develop a CO₂-switchable “pseudo-gemini” system with a common surfactant and a

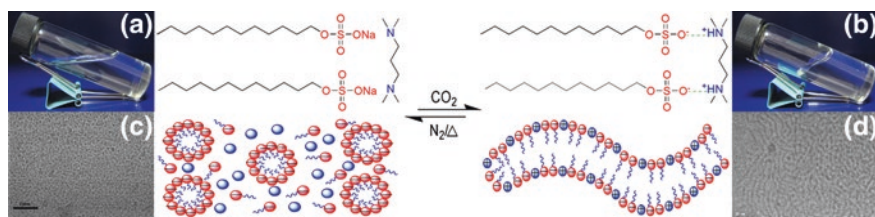


Fig. 5.1 Schematic illustration of the CO₂ switchability of the “pseudo-gemini” model composed of SDS and TMPDA. Adapted with permission from Ref. [28]. Copyright (2013) American Chemical Society

CO₂-sensitive hydrotrope. Thus, we chose the commodity anionic surfactant, sodium dodecyl sulphate (SDS), in combination with *N,N,N',N'*-tetramethyl-1,3-propanediamine (TMPDA, Fig. 5.1) to form a mixture in aqueous solution at the specific stoichiometric ratio of 2:1 (referred as “SDS–TMPDA”). It was found that the mixtures can reversibly be switched between either viscoelastic or low-viscosity fluids through several cycles of alternate bubbling and removal of CO₂ [28].

As exhibited in Fig. 5.1, the initial 250 mM SDS–TMPDA aqueous solution has low viscosity (Fig. 5.1a), while the CO₂-saturated mixture solution (SDS–TMPDA–CO₂) shows a substantially higher viscosity (Fig. 5.1b). More quantitatively, the viscosity of 250 mM SDS–TMPDA is around 1.5 mPa s, irrespective of the shear rate, thus showing a typical Newtonian fluid behaviour. However, after introducing CO₂, the zero-shear viscosity η_0 increases to 4,000 mPa s and shear-thinning behaviour is evidenced (Fig. 5.2a). In addition, before bubbling CO₂, the η_0 – C curve (Fig. 5.2b) of the mixture solution shows no obvious change over the whole concentration range, concurrent with the presence of spheric micelles only (Fig. 5.1c). Instead, after exposure to CO₂, η_0 increases linearly in the dilute regime ($C < C^*$) in accordance with the Einstein equation $\eta_0 = \eta_{\text{water}}(1 + KC)$, where K is of the order of unity; in the semi-dilute region ($C > C^*$), wormlike micelles are formed and start entangling (Figs. 5.1d and 5.2c), forming a dynamic transient network and thus imparting substantial viscosity enhancement to the solutions. In this case, η_0 increases exponentially by several orders of magnitude following the scaling law $\eta_0 \propto C^{2.8}$.

The dynamic rheogram (Fig. 5.2c) of 250 mM SDS–TMPDA–CO₂ aqueous solution also suggests the formation of WLMs, with an evident viscoelastic response: the behaviour is elastic (storage modulus $G' > \text{loss modulus } G''$) at high frequencies or short timescales, while it is viscous ($G' < G''$) at lower frequencies. Moreover, G' and G'' are well fitted by the Cole–Cole model in the low-to-medium frequency range, but deviation occurs at high frequencies owing to non-repetitive effects, further supporting the formation of WLMs [28].

Notably, the viscosity of SDS–TMPDA solutions can repeatedly be switched “on and off” when CO₂ is cyclically bubbled into and removed from the solution; these changes are easily cycled more than four times without any deterioration of the response (Fig. 5.2d).

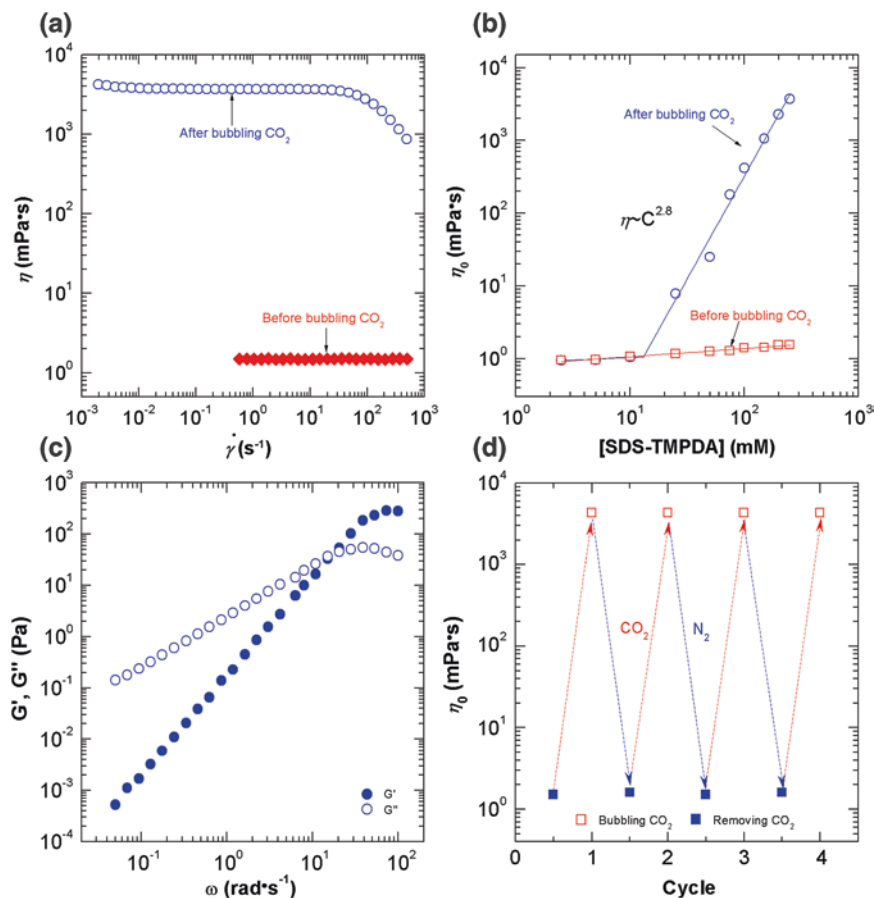


Fig. 5.2 **a** Steady-state rheogram of a 250 mM SDS–TMPDA solution. **b** Concentration dependence of the zero-shear viscosity. **c** Dynamic rheogram. **d** Reversible switchability over four repetitive cycles of alternately bubbling CO₂ and N₂. The gas flow rate is fixed at 0.1 L min⁻¹; CO₂ is bubbled at 25 °C, while N₂ bubbling is accompanied by heating at 75 °C. Adapted with permission from [28]. Copyright (2013) American Chemical Society

When streaming CO₂ into the 250 mM SDS–TMPDA solution, the conductivity rises evidently from 17.5 to 27.0 mS cm⁻¹, accompanied by a decrease in pH from approximately 12 to 8, indicative of the formation of protonated species from TMPDA. ¹H NMR characterization of the individual species, and the mixture with and without CO₂ show chemical shifts of the protons connected to the N atoms in TMPDA shift downfield, further confirming the protonation of TMPDA in the mixture, and ¹³C NMR spectrum shows that the protonated species of TMPDA belong to the ammonium hydrogen carbonate [28].

The microstructure morphology of SDS–TMPDA mixture was predicted by the packing parameter theory. For SDS alone in pure water, the packing parameter P

is 0.34, slightly above 1/3, suggesting that the formation of predominantly spherical micelles is favoured. This is in good line with small-angle neutron-scattering results showing that SDS forms ellipsoidal micelles in water [29]. The packing parameter of SDS–TMPDA mixtures without CO₂ was estimated at 0.11, thus indicating a preferential packing of the surfactants into spherical micelles. Upon treatment with CO₂, the solution pH decreases, inducing the protonation of the tertiary amine groups of TMPDA into ammonium ions. This results in one protonated TMPDA molecule acting as a spacer linking two SDS molecules non-covalently by electrostatic attraction between the positive ammonium group and negative sulphate group, forming a dynamic “pseudo-gemini” structure (Fig. 5.1), resulting in viscosity enhancement. In this case, the calculated P is 0.45, just falling in the range of 1/2–1/3, which is consistent with the formation of wormlike micelles. This agrees well with the prediction for gemini surfactants with short spacers that possess wedge-like molecular geometries and tend to aggregate into cylindrical micelles [30]. After removing CO₂, the ammonium groups are deprotonated back into tertiary amines, thus reducing the electrostatic attraction and dissociating the pseudo-gemini structure, restoring the viscosity to the water-like level due to the rupture of the wormlike micelles into spherical ones. As explained above, the rheological properties can be reversibly tuned by cyclically bubbling and removing CO₂. The morphological structures underlying the macroscopic changes correlate well with the predictions from the “packing parameter” theory.

The molar ratio of SDS to TMPDA plays a crucial role in determining the viscoelasticity of the mixture solutions. When bubbling CO₂ into pure SDS or TMPDA solution, no viscosity enhancement is evidenced, implying no WLMs are formed. When CO₂ is introduced into the mixtures, the peak of both viscosity and shear modulus is obtained at a ratio of 2:1 (Fig. 5.3) [28], indicating that this ratio is the optimum value for the “gemini” structure. In fact, this is consistent with the theoretical

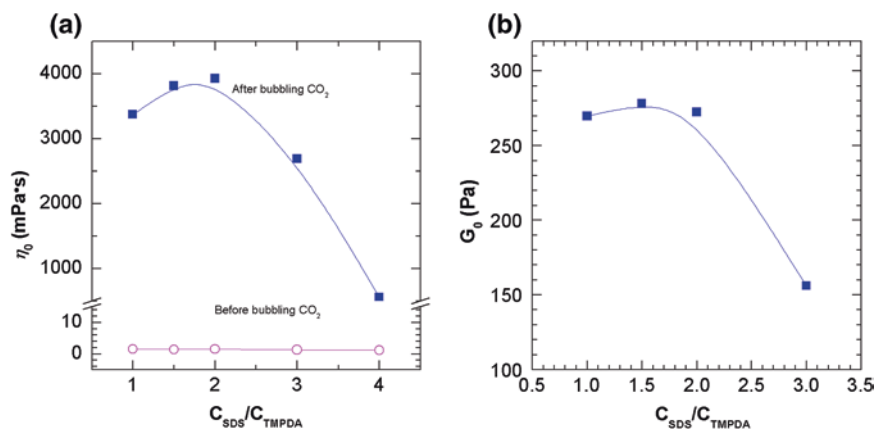


Fig. 5.3 An optimum molar ratio of 2:1 is found to achieve **a** zero-shear viscosity and **b** plateau modulus peaks for the 240 mM “SDS–TMPDA”. Reprinted with permission from [28]. Copyright (2013) American Chemical Society

scenario: for $C_{\text{SDS}}/C_{\text{TMPDA}} \leq 2$, all SDS molecules participate in the formation of pseudo-gemini surfactants because of the excess of TMPDA molecules, but the number of “pseudo-gemini” surfactants is still lower than at 2:1. On the other hand, when the molar ratio exceeds 2, the number of SDS molecules is in excess, implying less pseudo-gemini surfactants and thus less wormlike micelles formed, resulting in loose entanglements, and, as a result, both η_0 and G_0 decrease accordingly.

It is worth pointing out that the protonated organic TMPDA serves both as a spacer to link two C12 hydrophobic tails and two positive counterions neutralizing the negative sulphate moieties. As a result, the availability of low-cost, commercial SDS and TMPDA not only avoids the cumbersome organic synthesis of covalently linked gemini surfactants, but also paves the way for the fabrication of smart wormlike micelles by “tailoring” the pseudo-gemini structure with different tail lengths or different hydrophilic headgroups of anionic surfactants, such as alkyl sulphate, alkyl carboxylate, or even alkyl phosphonate.

Using a similar idea, Su et al. [31] demonstrated the reversible conversion of highly viscoelastic wormlike micellar solutions into low-viscosity spherical micelles when bubbling CO₂ in a mixture of sodium octadecyl sulphate (C18SNa) and 2-(dimethylamino) ethanol (DMAE). The mixture of 200 mM C18SNa and 200 mM DMAE was switched between low and high zero-shear viscosity states by alternating CO₂ and N₂ treatment over three cycles, combined with high temperature (60 °C). Another common hydrotrope, *N,N,N',N'*-tetramethyl-1,4-butanediamine (TMDAB), was also successfully used for switching the viscosity of the aqueous solution with C18SNa [31]. The viscosity can be reversibly controlled by the addition and removal of CO₂, and the viscosity reached a maximum for a molar ratio of TMDAB: C18SNa of 1:2.

5.2 CO₂-Switchable WLMs Based on a C18-Tailed Polyamine

One limitation of binary systems such as those described in the previous section is that the mixtures may result in “chromatographic fractionating effect” when passing through porous media, for example, as used in the oil production process. To this end and to simplify the formulation, we next developed single-component CO₂-switchable WLMs. The first of such systems is based on a newly synthesized C18-tailed polyamine–octadecyl dipropylene triamine (ODPTA, Fig. 5.4), whose polyamine headgroup responds to the stimulus of CO₂, and the long hydrocarbon chain is amenable to spontaneous assembly into WLMs [32]. This wormlike micellar system can undergo a fully reversible, cyclable “sol/gel” transition upon alternative treatment of CO₂ and N₂, while the more traditional treatment with HCl imparts quite different function to this system, even at the same pH as the one reached with CO₂.

As shown in Fig. 5.5a, the original 2.0 wt% ODPTA dispersion is milky and shows a weak shear-thinning response, with a maximum viscosity of only 5 mPa s,

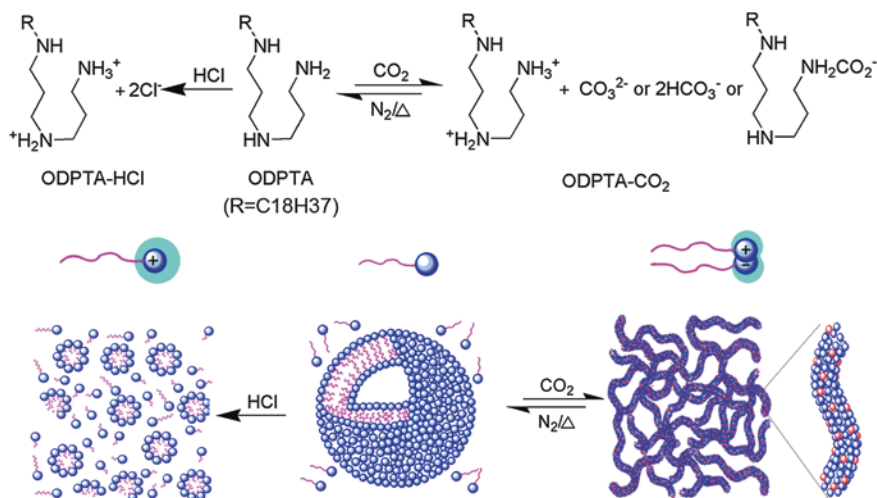


Fig. 5.4 Schematic comparison of treatment by CO₂ or HCl in regulating micellar self-assembly of ODPTA. Reproduced from Ref. [32] by permission of The Royal Society of Chemistry

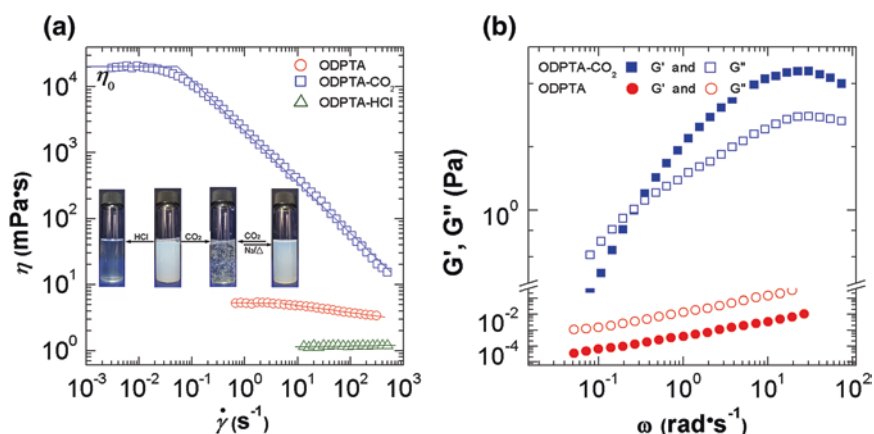


Fig. 5.5 **a** Steady-state and **b** dynamic rheology of a 2.0 wt% ODPTA dispersion at 30 °C showing the effect of bubbling CO₂ and addition of HCl. *Insets* snapshots of the original 2.0 wt% ODPTA aqueous dispersion, after bubbling CO₂ (0.1 MPa), replacing CO₂ by N₂ (0.1 MPa) at 75 °C, and adjusting to the same equilibrium pH with HCl. Adapted from Ref. [32] by permission of The Royal Society of Chemistry

but instantaneously switches to a transparent viscoelastic “gel” with η_0 as high as 2×10^4 mPa s after 2 min of CO₂ bubbling (“ODPTA–CO₂”), characteristically trapping bubbles over a long period of time (Fig. 5.5a, inset). When CO₂ is displaced with N₂ at 75 °C for about 45 min, the “gel” recovers its initial appearance (Fig. 5.5a, inset).

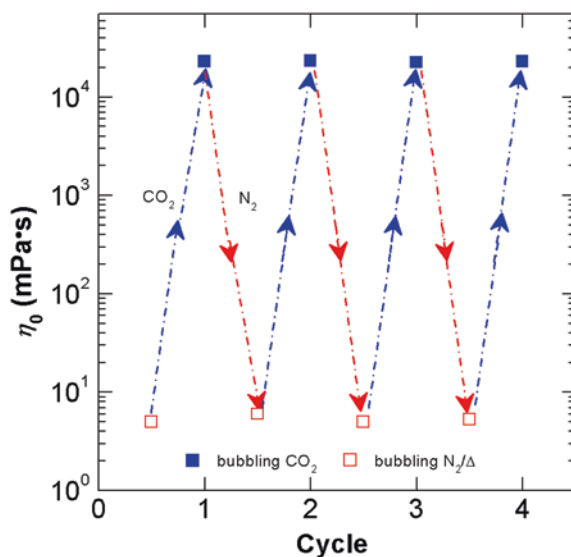
However, when adjusting the pH of ODPTA dispersions with HCl to that of “ODPTA–CO₂”, the dispersion turns into a transparent, water-like fluid displaying a typical Newtonian behaviour with a viscosity around 1 mPa s, and with none of the viscoelastic characteristics of “ODPTC–CO₂”. Oscillatory shear measurements (Fig. 5.5b) also corroborate the formation and break-up of ODPTA WLMs. The dependence of the storage (G') and loss modulus (G'') with frequency show a liquid-like behaviour in the absence of CO₂ ($G'' > G'$), while bubbling CO₂ induces a predominantly solid-like viscoelastic response, with G' above G'' over a large range of frequencies.

Of special interest is that such a CO₂-responsive behaviour is reversible when cyclically bubbling and removing CO₂, and after 4 cycles, the sample still reverts back to exactly its original value, without any deterioration of the response (Fig. 5.6).

Cryo-TEM visualization before and after CO₂ treatment reveals a microstructural transition from spherical micelles and vesicles to WLM networks, which thus explains the observed rheological response. In the absence of CO₂ or HCl, vesicles are observed in 2 wt% aqueous dispersions (Fig. 5.7a). After CO₂ uptake, networks of elongated thread-like micelles are visible (Fig. 5.7b); these WLMs have diameters of several nanometres and are several hundred nanometres long (Fig. 5.7c). When CO₂ is removed, the networks revert back to vesicles (Fig. 5.7d). In comparison, only spherical micelles are detected in ODPTA aqueous dispersions with HCl (Fig. 5.7e). Thus, the dramatic rheological changes observed in ODPTA dispersions can clearly be ascribed to the transition between entangled networks of WLMs to vesicles.

To gain insight into the different mechanisms of CO₂ and HCl, both UV/vis spectroscopy and NMR techniques were used. UV/vis measurements using Nile

Fig. 5.6 Zero-shear viscosity (η_0) of a 2.0 wt% ODPTA dispersion measured over repeated cycles of bubbling and removing CO₂. Adapted from Ref. [32] by permission of The Royal Society of Chemistry



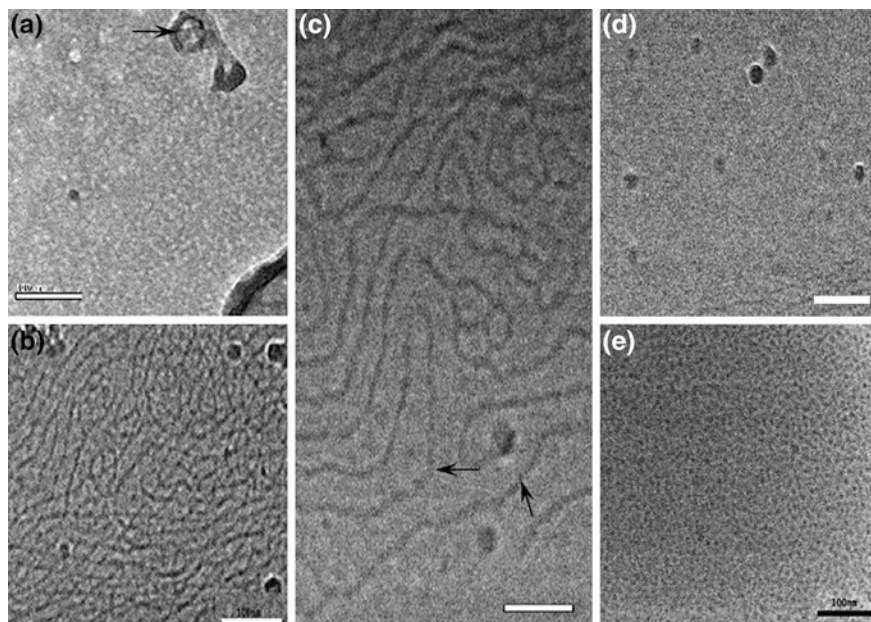


Fig. 5.7 Cryo-TEM micrographs of 2.0 wt% ODPTA at 30 °C. **a** Before bubbling CO₂; **b** and **c** after bubbling CO₂; **d** removal of CO₂; **e** with HCl to adjust the pH. Bars in **(a, b, d)**, and **(e)** are 100 nm and 50 nm in **(c)**. Reproduced from Ref. [32] by permission of The Royal Society of Chemistry

red as a probe demonstrate that both the bubbling of CO₂ or the addition of HCl significantly increase the polarity of ODPTA dispersions, but the effect is significantly stronger with HCl. Further pH titration reveals that a viscosity enhancement is also observed when adding HCl, but only at high pH values. Indeed, η_0 increases similarly for both “ODPTA–CO₂” and “ODPTA–HCl” when reducing the pH from 11.0 to 9.8. Beyond that point, further addition of HCl lowers the viscosity below its original value, while the addition of CO₂ increases it by 4 orders of magnitude, up to the equilibrium pH value of ~6.0, as discussed above.

¹H NMR measurements bring further clarification on the different effect of CO₂ and HCl on the viscosity (Fig. 5.8). After bubbling CO₂ or adding HCl, the chemical shifts of all protons in CH₂-neighbouring amine groups (*a, b, c*, and *d*, except *f* and *g*) shift downfields, implying that the primary and middle secondary amine groups of ODPTA have been protonated. However, the distributions of these peaks are not identical, which may be ascribed to the different structures of the protonated products. The ¹³C NMR spectra reveal that the by-products of “ODPTA–HCl” and “ODPTA–CO₂” are quite different: the former only has a single ammonium hydrochloric acid, while the latter is a mixture of ammonium carbamate, carbonate, and bicarbonate. According to the three distinctly different aqueous p*K*_{aH} values at 10.08, 7.41, and 4.64 from the primary, middle secondary, and another secondary amine groups along the ODPTA skeleton, two predominant

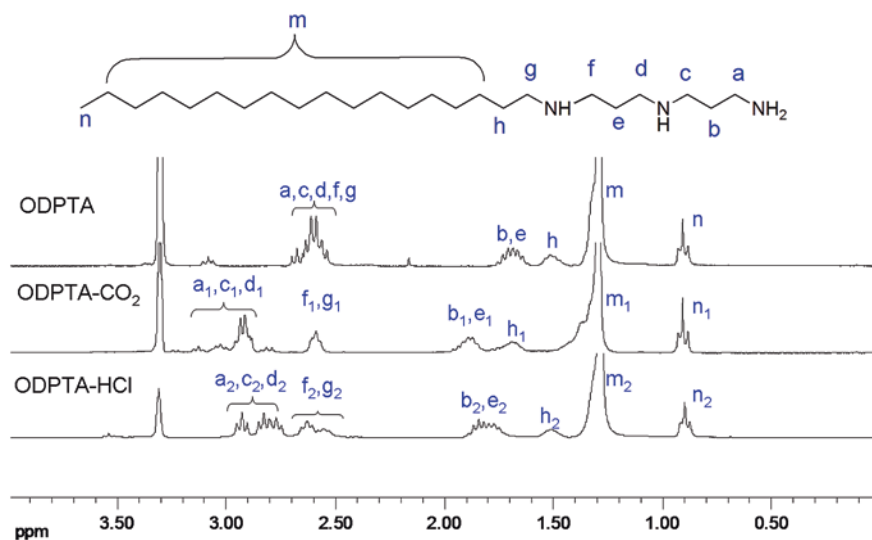
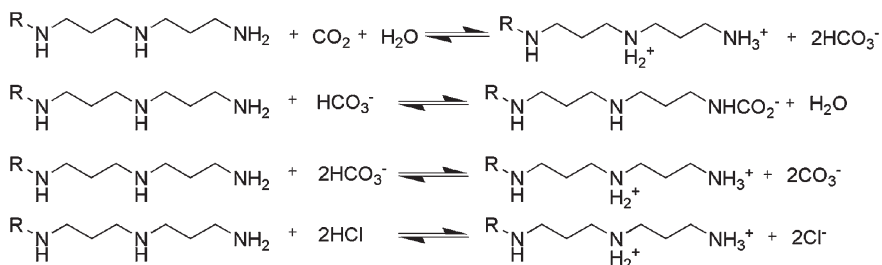


Fig. 5.8 Comparison of ¹H NMR spectra (CD₃OD/D₂O, v/v = 5:1) of ODPTA before and after reacting with CO₂ or HCl. Reproduced from Ref. [32] by permission of The Royal Society of Chemistry

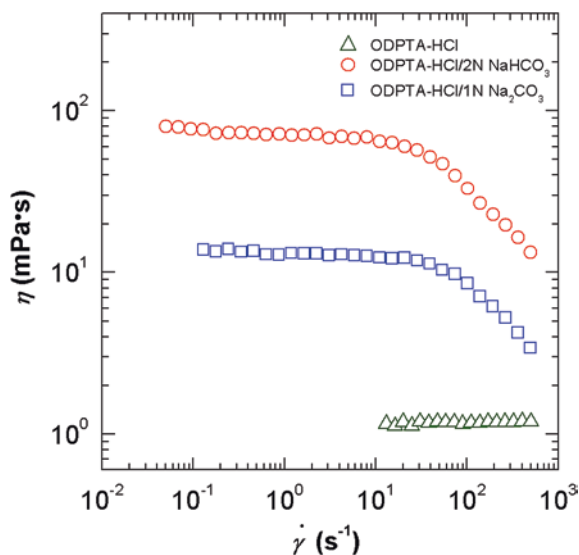
protonated species and two by-products are expected from “ODPTA–CO₂” at pH 6.0 (Scheme 5.1): the C18-tailed ammonium C₁₈H₃₇–NH–(CH₂)₃–NH₂⁺–(CH₂)₃–NH₃⁺ and C18-tailed carbamate C₁₈H₃₇–NH–(CH₂)₃–NH–(CH₂)₃–NH₂–CO₂[–], as well as CO₃^{2–} and HCO₃[–]; on the contrary, only one protonated product (C₁₈H₃₇–NH–(CH₂)₃–NH₂⁺–(CH₂)₃–NH₃⁺) and one by-product (Cl[–]) are produced from “ODPTA–HCl” at the same pH. Thus, the different macroscopic behaviour of “ODPTA–HCl” and “ODPTA–CO₂” quite possibly originate from the impact of both the main protonated products and the by-products, which may function as counterions.

To confirm the influence of the by-products on the viscosity of protonated ODPTA, NaHCO₃ or Na₂CO₃ was added to the “ODPTA–HCl” solution at pH 6.0 (Fig. 5.9). It was found that CO₃^{2–} and HCO₃[–] can increase the viscosity tenfold



Scheme 5.1 Reaction of ODPTA with CO₂ or HCl at pH 6.0. Reproduced from Ref. [32] by permission of The Royal Society of Chemistry

Fig. 5.9 Both CO₃²⁻ and HCO₃⁻ can increase the viscosity of 2 wt% “ODPTA-HCl” at pH 6.0. Reproduced from Ref. [32] by permission of The Royal Society of Chemistry



and nearly 100 times, respectively, compared to the original “ODPTA-HCl” solution. This means that both CO₃²⁻ and HCO₃⁻ show a much stronger ability than Cl⁻ to induce the growth of wormlike micelles, because Cl⁻ is more readily hydrated than the two other anions.

In terms of protonated products, the C18-tailed ammonium C₁₈H₃₇-NH-(CH₂)₃-NH₂⁺-(CH₂)₃-NH₃⁺ and C18-tailed carbamate C₁₈H₃₇-NH-(CH₂)₃-NH-(CH₂)₃-NH₂-CO₂⁻ are typical cationic and anionic surfactants, respectively (Scheme 5.1), and it is well recognized that such cationic-anionic ion pairs can facilitate the formation of WLMs through effectively screening the electrostatic repulsion between ionic headgroups [33]. Above C*, the WLMs overlap and entangle into a transient network, resulting in the observed enhancement of the viscoelasticity of the solutions.

Based on the different functions of different protonated products and by-products, as well as the different macroscopic behaviours and microstructure morphologies, the different mechanisms of CO₂ and HCl to induce the formation of micelles are compared in Fig. 5.4. As a long-chain polyamine, ODPTA is not ionized in water, and self-assembles into small vesicles, displaying low viscosity. After bubbling CO₂, the nonionic ODPTA converts into long-chain cationic ammonium and anionic carbamate accompanied by the formation of CO₃²⁻ and HCO₃⁻. The two long-chain surfactants (ammonium and carbamate) can form ion pairs to promote the growth of WLMs, and both CO₃²⁻ and HCO₃⁻ can significantly increase the viscosity of the protonated ODPTA aqueous solution as well. When CO₂ is depleted by N₂, the protonated amine groups return back to their nonionic form, the hydration of the headgroup weakens, the electrostatic attraction disappears, and thus, ODPTA reverts back to its initial structure and packing, leading to a drop in the viscosity. Nevertheless, the single C18-tailed protonated

ammonium cannot effectively self-assemble into WLMs, and the counterion Cl⁻ does not induce the growth of micelles either. As a result, “ODPTA–HCl” does not result in the strong viscosity enhancement observed in the “ODPTA–CO₂” system. This demonstrates the potential differences between CO₂ as a trigger versus the more conventional pH trigger obtained by acid titration, due to the importance of the nature of the counterions formed in driving WLM formation.

5.3 CO₂-Switchable WLMs Formed from a C22-Tailed Tertiary Amine

The reversibility of the systems described in the previous two sections is not “symmetrical”; in other words, the temperature used when bubbling and removing CO₂ is not the same, and in the latter case, heating to relatively high temperature is necessary to displace CO₂. In addition, an inert gas is usually needed to achieve full reversibility of the systems. We describe in this section WLMs formed from the single UC22AMPM surfactant that can be switched “on” and “off” by CO₂ and air at ambient pressure and room temperature, without the need of either inert gas or heating [34].

Upon bubbling CO₂ for ~10 min at room temperature, a 100 mM UC22AMPM solution immediately becomes homogeneous, transparent, and highly viscoelastic and can retain bubbles over a long time. The gel-like fluid returns to a low-viscosity emulsion-like solution by bubbling air for 30 min or exposing to air for ~4 days at ambient temperature. Steady-state rheological experiments indicate that η_0 increases by more than 5 orders of magnitude upon CO₂ trigger (Fig. 5.10a).

Similarly to the previous two systems, low and high viscosity of 100 mM UC22AMPM aqueous solution can be reversibly obtained when cyclically bubbling CO₂ and air (Fig. 5.10a). As established above, the initial η_0 of UC22AMPM–CO₂ is five orders of magnitude higher than that of UC22AMPM–air. After three cycles of CO₂ and air sparging, η_0 can still return back to exactly its original value, without any deviation. Cryo-TEM observation corroborates the nature of the structures formed in the system: elongated, flexible wormlike micelles that entangle with each other are present in “UC22AMPM–CO₂” solution, and these aggregates have diameters of several nanometres and lengths in the micrometre range (Fig. 5.10b); instead, only small spherical micelles are evidenced in “UC22AMPM–air” solution (Fig. 5.10c). Therefore, the dramatic rheological changes observed in UC22AMPM solution can clearly be ascribed to the transition from an entangled network of wormlike micelles (CO₂) to spherical micelles (air).

More remarkably even, simple exposure of the UC22AMPM solution to air at room temperature can also decrease the viscosity. As shown in Fig. 5.11a, initially, the solution is a homogeneous viscoelastic fluid trapping numerous bubbles; when exposing the solution to air over time, first an emulsion-like phase is formed on the surface, which progressively expands to the bulk, eventually forming a

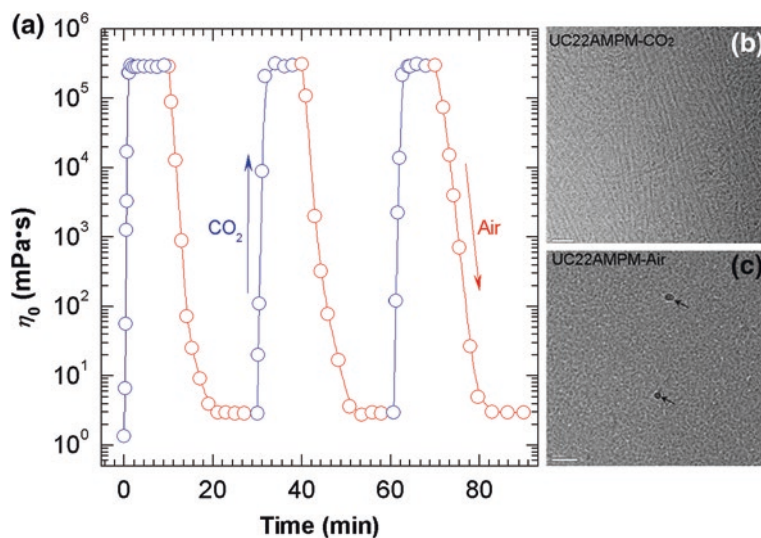


Fig. 5.10 **a** Zero-shear viscosity (η_0) of the 100 mM UC22AMPM solution measured during the repeated cycles of bubbling CO₂ and air at 25 °C; **b** micrographs of UC22AMPM-CO₂ and **c** UC22AMPM-air observed by Cryo-TEM. The scale bar is 50 nm for UC22AMPM-CO₂ and 100 nm for UC22AMPM-air, respectively. Adapted from Ref. [34] by permission of The Royal Society of Chemistry

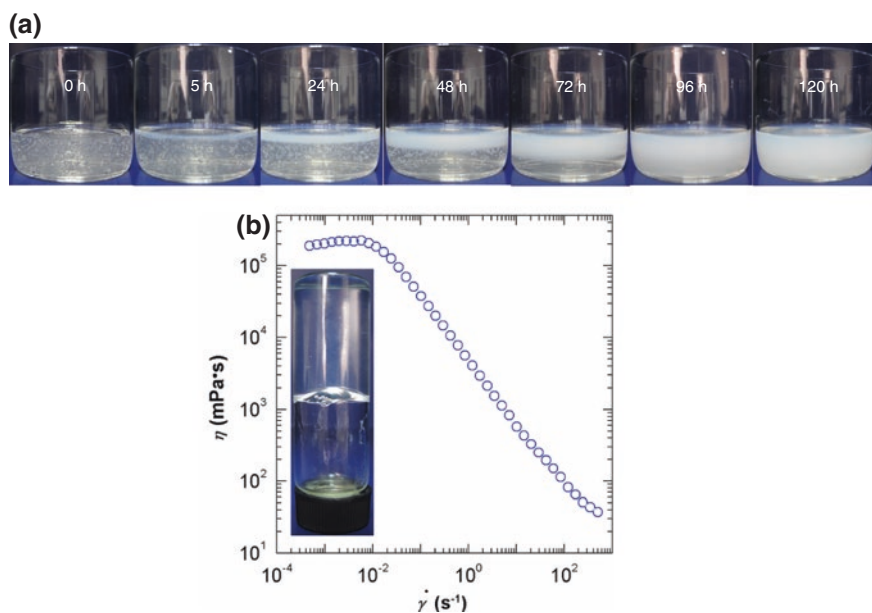


Fig. 5.11 **a** Evolution of the appearance of 100 mM UC22AMPM-CO₂ solutions over time when exposed to air; **b** high viscosity is still evidenced after 6 months of storage of the 100 mM UC22AMPM-CO₂ solution sealed in a vial. Adapted from Ref. [34] by permission of The Royal Society of Chemistry

low-viscosity opaque solution. In contrast, when the “UC22AMPM–CO₂” sample is kept in a sealed vessel for six months, it still appears as a transparent viscoelastic fluid, and η_0 is as still high as 280,000 mPa s (Fig. 5.11b), very close to the initial value of that present in Fig. 5.10a, thus showing the strong air sensitivity of the system.

5.4 CO₂-Rupturing WLMs Formed from Sodium Erucate

As a trigger, CO₂ can not only thicken surfactant solutions, but also decrease the viscosity of high-viscosity surfactant solutions. As shown in Fig. 5.12a, a sodium erucate (NaOEr) solution at pH 11.34 before CO₂ treatment appears as homogeneous viscoelastic fluid which can trap numerous air bubbles in the bulk [35]. This appearance changes when continuously bubbling CO₂ into the NaOEr aqueous solution at 60 °C at a fixed rate of 0.1 L min⁻¹. After only 10 s of bubbling, an emulsion-like phase is formed on the surface. With the increase in the time of bubbling CO₂, the emulsion-like phase progressively diffuses throughout the whole solution, eventually forming a low-viscosity opaque solution within 1 min.

Initially, at pH 11.34, erucic acid molecules are neutralized into erucate ions, behaving like ultra-long-chain anionic surfactants, which can self-assemble into long wormlike micelles at a low concentration and then entangle into transient networks responsible for the viscoelasticity (Inset, Fig. 5.12b), with η_0 as high as 60,000 mPa s.

When CO₂ is bubbled, η_0 drops dramatically over a short timescale (0–40 s) (Fig. 5.12b), and then levels off for times longer than 40 s, which signifies that the content of NaOEr in the solutions gradually decreases with CO₂ bubbling. Correspondingly, both plateau modulus (G_0) and relaxation time (τ_R) (Fig. 5.12c) decrease over bubbling time. Concurrently, the pH value of the solution decreases due to the formation of H₂CO₃, which results in the conversion of erucate ions into nonionic erucic acid molecules. With increasing CO₂ bubbling time, increasing amounts of anionic surfactant NaOEr convert to erucic acid, which break away from the surfactant aggregates. As a result, the effective surfactant concentration (or the number of surfactant molecules involved in forming wormlike micelles) decreases. With the decrease in surfactant concentration, the length and flexibility of the wormlike micelles decrease concomitantly and result in a decrease of η_0 and τ_R . The shortening of the wormlike micelles leads to a decrease of the mesh size of the network, and thus, G_0 decreases upon increasing the time of bubbling CO₂. G_0 correlates with mesh size and thus normally scales with surfactant concentration; thus, the decrease in G_0 with the time of CO₂ bubbling also confirms the decrease in wormlike micelles concentration, because less NaOEr molecules are generated and dispersed when decreasing the pH.

Finally, the original viscoelastic wormlike micelle solutions are converted into low-viscosity spherical micelles or free monomer solutions. However, it is worth pointing out that, when bubbling N₂ to displace CO₂ at 80 °C for one day, the pH

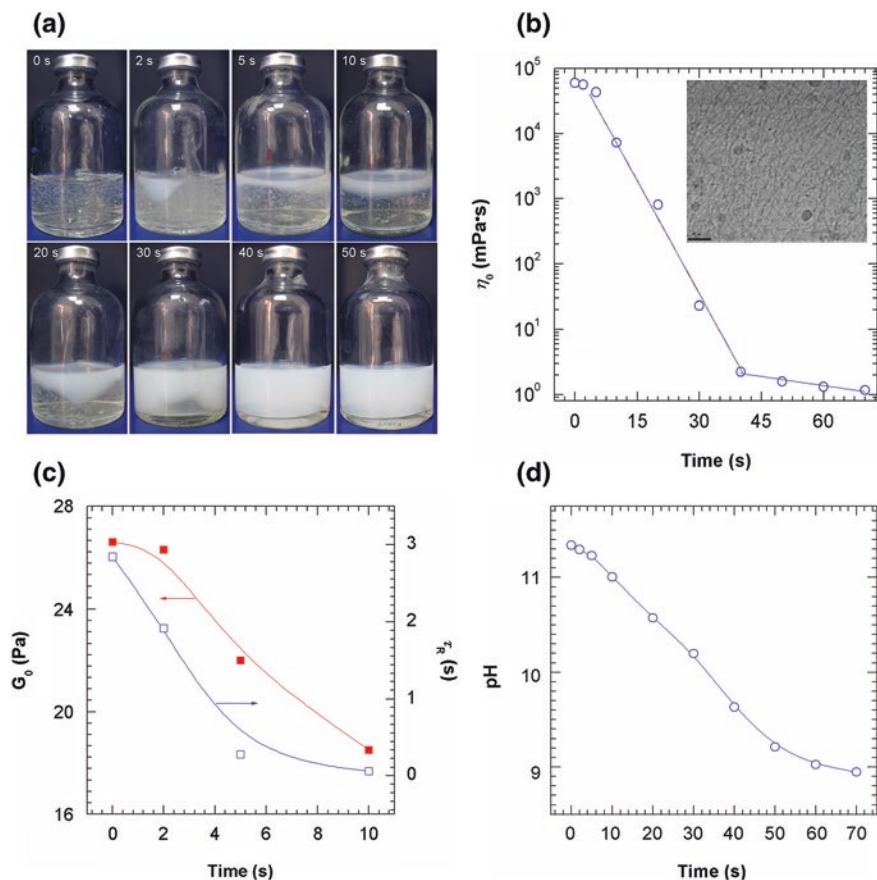


Fig. 5.12 Evolution of **a** appearance, **b** zero-shear viscosity (η_0), **c** plateau modulus (G_0) and relaxation time (τ_R), and **d** pH of 100 mM NaOEr solution (pH = 11.34) as a function of CO₂ bubbling time at 60 °C. Adapted from Ref. [35], Copyright (2014) ICE Publishing

value of the sample only increases back to ~ 9.22 , which is insufficient to drive wormlike micelle formation. Hence, in the present system, the viscoelastic fluid does not recover its original state by depleting CO₂ with N₂, a common method used in other wormlike micellar systems.

Su et al. [31] also developed a CO₂-thinning solution system but showing viscosity switchability by bubbling/removing CO₂ into/from the aqueous mixture of sodium stearate (C18CNa) and NaNO₃. Before introducing CO₂, the highest η_0 of 200 mM of the solution was 12,400 mPa s at 80 °C; after CO₂ was bubbled throughout the solution for 10 min at the same temperature, the mixture became milky and displayed a much lower η_0 at only 2.0 mPa s. In this state, the aqueous solution has become a suspension of particles with an average particle size of 946 nm and a zeta potential of -23 mV. After N₂ was bubbled through the suspension for about 40 min at 80 °C, the viscosity increased back to 12,360 mPa s. The

authors attributed the slight decrease in the maximum viscosity to the incomplete conversion of switchable moieties back to the neutral form. Although the Krafft point (T_K) of C18CNa is 71 °C, these authors also obtained switchable viscosity with an aqueous solution of C18CNa and tetrabutylammonium bromide (TBAB) at 60 °C because the addition of TBAB decreases the T_K of sodium carboxylate soaps and increases their solubility in aqueous solution.

In summary, we presented in this chapter four classes of CO₂-responsive wormlike micellar systems, three of which are based on amines either on the hydrotrope molecules or on the skeleton of long-chain surfactants. Carboxylate-based anionic WLMs are also sensitive to CO₂, but unlike the previous systems, the pre-formed WLMs are destroyed by the presence of CO₂, and thus, the macroscopic viscosity drops.

In terms of formulation, the binary “pseudo-gemini” system and the anionic one are more readily obtained and more environment-friendly because they can be formed by a common anionic surfactant or natural erucic acid solutions without the need of complex organic synthesis. The “CO₂/air” switchable system is particularly attractive for practical applications—it provides an economical, environment-friendly, and low-energy-cost way to regulate the viscoelasticity in aqueous media, since it can be achieved by simply bubbling CO₂ or air at ambient temperature, not requiring heat or the use of an inert gas such as N₂ or Ar.

References

1. Jessop PG, Mercer SM, Heldebrant DJ (2012) CO₂-triggered switchable solvents, surfactants, and other materials. *Energy Environ Sci* 5:7240–7253
2. Tour JM, Kittrell C, Colvin VL (2010) Green carbon as a bridge to renewable energy. *Nat Mater* 9:871–874
3. Seifter JL (2011) Acid-base disorders. In: Goldman L, Schafer AI (eds) *Goldman's Cecil medicine*, 24th edn. Elsevier, Saunders, pp 741–753
4. Gutknecht J, Bisson MA, Tosteson FC (1977) Diffusion of carbon-dioxide through lipid bilayer membranes—effects of carbonic—anhydrase, bicarbonate, and unstirred layers. *J Gen Physiol* 69:779–794
5. Yan Q, Zhao Y (2013) CO₂-stimulated diversiform deformations of polymer assemblies. *J Am Chem Soc* 135:16300–16303
6. Yan Q, Zhou R, Fu C, Zhang H, Yin Y, Yuan J (2011) CO₂-responsive polymeric vesicles that breathe. *Angew Chem Int Ed* 50:4923–4927
7. Yan Q, Zhao Y (2013) Polymeric microtubules that breathe: CO₂-driven polymer controlled-self-assembly and shape transformation. *Angew Chem Int Ed* 52:9948–9951
8. Yan Q, Wang J, Yin Y, Yuan J (2013) Breathing polymersomes: CO₂-tuning membrane permeability for size-selective release, separation, and reaction. *Angew Chem Int Ed* 52:5070–5073
9. Liu YX, Jessop PG, Cunningham M, Eckert CA, Liotta CL (2006) Switchable surfactants. *Science* 313:958–960
10. Scott LM, Robert T, Harjani JR, Jessop PG (2012) Designing the head group of CO₂-triggered switchable surfactants. *RSC Adv* 2:4925–4931
11. Phan L, Jessop PG (2009) Switching the hydrophilicity of a solute. *Green Chem* 11:307–308
12. Han DH, Tong X, Boissiere O, Zhao Y (2012) General strategy for making CO₂-switchable polymers. *ACS Macro Lett* 1:57–61

13. Guo Z, Feng Y, Wang Y, Wang J, Wu Y, Zhang Y (2011) A novel smart polymer responsive to CO₂. *Chem Commun* 47:9348–9350
14. Yan Q, Zhao Y (2014) Block copolymer self-assembly controlled by the “green” gas stimulus of carbon dioxide. *Chem Commun* 50:11631–11641
15. Li WJ, Zhang ZF, Han BX, Hu SQ, Song JL, Xie Y, Zhou XS (2008) Switching the basicity of ionic liquids by CO₂. *Green Chem* 10:1142–1145
16. Li XY, Hou MQ, Zhang ZF, Han BX, Yang GY, Wang XL, Zou LZ (2008) Absorption of CO₂ by ionic liquid/polyethylene glycol mixture and the thermodynamic parameters. *Green Chem* 10:879–884
17. Wang CM, Mahurin SM, Luo HM, Baker GA, Li HR, Dai S (2010) Reversible and robust CO₂ capture by equimolar task-specific ionic liquid-superbase mixtures. *Green Chem* 12:870–874
18. Wang CM, Luo HM, Jiang DE, Li HR, Dai S (2010) Carbon dioxide capture by superbase-derived protic ionic liquids. *Angew Chem Int Ed* 49:5978–5981
19. Hoshino Y, Imamura K, Yue MC, Inoue G, Miura Y (2012) Reversible absorption of CO₂ triggered by phase transition of amine-containing micro- and nanogel particles. *J Am Chem Soc* 134:18177–18180
20. Han DH, Boissiere O, Kumar S, Tong X, Tremblay L, Zhao Y (2012) Two-way CO₂-switchable triblock copolymer hydrogels. *Macromolecules* 45:7440–7445
21. Guo Z, Feng Y, He S, Qu M, Chen H, Liu H, Wu Y, Wang Y (2013) CO₂-responsive “smart” single-walled carbon nanotubes. *Adv Mater* 25:584–590
22. Jessop PG, Heldebrant DJ, Li XW, Eckert CA, Liotta CL (2005) Reversible nonpolar-to-polar solvent. *Nature* 436:1102
23. Heldebrant DJ, Koech PK, Ang MTC, Liang C, Rainbolt JE, Yonkera CR, Jessop PG (2010) Reversible zwitterionic liquids, the reaction of alkanol guanidines, alkanol amidines, and diamines with CO₂. *Green Chem* 12:713–721
24. Zhao Y, Landfester K, Crespy D (2012) CO₂ responsive reversible aggregation of nanoparticles and formation of nanocapsules with an aqueous core. *Soft Matter* 8:11687–11696
25. Harjani JR, Liang C, Jessop PG (2011) A synthesis of acetamidines. *J Org Chem* 76:1683–1691
26. Jing YQ, Thomas PD, Andrew BL (2013) Amidine functionality as a stimulus-responsive building block. *Chem Soc Rev* 42:7326–7334
27. Chu Z, Feng Y (2010) pH-switchable wormlike micelles. *Chem Commun* 46:9028–9030
28. Zhang Y, Feng Y, Wang Y, Li X (2013) CO₂-switchable viscoelastic fluids based on a pseudogemini surfactant. *Langmuir* 29:4187–4192
29. Kumar S, David SL, Aswal VK, Goyal PS, Kabir-ud-Din (1997) Growth of sodium dodecyl sulfate micelles in aqueous ammonium salts. *Langmuir* 13:6461–6464
30. Manne S, Schäffer TE, Huo Q, Hansma PK, Morse DE, Stucky GD, Aksay IA (1997) Gemini surfactants at solid-liquid interfaces: control of interfacial aggregate geometry. *Langmuir* 13:6382–6387
31. Su X, Cunningham MF, Jessop PG (2013) Switchable viscosity triggered by CO₂ using smart worm-like micelles. *Chem Commun* 49:2655–2657
32. Zhang Y, Feng Y, Wang J, He S, Guo Z, Chu Z, Dreiss CA (2013) CO₂-switchable wormlike micelles. *Chem Commun* 49:4902–4904
33. Eastoe J, Hatzopoulos MP, Dowding PJ (2011) Action of hydrotropes and alkyl-hydrotropes. *Soft Matter* 7:5917–5925
34. Zhang Y, Chu Z, Dreiss CA, Wang Y, Fei C, Feng Y (2013) Smart wormlike micelles switched by CO₂ and air. *Soft Matter* 9:6217–6221
35. Zhang Y, Yin H, Feng Y (2014) CO₂-responsive anionic wormlike micelles based on natural erucic acid. *Green Mater* 2:95–103

Chapter 6

Other Types of Smart Wormlike Micelles

Abstract In comparison with the widely reported triggers described in previous chapters—namely temperature, pH, and light—this chapter discusses triggers which have been far less documented: redox potential and hydrocarbons and their use to control the assembly and properties of wormlike micelles. In addition, recent reports of multiple stimuli-responsive wormlike micelles are also described, as well as smart reverse wormlike micelles, to complete this collection of “unconventional” smart wormlike micelles.

Keywords Redox-responsive · Hydrocarbon-responsive · Multi-responsive · Smart reverse wormlike micelles

6.1 Redox-Responsive WLMs

The first redox-sensitive surfactant was reported nearly 30 years ago by Saji et al. [1, 2]. They incorporated a ferrocene-based moiety into the surfactant and found that the CMC and micellization behaviour were altered under the stimulus of electron transfer, and they observed that micelles could be broken up into monomers by oxidation and re-formed by reduction. More details on this type of surfactants can be found in recent reviews by Abbott [3] and Eastoe [4].

Despite this prior work, the only example of redox-sensitive WLMs, to our knowledge, was reported by Abe et al. [5] in 2004, and motivated by the development of electro-rheological (ER) fluids. ER fluids are colloidal dispersions whose viscosity can be controlled by an applied electric potential and are regarded as versatile materials for building up smart structures and machines. These fluids have applications in valves and clutches for transmission and precise control of mechanical positioning. They are conventionally produced by dispersing solid particles within a liquid. The application of an alternating electric field to the ER dispersions produces a viscosity increase mainly in the direction perpendicular to the field, because the dispersed particles align to form strings in the direction parallel

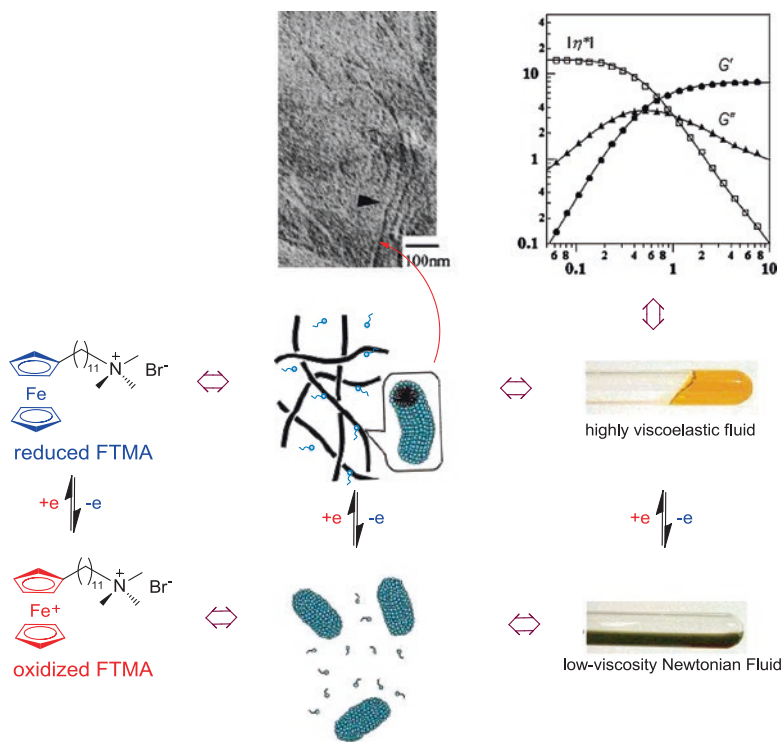


Fig. 6.1 Electro-stimulus response of FTMA wormlike micelles: rheological response, mechanism, and FF-TEM image. Adapted with permission from Ref. [5]. Copyright (2004) American Chemical Society

to the field due to the attraction of induced dipoles. These conventional ER fluids, however, have many disadvantages. In particular, a high voltage and a high particle concentration are required and their stability is usually poor; this has hampered their industrial applications.

To overcome the above deficiencies, and inspired by the fact that the surface tension [6], as well as the aggregate microstructure [7–9] of ferrocene-containing surfactants can be reversibly and dramatically controlled by oxidation, the team of Abe [5] developed a novel type of ER fluids through a simple redox reaction of a ferrocenyl surfactant [(11-ferrocenylundecyl) trimethyl-ammonium bromide] (FTMA).

As illustrated in Fig. 6.1, when the redox-active ferrocenyl group positioned at the end of alkyl chain is reduced, it becomes hydrophobic, while the ferricinium cation (oxidized form) acts as a hydrophilic group. This causes a remarkable change in the hydrophilic–lipophilic balance of FTMA, thereby altering its aggregation state, as well as the viscoelasticity of aqueous FTMA/NaSal mixtures.

The viscosity of 50 mM reduced FTMA/NaSal mixture solution increases upon increasing the molar ratio of NaSal to FTMA from 0 to 0.4, at which point the solution becomes a gel. Rheological measurements show that the mixture solution

displays typical behaviour of a non-Newtonian viscoelastic fluid: η_0 reaches 15,000 mPa s, 4 orders of magnitude higher than pure water; the storage modulus G' is lower than the loss modulus G'' at low frequencies, while it dominates over G'' and exhibits a definite plateau at high frequencies. This increased viscoelasticity is ascribed to the three-dimensional network from the entanglement of WLMs, which could be verified by freeze-fracture transmission electron microscopy (FF-TEM) observation.

Instead, when FTMA is oxidized, the mixture solution flows easily (Fig. 6.1), behaving like a Newtonian fluid with no elasticity. Its viscosity sharply decreases to 2.5 mPa s, 1/6000th of that of the reduced sample. This remarkable viscoelasticity decrease is caused by a significant shortening of the WLMs, thus rupturing the network structure.

6.2 Hydrocarbon-Responsive WLMs

Unlike the stimuli described above, which are usually the result of careful design, the addition of hydrocarbons affects the behaviour of the vast majority of WLMs. Generally, entangled WLMs networks can be disrupted and broken up by the addition of minute amounts of hydrocarbons, and thus the initial viscoelastic fluids turn into water-like solutions [10].

Surfactant micellar solutions have a general tendency to solubilize a certain amount of hydrocarbons because of the interaction between the hydrocarbon and the micellar core. Aqueous solutions composed of globular micelles can normally trap a small amount of hydrocarbon, and the maximum concentration of the dispersed hydrocarbon is typically at least one order of magnitude lower than that of the surfactant. However, as reported by Hoffmann et al. [10, 11], WLM solutions can solubilize rather larger amounts of hydrocarbons, compared to globular micelle solutions; in favourable cases, the hydrocarbon/surfactant ratio in a saturated solution has a value of about one [10]. The added hydrocarbon can be considered as a stimulus, as it induces the transformation of entangled WLMs into isolated globular aggregates with radii from 20 to 500 Å. As a result, the viscoelasticity is lost and the solution behaves like a low-viscosity Newtonian liquid with a shear-independent viscosity [10, 11].

Philippova's team [12] observed a substantial viscosity decrease after saturating potassium oleate WLMs solutions with *n*-heptane or *n*-dodecane. The viscosity change was attributed to the transformation of WLMs into spherical aggregates consisting of "drops" of hydrocarbon surrounded by surfactant micelles, as confirmed by SANS.

This specific property of WLMs has found numerous practical applications, particularly as viscoelastic fluids in the oilfield industry [12, 13]. It was suggested that hydrocarbon-responsive WLMs are very promising for use as clean fracturing fluids, in particular, at the stage where the porous space needs to be cleaned from the residuals of the viscous fluid in order to allow the oil to drain into the wellbore [14, 15].

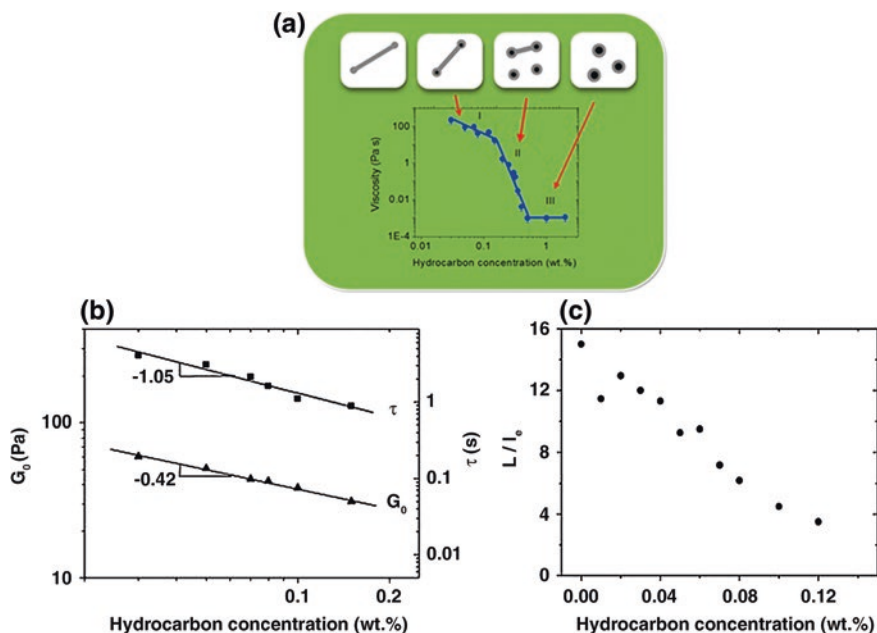


Fig. 6.2 The dependence of **a** zero-shear viscosity, **b** plateau shear modulus G_0 and relaxation time τ , and **c** the ratio of the average contour length of micelles L to the entanglement length l_e , on the hydrocarbon (*n*-dodecane) concentration for 3 wt% potassium oleate solution. Temperature: 20 °C; solvent: 6 wt% KCl aqueous solution. Adapted with permission from Ref. [16]. Copyright (2014) American Chemical Society

Very recently, Philippova and co-workers [16] gained more detailed insight into the effect of hydrocarbon addition on the rheological properties and structure of wormlike micellar solutions of potassium oleate. They found that a viscoelastic solution of entangled micellar chains was extremely responsive to hydrocarbons: the addition of only 0.5 wt% *n*-dodecane resulted in a drastic drop in viscosity by up to 5 orders of magnitude (Fig. 6.2a), due to the complete disruption of micelles and the formation of microemulsion droplets. Structural transitions of WLMs into microemulsion droplets could be divided into three regions: (i) high-viscosity solution ($\sim 10,000$ – $350,000$ mPa s), the micelles are entangled but their length is reduced by the solubilization of hydrocarbons; (ii) unentangled regime, the viscosity sharply decreases as a result of further micelle shortening and the appearance of microemulsion droplets; (iii) low-viscosity region (~ 1 mPa s), only microemulsion droplets remain.

Concomitantly, with increasing the concentration of *n*-dodecane (C_h), both plateau modulus (G_0) and relaxation time τ decreased following the scaling law (Fig. 6.2b): $G_0 \sim C_h^{-0.42}$ and $\tau \sim C_h^{-1.35}$. This behaviour could be explained by an increase rigidity of the WLMs when hydrocarbon accumulates inside. The ratio of average contour length L of the micelles relative to their entanglement length

l_e decreased with the addition of hydrocarbon (Fig. 6.2c), approaching the limit $L \approx l_e$ at an oil content of about 0.15 wt% for 3 wt% potassium oleate solutions. With $C_h > 0.15$ wt%, the WLMs were too short to be entangled and the solution lost its elasticity.

On the basis of rheological and SANS results, the authors proposed the following mechanisms: the micelle shortening results from the preferential accumulation of the solubilized hydrocarbon in the spherical end caps of WLMs, which makes the end-caps thermodynamically more favourable; the onset of the sharp drop in viscosity correlates with the crossover from the entangled to the unentangled regime, which results from the shortening of the micellar chains; in the unentangled regime, short cylindrical micelles coexist with microemulsion droplets.

6.3 Multi-stimuli-Responsive WLMs

While previous chapters have discussed SWLMs which modify their rheological behaviour in reaction to a given trigger, most life processes are reliant on responsiveness to multiple—rather than single—stimuli. Fundamental events, such as the complex folding of proteins and nucleic acids or selective transport of ions and molecules across cell membranes, all result from sensing and responding to a combination of environmental changes, rather than a single trigger. Synthetic materials that respond to several stimuli in a predictable manner have started to emerge, but are still in their infancy [17–19]. “Mimicking nature” is obviously not the sole motivation for embarking on the design of complex responsive modes. However, it is clear for instance that the introduction of synthetic materials in the biological environment (for pharmaceutical or biomedical applications) implies the requirement for the materials to demonstrate multi-responsive behaviour. In addition, engineering responsiveness to two, three or more individual stimuli and convoluted combinations of them allow a high degree of control on functionality, which is of particular interest for instance to fine-tune drug release profiles or to achieve delivery of a payload in specific compartments of the body. While still a field in its early stage, the majority of multi-stimuli-responsive materials reported to date have been polymeric in nature [17–22], only a few systems based on small molecular assemblies have been described very recently [21, 23, 24], among which just a very few studies dealing with multi-stimuli-responsive WLMs, which are discussed below.

Low molecular weight gelators, compared to polymers, present the advantage of being easier to degrade, thus more amenable to biological applications and self-assembled structures (thus gelation and micellization behaviour) and are usually more sensitive to small changes in temperature, pH or salinity; therefore, multi-stimuli responsiveness is likely to involve less convoluted synthesis [25, 26]. Probably the first example pertaining to the field of WLMs was recently reported by Graf et al. [25] where they exploited the aggregation behaviour and rheological properties of bolaamphiphiles or bolalipids (lipids consisting of a hydrophobic spacer connected to

hydrophilic groups at both ends), displaying a behaviour intermediate between helical nanofibres and WLMs. The elongated structures entangled into a network, imparting gel-like properties, which could be switched “on” and “off” by pH and salinity.

Also relevant to the field of WLMs, because it suggests potential non-covalent routes to impart them, multi-stimuli responsiveness is the work reported by Huang and co-workers [27] on surfactant aggregates. Multi-stimuli responsiveness was imparted to otherwise responsiveness catanionic (mixtures of cationic and anionic) surfactants by the simple addition of a “responser” (a multi-stimuli-responsive molecule) in sodium cholate (SC), which has three temperature-responsive hydroxyl groups, a pH-responsive carboxylate group and a hydrophobic steroid skeleton. For a given amount of SC, its effect on self-assembled architectures depends on its aggregate/water distribution ratio and its orientation inside the aggregates, both of which are affected by pH and temperature. The very high sensitivity of this system to low amounts of SC was attributed to the use of a mixture of cationic/anionic surfactants, rather than a single surfactant. Similar strategies have been employed for WLMs, but using only one stimulus [28–30]. For example, Raghavan et al. [28]—as mentioned above—designed a PR fluid requiring no specialized synthesis, simply by mixing the cationic surfactant CTAB with a photo-responsive organic derivative, *trans*-OMCA. Upon irradiation by UV light, OMCA undergoes a photo-isomerization from *cis* to *trans*, altering molecular packing at the interface, thus drastically reducing micellar length and resulting in a viscosity decrease by four orders of magnitude. The strategy proposed by Jiang et al. [27] was successfully extended to other surfactants mixtures. It has the obvious advantage of sidestepping difficult synthesis, while the nature of the responder can easily be extended to a range of molecules, as long as they present some hydrophobicity, so that they can spontaneously be incorporated into micellar aggregates: hydrotropes, dyes, light-responsive cinnamic acid, redox-responsive ferrocene carboxylic acid, and pH-responsive malachite green. We envisage that this strategy could easily be adapted to WLMs systems.

The combination of pH [31] and temperature [32] as stimuli has obvious relevance to biological applications in protein reconstitution, gene delivery, and controlled release of drugs, since sick tissues and organs often display abnormal temperature and/or pH. Recently, Zhang et al. [33] found that pH-switchable worm systems based on a C22-tailed anionic surfactant could form a solid-like highly viscoelastic material when decreasing the temperature and recovered their fluid-like properties when increasing back the temperature. To our knowledge, this is the first reported pH- and temperature-responsive WLMs.

A rather convoluted approach to impart multi-stimuli responsiveness would obviously involve the introduction of more than one stimuli-responsive chemical group on surfactant molecules: for instance, tertiary amine, azobenzene, and polyoxyethylene as pH-, photo-, and thermo-responsive functionalities, thus controlling the “on” and “off” switch. Alternatively, combining single-stimulus WLMs-forming surfactants could be a simple route worth exploring to design multi-stimuli WLMs.

It is not excluded that the scarcity of reports on multi-responsive WLMs is not a reflection of their inexistence, but simply the fact that the field of smart WLMs is

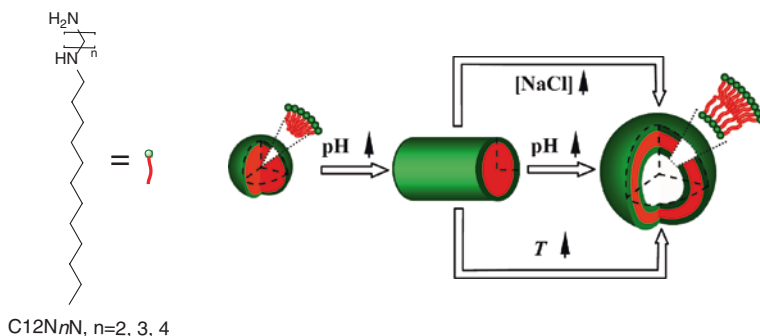


Fig. 6.3 Schematic illustration of the influence of pH, temperature and electrolyte on the morphological transition of the aggregates formed from *N*-dodecyl-1, ω -diaminoethane. Adapted with permission from Ref. [34]. Copyright (2012) Elsevier

still in its early stages, and the focus to date has been on carefully designing “one stimulus” systems while ignoring the potential existence of others. For instance, the majority of WLMs are sensitive to temperature (to various extents) and smart wormlike micelles designed to respond to other triggers, such as light or pH, may well also be “thermo-sensitive”. Similarly, pH-responsive micelles are probably sensitive to ionic strength, and most smart wormlike micelles are likely to respond to other “external” triggers.

Recently, WLMs responsive to multiple triggers were reported by Li et al. [34] in a series of homologues, *N*-dodecyl-1, ω -diaminoethane (C12N n N, $n = 2, 3, 4$). Light scattering, viscosity, and cryo-TEM results revealed that the aggregates changed from spherical micelles to vesicles via WLMs as the pH was gradually varied from acidic to basic conditions. In addition, the WLMs could also switch to vesicles upon heating. For $\omega = 2$, the transition from WLMs to vesicles could also be obtained by the addition of NaCl (Fig. 6.3).

Very recently, Yang and co-workers reported a new C22-tailed sarcosinate anionic surfactant, 2-(*N*-erucacyl-*N*-methyl amido) acetate (EMAA), synthesized by using erucic acid and a hydrotrope—sarcosine. In contrast to the traditional way of forming wormlike micelles, in which both a hydrotrope and a surfactant are mixed together, the EMMA reported here is prepared by chemical modification of an anionic surfactant with sarcosine. This long-chain anionic surfactant shows pH-controllable micelle-vesicle-WLM transition. Besides pH, the rheological properties of EMMA are also affected by temperature and salt [24].

6.4 Responsive Reverse WLMs

To close this collection of “unconventional” SWLMs, we report on reverse wormlike micelles (RWLMs), namely worms assembled from surfactants in non-aqueous media [35], the archetypal example of which is lecithin [35, 36]. Specifically,

the non-polar tails are directed outwards into the organic solvent, while the polar heads point inwards [37].

A number of RWLMs systems have been reported; however, stimuli-responsive properties are scarce and mostly limited to the effect of additives. Raghavan and co-workers [37] pioneered the work on stimuli-responsive RWLMs, where lecithin was used as an amphiphile, *para*-coumaric acid (PCA) as a photo-responder, and cyclohexane as a solvent. The combination of lecithin with the *trans* form of PCA induces the formation of reverse worms and thereby imparts viscoelasticity to the bulk solution. This arises from the ability of *trans*-PCA to form H-bonds with the headgroups of lecithin, which alters the geometry of the amphiphiles to favour cylindrical micelles at the expense of spherical ones. Upon UV irradiation, *trans*-PCA is photo-isomerized to its *cis* isomer, which is less polar and thus less capable of H-bonding with lecithin; as a result, the micelles revert to much smaller sizes, leading to a viscosity drop of more than 1000-fold. It was observed that the

Fig. 6.4 Reversible PR fluid formed by SP-doped reverse-phase wormlike micelles

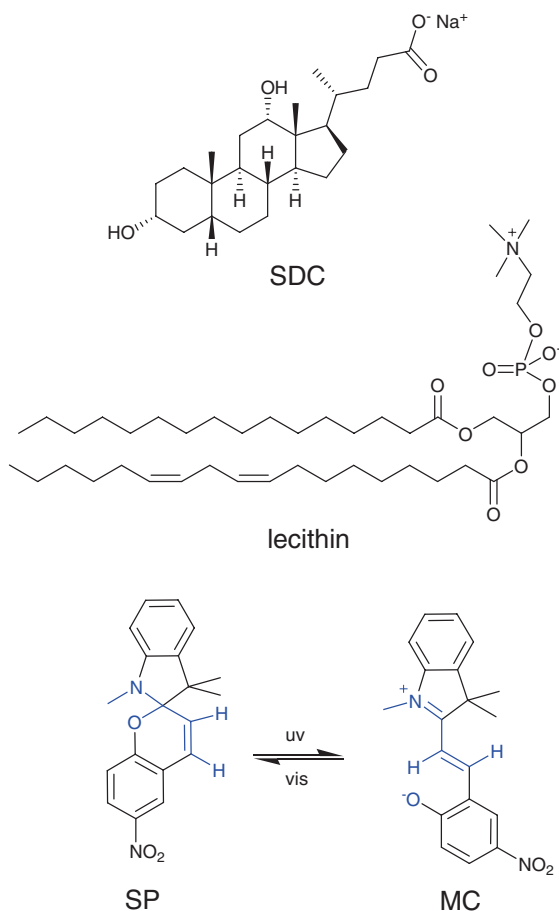


photo-responsive reverse WLMs could be equally formed in a variety of organic solvents such as alkanes, alkenes, and fatty acid esters.

In a very recent study, the same team [38] described an alternative protocol to prepare a photo-switchable RWLMs fluid, which was achieved by doping lecithin/sodium deoxycholate (SDC) reverse micelles with a photo-chromic compound, spiropyran (SP). The lecithin/SDC/SP mixtures dispersed in cyclohexane were highly viscoelastic, implying the presence of long, flexible WLMs. Upon UV irradiation, SP molecules were isomerized to an open merocyanine MC structure (Fig. 6.4), causing a remarkable decrease in the viscosity. By switching off the UV light, the MC reverted to the SP form, and the viscosity reverted back to its initial value. This cycle could be repeated several times without altering the response. This rheological transition was attributed to a change in the length of the reverse worms.

In spite of the importance and relevance of imparting multiple responsiveness, multi-stimuli-responsive WLMs systems are still in their infancy, and combinations of triggers reported to date relatively conventional (pH, heat, and electrolyte). Redox-sensitive surfactants have been extensively investigated, yet WLMs switched by an electrical field have been less reported. Hydrocarbon-sensitive WLMs have received more attention lately and may help us understand better the mechanisms of clean fracturing fluids, in which WLMs are disrupted upon contact with hydrocarbon from natural gas or the light portion of crude oil.

References

1. Saji T, Hoshino K, Aoyagui S (1985) Reversible formation and disruption of micelles by control of the redox state of the head group. *J Am Chem Soc* 107:6865–6868
2. Saji T, Hoshino K, Aoyagui S (1985) Reversible formation and disruption of micelles by control of the redox state of the surfactant tail group. *J Chem Soc Chem Commun* 13:865–866
3. Liu X, Abbott NL (2009) Spatial and temporal control of surfactant systems. *J Colloid Interface Sci* 339:1–18
4. Brown P, Butts CP, Eastoe J (2013) Stimuli-responsive surfactants. *Soft Matter* 9:2365–2374
5. Tsuchiya K, Orihara Y, Kondo Y, Yoshino N, Ohkubo T, Sakai H, Abe M (2004) Control of viscoelasticity using redox reaction. *J Am Chem Soc* 126:12282–12283
6. Aydogan N, Gallardo BS, Abbott NL (1999) A molecular-thermodynamic model for Gibbs monolayers formed from redox-active surfactants at the surfaces of aqueous solutions: redox-induced changes in surface tension. *Langmuir* 15:722–730
7. Aydogan N, Abbott NL (2001) Comparison of the surface activity and bulk aggregation of ferrocenyl surfactants with cationic and anionic headgroups. *Langmuir* 17:5703–5706
8. Sakai H, Imamura H, Kondo Y, Yoshino N, Abe M (2004) Reversible control of vesicle formation using electrochemical reaction. *Colloid Surf A Physicochem Eng Asp* 232:221–228
9. Tsuchiya K, Sakai H, Saji T, Abe M (2003) Electrochemical reaction in an aqueous solution of a ferrocene-modified cationic surfactant mixed with an anionic surfactant. *Langmuir* 19:9343–9350
10. Hoffmann H, Ebert G (1988) Surfactants, micelles and fascinating phenomena. *Angew Chem Int Ed Engl* 27:902–912
11. Hoffmann H, Ulbricht W (1987) The rheological behavior of different viscoelastic surfactant solutions. *Tenside, Surfactants, Deterg* 24:23–31

12. Molchanov VS, Philippova OE, Khokhlov AR, Kovalev YA, Kuklin AI (2007) Self-assembled networks highly responsive to hydrocarbons. *Langmuir* 23:105–111
13. Philippova OE, Khokhlov AR (2010) Smart polymers for oil production. *Petro Chem* 50:266–270
14. Maitland GC (2000) Oil and gas production. *Curr Opin Colloid Interface Sci* 5:301–311
15. Chase B, Chmiliowski W, Marcinew R, Mitchell C, Dang Y, Krauss D, Nelson E, Lantz T, Parham C, Plummer J (1997) Clear fracturing fluids for increased well productivity. *Oilfield Rev* 9:20–33
16. Shibaev AV, Tamm MV, Molchanov VS, Rogachev AV, Kuklin AI, Dormidontova EE, Philippova OE (2014) How a viscoelastic solution of wormlike micelles transforms into a microemulsion upon absorption of hydrocarbon: new insight. *Langmuir* 30:3705–3714
17. Cohen Stuart MA, Huck WTS, Genzer J, Müller M, Ober C, Stamm M, Sukhorukov GB, Szleifer I, Tsukruk VV, Urban M, Winnik F, Zauscher S, Luzinov I, Minko S (2010) Emerging applications of stimuli-responsive polymer materials. *Nat Mater* 9:101–113
18. Schattling P, Jochum FD, Theato P (2014) Multi-stimuli responsive polymers—the all-in-one talents. *Polym Chem* 5:25–36
19. Li RR, Feng FL, Wang YS, Yang XY, Yang XL, Yang VC (2014) Folic acid-conjugated pH/temperature/redox multi-stimuli responsive polymer microspheres for delivery of anti-cancer drug. *J Colloid Interface Sci* 429:34–44
20. Zhuang JM, Gordon MR, Ventura J, Li LY, Thayumanavan S (2013) Multi-stimuli responsive macromolecules and their assemblies. *Chem Soc Rev* 42:7421–7435
21. Wang F, Klaukherd A, Thayumanavan S (2011) Temperature sensitivity trends and multi-stimuli sensitive behavior in amphiphilic oligomers. *J Am Chem Soc* 133:13496–13503
22. Klaukherd A, Nagamani C, Thayumanavan S (2009) Multi-stimuli sensitive amphiphilic block copolymer assemblies. *J Am Chem Soc* 131:4830–4838
23. Fameau A-L, Lam S, Velev OD (2013) Multi-stimuli responsive foams combining particles and self-assembling fatty acids. *Chem Sci* 4:3874–3881
24. Yao RC, Qian JS, Li HZ, Yasin A, Xie YJ, Yang HY (2014) Synthesis and high-performance of a new sarcosinate anionic surfactant with a long unsaturated tail. *RSC Adv* 4:2865–2872
25. Graf G, Drescher S, Meister A, Dobner B, Blume A (2011) Self-assembled bolaamphiphile fibers have intermediate properties between crystalline nanofibers and wormlike micelles: formation of viscoelastic hydrogels switchable by changes in pH and salinity. *J Phys Chem B* 115:10478–10487
26. Tung S-H, Huang Y-E, Raghavan SR (2007) Contrasting effects of temperature on the rheology of normal and reverse wormlike micelles. *Langmuir* 23:372–376
27. Jiang LX, Wang K, Ke FY, Liang DH, Huang JB (2009) Endowing catanionic surfactant vesicles with dual responsive abilities via a noncovalent strategy: introduction of a responder, sodium cholate. *Soft Matter* 5:599–606
28. Ketner AM, Kumar R, Davies TS, Elder PW, Raghavan SR (2007) A simple class of photorheological fluids: surfactant solutions with viscosity tunable by light. *J Am Chem Soc* 129:1553–1559
29. Davies TS, Ketner AM, Raghavan SR (2006) Self-assembly of surfactant vesicles that transform into viscoelastic wormlike micelles upon heating. *J Am Chem Soc* 128:6669–6675
30. Buwalda RT, Stuart MCA, Engberts JBFN (2000) Wormlike micellar and vesicular phases in aqueous solutions of single-tailed surfactants with aromatic counterions. *Langmuir* 16:6780–6786
31. Ganta S, Devalapally H, Shahiwala A, Amiji M (2008) A review of stimuli-responsive nano-carriers for drug and gene delivery. *J Control Release* 126:187–204
32. Mano JF (2008) Stimuli-responsive polymeric systems for biomedical applications. *Adv Eng Mat* 10:515–527
33. Zhang Y, Han Y, Chu Z, He S, Zhang J, Feng Y (2013) Thermally-induced structural transitions from fluids to hydrogels with pH-switchable anionic wormlike micelles. *J Colloid Interface Sci* 394:319–328

34. Yang Y, Dong J, Li X (2012) Micelle to vesicle transitions of N-dodecyl-1, ω -diaminoalkanes: effects of pH, temperature and salt. *J Colloid Interface Sci* 380:83–89
35. Palazzo G (2013) Wormlike reverse micelles. *Soft Matter* 9:10668–10677
36. Hashizaki K, Taguchi H, Saito Y (2009) A novel reverse worm-like micelle from a lecithin/sucrose fatty acid ester/oil system. *Colloid Polym Sci* 287:1099–1105
37. Kumar R, Ketner AM, Raghavan SR (2010) Nonaqueous photorheological fluids based on light-responsive reverse wormlike micelles. *Langmuir* 26:5405–5411
38. Lee HY, Diehn KK, Sun KS, Chen TH, Raghavan SR (2011) Reversible photorheological fluids based on spiropyran-doped reverse micelles. *J Am Chem Soc* 133:8461–8463

Chapter 7

Applications of Smart Wormlike Micelles

Abstract The end purpose of formulating smart wormlike micelles is undoubtedly to use them for practical applications. Their micellar structure and reversibly switchable viscoelastic properties offer opportunities for uses where controllable encapsulation and thickening are needed. A series of potential applications are described in this chapter, including biomedicine, cleaning, as electrorheological and photo-rheological fluids, for templating, and drag reduction, amongst others. However, the only current success stories of SWLMs commercial applications come from oil well stimulation processes, including as clean fracturing fluids and for self-diverting acidizing, which are discussed at length in this chapter.

Keywords Applications of SWLMs • Oil well stimulation • Clean fracturing fluids • Self-diverting acidizing • Drag reduction • Biomedicine • Electrorheological fluids • Photo-rheological fluids

The field of stimuli-responsive materials, in particular applied to hydrogels, has grown considerably over the past decade [1]. A plethora of “intelligent” nanostructured systems has emerged and been proposed for a wide range of applications, for instance, in electronic devices, as “smart” optical systems [2], micro-electromechanical systems, in coatings, and quite significantly in the biomedical field for drug delivery, diagnostics, bioseparation, as biosensors, and artificial organs and tissues [1–3]. Traditionally, these materials have been based predominantly on polymers; however, as previous chapters have shown, smart WLMs can display properties of “soft” gels, as a result of their entanglements [4–7]. Their micellar nature provides an opportunity for encapsulation and release, particularly relevant to the areas of drug delivery, the liberation of perfumes or to cleaning processes.

Being still a very young field, applications of SWLMs as such are still largely speculative. While many of the advances discussed in this book respond to specific needs and are driven by a final use, they have not yet reached commercialization. Perhaps the only success stories of scale-up applications originate from the oil industry, where SWLMs have been extensively used in the various stages of the process,

including drilling, gravel packing, fracturing fluid, and self-diverting acidizing [8]; we therefore focus the discussion mainly on oil well stimulation. Other areas where clear opportunities for applications of SWLMs have been identified are as follows: biomedicine, cleaning processes, electro- and photo-rheological fluids, and drag reduction; they are discussed under corresponding subheadings in this chapter.

7.1 Biomedicine

The last decade or so has witnessed an upsurge of “smart” hydrogels in the biomedical field [1, 3, 9–11]. Hydrogels are appealing because of their high water content and nanoscale structure, reminiscent of natural tissues such as the extracellular matrix, thus providing a positive environment for the growth of cells in tissue engineering applications [12], while responsive hydrogel swelling can be conveniently exploited as a mechanism for drug release.

WLMs provide an alternative to traditional polymeric materials for biomedical applications; they are easier to degrade, therefore likely to be more biocompatible; they are more amenable to responsiveness to a range of stimuli, due to their self-assembled nature; they naturally incorporate a hydrophobic core, which can serve as a solubilization locus for pharmaceutical oils and drugs [13, 14]. In tissue engineering, scaffolds which gel upon exposure to body temperature offer the significant advantage of avoiding surgical procedures and complications associated with implants [15]. A considerable challenge of drug delivery lies in the release of an active agent at the pathological site, in order to maximize therapeutic effect, while limiting side-effects; this challenge is well epitomized in cancer therapy. The incorporation of stimuli-responsiveness in “intelligent” materials promises to overcome some of the systemic and intracellular delivery barriers. Various triggers are particularly relevant to the biomedical field, as they often appear as the result of pathology: pH, temperature, and redox potential [16, 17]. For instance, in solid tumours, the extracellular pH is significantly more acidic (6.5) than the pH in the blood (7.4) [18]. In addition, the pH of endosomal and lysosomal vesicles inside cells is significantly lower than the cytosolic pH. Temperature is also an obvious “biologically relevant” trigger; body temperature is used to trigger gelation in “injectable” scaffolds [15], while local hyperthermia is also employed to achieve drug release to a specific target site [16]. Finally, redox potential has been proposed as a stimulus for gene delivery as a high redox potential difference exists between the reducing intracellular space and the oxidizing extracellular space [16]. External stimuli can also be employed to target delivery to specific sites, in particular via the application of (localized) light [19], ultrasound, or magnetic field.

Previous chapters have reviewed examples of pH-, thermo-, light-, redox-, and CO₂-responsive WLMs reported in the literature, where application of a specific trigger switched the rheological behaviour from Newtonian to “gel-like”, thus demonstrating the availability of a wide variety of strategies and systems. Based on these findings, we foresee that many SWLMs systems could find applications as

vehicles for controlled and targeted delivery. Alternative “biologically relevant” triggers could also be developed, such as responsiveness to glucose for the treatment of diabetes [20] or the presence of metabolites [21].

Polymeric micelles/nanoparticles hybrids have been extensively investigated for the solubilization and cellular delivery of poorly water-soluble drugs or imaging contrast agents. To target the acidic micro-environment in early endosome and late endosome/lysosome, Yu et al. [22] reported pH-responsive WLMs composed of the diblock co-polymer, poly(ethylene glycol)-block-poly(2-diisopropylamino ethyl methacrylate) (PEG-*b*-PDPA) to deliver hydrophobic drugs. To impart pH-responsiveness to the micelles, hydroxyl pendant groups were introduced onto the PDPA block, and the polymer was labelled with a pH non-responsive fluorescence dye, tetramethyl rhodamine (TMR). For pH > 6.3, the fluorophore signal produced from the micellar solution was negligible, owing to the aggregation of TMR molecules inside the micelle core; while at pH < 6.3, the PDPA segment was protonated and became water-soluble, thus leading to micelle disassembly and dramatic increase in fluorescence emission [23].

The TMR-conjugated wormlike micelles were further investigated for their intracellular uptake and activation in A-549 lung cancer cells. Punctuated fluorescence dots appeared inside the cells 30 min after micelle incubation, indicating the efficient uptake and activation of the TMR-labelled micelles inside the acidic endosomes. The number of red fluorescence dots increased gradually due to cellular accumulation of the wormlike micelles. These results suggest that pH-responsive wormlike micelles are potent candidates for the intracellular delivery of hydrophobic drugs.

7.2 Oil Upstream Industry

From an engineering point of view, the interest of WLMs in the oil industry is motivated by their remarkable rheological properties and capacity to recover (due to their micellar nature, as compared to polymers). While recent reports demonstrate that WLMs can be extensively used in different stages of oil production, ranging from drilling, gravel packing, oilwell stimulation stimulation [8, 24–26] to tertiary oil recovery [27–35, 44], only in oilwell stimulations have WLMs been successfully used. Their responsiveness to specific triggers is exploited in these processes: the hydrocarbon-responsive character of WLMs is used in clean fracturing fluid, and pH-sensitivity is demonstrated in the self-diverting acidizing process. These are discussed in detail in the following subsections.

7.2.1 *Hydrocarbon-responsive SWLMs Used as Clean Fracturing Fluids*

Once an oil or gas well has been drilled, its production can be limited by low natural reservoir permeability or by permeability reduction induced by

particulate damage to the rock pore space either during drilling or production [36]. Stimulation technique including hydraulic fracturing and matrix acidizing is generally used to remove formation damage, and increase hydrocarbon production to levels far exceeding the rates that would be possible under natural flow conditions.

Hydraulic fracturing involves the injection of a highly pressurized fluid into the well at rates that cause the channels of the reservoir rock, along which gas and petroleum from source rocks, to migrate to wells, and thus the ultimate recovery of hydrocarbons is increased. The fracturing fluids consist primarily of water, but also include special polymer gels, silica sand, and gel breakers. These fluids transmit hydraulic pressure to the rock to induce fractures in the formation, into which sand or other ceramic “proppants” carried by the “gel” are transported and retained to keep the fractures open on removal of the fluid and cessation of pumping.

Conventional fracturing fluids mainly employ natural guar gum cross-linked by a transition metal to impart viscoelasticity. Once the proppant is in place, the gelling agent is deactivated in situ by oxidative or enzymatic breakers, so as to ensure it to flow back to the surface. Nevertheless, a serious limitation of guar gum is the degraded small cross-linked fragments that block the sandpack pore throats and reduce the hydraulic conductivity of the pack significantly [36]. Thus, WLMs-based fracturing fluid has been introduced to address this problem. Similar to polymer gels, entanglements between these WLMs impart solution viscoelasticity to suspend the proppants. However, unlike polymer gels, WLMs collapse spontaneously into spheres or microemulsions when coming into contact with hydrocarbon produced from the fracture through the proppant pack, resulting in a substantial drop in viscoelasticity and leaving little or no residue [37]. Thus, the fluid flows easily out of the pack and does not clog the pore, significantly improving the fracture clean-up [38]. Because the wormlike micellar structures can be destroyed upon exposure to hydrocarbon fluids, the viscoelastic surfactant (VES) fluids used in the fracturing process are also called “hydrocarbon-responsive” WLMs or “cleaning” fracturing fluids [25, 37, 39–41].

7.2.2 pH-responsive SWLMs in Self-diverting Acidizing

Matrix acidization involves the treatment of a reservoir formation with a stimulation fluid containing a reactive acid (typically, HF and HCl). When flowing into the formation, the acid reacts with the soluble substances in the sandstone formation matrix or dissolves the entire formation matrix in carbonate formations to form dendritic holes, so as to enlarge the pore spaces. For efficient stimulation, the wormhole network should uniformly cover the formation interval; unfortunately, high-permeability zones preferentially take the acid and leave zones with lower permeability untreated, which means less production and lost reserves. Various mechanical and chemical methods have been developed to force acid away from the primary wormholes and create new ones, or to ensure treatment of lower

permeability intervals. This process is called diversion. Conventional chemical diversion methods include nitrogen foam, bridging agents such as benzoic acid, and cross-linked polymer gels.

Specially-designed acidic polymer gel systems initially have a low viscosity to facilitate pumping, but once the fluid enters a carbonate formation and the acid spends, the polymer cross-links with the pH rise, increasing fluid viscosity. The viscosity increase restricts further flow of new acid through the wormholes, thereby diverting fresh acid to lower permeability zones. As the acid continues to dissolve the rock, the pH increases further. Once the pH reaches critical values, the gelled acid breaks, reducing the viscosity and enabling fluids to flow back and clean-up. Nevertheless, these polymer-based acid systems have several drawbacks [25]. Because of the narrow pH window, the cross-linking and breaking can be difficult to control. Moreover, the stability of polymer systems degrades as the bottomhole where temperature increases. This instability hinders proper diversion or, at worst, permanently damages the formation to the point of preventing flow.

VES-based self-diverting acidizing system can overcome the drawbacks of polymer gels. At a certain concentration of acid, the viscosity of VES fluid is low. As the acid is consumed through the reaction with CaCO_3 in calcite or MgCO_3 in dolomite, the fluid gels and diversion commence. Two factors trigger the gelation process of surfactant solutions [25]. When the acid spends, the increased pH allows the surfactant molecules to form WLMs. The carbonate dissolution also results in the formation of CaCl_2 brine, further stabilizing the WLMs. This WLMs-based system is easier to control than polymer gels because the surfactant gel breaks upon contact with produced hydrocarbon and does not rely on pH. The absence of insoluble residue further improves permeability after the treatment. The higher temperature that this acid system can be used is up to 149 °C [25].

7.2.3 Classes of Surfactants Used in SWLMs for Oilwell Stimulation

To date, three classes of VES have been employed in oilfield applications—cationic, anionic, and zwitterionic [25]. The most common VES fluid is based on cationic quaternary ammonium salts with carbon chain length ranging from C_{18} to C_{22} . The maximum practical fluid temperature for rapeseed-based quaternary ammonium salt systems is only 54 °C, while the erucic acid-based EHAC VES fluid is effective at temperatures up to about 79 °C and can be extended to 93 °C by adding sodium salicylate as a counterion to enhance micelle growth [25]. A major advantage of cationic VES surfactants is their low sensitivity to the ionic strength of the water quality, divalent cations in particular. The disadvantages are their high cost, their propensity to form emulsions with some crude oils [25], and their strong adsorption on the negatively charged sand stones.

Anionic VESs can address the cost disadvantage and emulsion problem of its cationic counterparts. This type of VES solution is usually prepared at the wellsite by

neutralizing oleic acid with NaOH or KOH, and then immediately pumped down-hole. Nevertheless, its maximum practical fluid temperature is only 54 °C [25]. Unlike the quaternary ammonium salts, anionic VES fluids are sensitive to water hardness and will react with the Ca^{2+} and Mg^{2+} to form an insoluble precipitate. Eventually, the fluid viscosity is deteriorated, and the precipitate may block the pore throat in the producing reservoir.

The third type of VES for oilfield use is zwitterionic, normally EDAB [42, 43], whose advantage is its efficacy at high fluid temperatures up to 121 °C [25].

Compared with polymer gelators, WLMs-based VESs are more expensive, but easier to prepare just with a simple dilution of the commercial surfactant slurry, and fewer additives are required for performance adjustments [24].

Another important advantage of VES fluids is their ability to fully regain viscosity after exposure to high shear rates. This occurs when fluids are pumped at high rates through tubing or when the fluid passes through casing perforations. High shear rates can physically break down the polymer or destroy irreversible cross-links, thus permanently damage the performance of polymer-based fluids.

Thousands of well stimulation cases worldwide from South America, North America, the North Sea, the Caspian Sea, and the Middle East to China clearly demonstrate that these wormlike micellar solutions can help engineers optimize oil and gas asset performance and improve hydrocarbon recovery [8]. Nevertheless, some disadvantages have also been experienced with the VES fluids used in the oil well stimulation process. The first one is their limited ceiling temperature, and the second problem is breakers are also necessary when encountering dry gas wells that contain a small amount of liquid hydrocarbons. The third problem of VES fluids is their poor ability to bind free water to avoid their penetration into the target oil or gas zone.

7.2.4 WLMs for Enhanced Oil Recovery

Although several recent studies [27–32, 44] all claimed that WLMs can be used as a displacing fluid in the enhanced oil recovery (EOR) process, the hydrocarbon-sensitive character probably deteriorates the production efficiency because the light portion in the crude oil will disrupt the entanglements of WLMs in the VES fluids, thus significantly weakening the thickening ability of the chasing fluid, and finally only a limited recovery factor is obtained. This is also probably why wormlike micelle solutions are more suitable for heavy oil recovery [32]. Secondly, the entangled WLMs will be constantly sheared when they are passing through the pore throat of oil reservoir underground, leading to the disruption of the WLMs into spherical micelles, and WLMs may not be reformed when they pass through the next throat, thus the thickening efficiency is also weakened. Thirdly, the strong adsorption of cationic and zwitterionic WLMs onto the sand rock surface will diminish the concentration of surfactant, which also impairs the viscoelasticity. All of these processes may significantly decrease the viscosity of the surfactant solution, and thus limit the use in EOR. However, addition of a pre-flush slug or post-flush of polymer will remarkably increase the oil recovery factor [33].

Very recently, Akbulut and co-workers [44] reported pH-responsive WLMs as displacing fluids for EOR. Such a WLM system is composed of an amino-amide (*N*-oleicamidopropyl-*N,N*-dimethylamine) and maleic acid, which borrows the previously reported “pseudo-gemini” concept [45]. It was found that addition of such a mixture solution can increase the viscosity of water by a factor of 4.5×10^5 . The authors ascribed such a superior viscosity behaviour to the formation and entanglements of layered cylindrical supramolecular assemblies with diameters of several hundred nanometers. They also observed that the viscosity could be reversibly tuned by changing the pH from 4 to 8. The authors claimed that such a switchable property can be very beneficial for EOR applications when the injectivity became a limitation and can reduce the energy cost associated with pumping large volumes of the viscous displacement fluids. More importantly, at pH 8, the authors found that 0.4 wt% of the mixture solution had a much higher efficiency than that of normal polyacrylamide, which is widely used in tertiary oil recovery process. Surprisingly, the authors attributed the increased viscosity, thus improved oil recovery efficiency, to the transition from dimer to trimer type of complexes at basic pH values, and they also postulated that the protonated long-chain quaternary ammonium could complex with itself or with the un-protonated tertiary amine; they were, however, unable to identify the forces driving this complexation.

7.3 Cleaning Processes

Another area where traditional WLMs are already present is consumer products for cleaning and personal care [46, 47]. It is expected that smart micelles can advance the applicability of WLMs in cleaning processes, for instance in processes such as water treatment. While emulsions containing undesirable species (dirt/oil) are useful at one stage of a process, the surfactant then becomes a liability that hinders the separation of the components. While cleavable surfactants can be employed, triggers are more advantageously used to break surfactant-stabilized emulsions, enabling a fully reversible interconversion between an active and an inactive form, which could thus be recovered and reused.

7.4 Electrorheological Fluids

An area which has nurtured a few of the examples of SWLMs discussed in previous sections is ER fluids, which, as explained, have traditionally been colloidal dispersions whose viscosity can be controlled by an alternating electric field (the viscosity rises in the direction perpendicular to the field as particles align to form strings parallel to the field because of induced dipoles attraction) [48]. These smart fluids can be applied to clutches for transmission, valves, dampers, and precise control of mechanical position [49]. However, industrial application of traditional

ER fluids has been hampered by their poor stability and the need of high voltage and high particle concentration. ER fluids based on SWLMs represent a new avenue for ER fluids. For instance, Abe et al. [49] have reported a system based on the redox-switchable ferrocenyl surfactant (FTMA) that self-assembles into WLMs in the presence of NaSal. The viscoelasticity is tuned by controlling the degree of entanglement of the micelles through a redox reaction of FTMA. The system presents numerous advantages over conventional ER fluids and has great potential to be applied to inkjet printer inks and the controlled release of dyes and perfumes.

7.5 Photo-rheological Fluids

Extending to light as an alternative trigger, PR fluids follow the path of ER or magnetorheological fluids [50]. Conventional PR fluids are typically a two-phase system that aggregates or settles with time. A new class of WLMs-based PR fluids have been proposed by the group of Raghavan [50–52], based on widely available photo-sensitive organic acids or salts mixed with conventional WLMs-forming surfactants: for instance CTAB [50] or EDAB [51] in the presence of OMCA, or lecithin with PCA [52]. PR fluids promise to be true, single-phase solutions, structured at the nanoscale. As mentioned above, light presents the additional benefit of precise localization, making it useful in numerous nanotechnological applications, sensor systems, nanoelectronics, microfluidics, molecular devices, logic gates, information storage devices [53]. Smart WLMs represent an emerging class of materials in this area; while current solutions rely on the involved synthesis of specialized photo-responsive molecules, WLMs, through spontaneous self-assembly, offer an alternative with simple, inexpensive chemical components, commercially available. Upon irradiation, viscosity was shown to drop by 4 orders of magnitude because of the *trans*-to-*cis* photo-isomerisation of the double-bond in OMCA [50], thus impacting the molecular packing. This simple approach could easily be extended to a range of aromatic derivatives [54], where the photo-isomerisation can be reversed by irradiation at different wavelengths. Advantageously, these fluids are likely to tolerate the addition of electrolytes, macromolecules, or nanoparticles. Applications in bioseparation are anticipated, as well as capillary electrophoresis, where the photo-gelling carrier fluid can be loaded into the capillary while it is thin and later transformed into a gel-like state by UV irradiation [52]. Other groups have reported photo-switchable fluids [55, 56] based on similar principles.

7.6 Drag Reduction with Light-responsive WLMs

While high-molecular-weight polymers with flexible chains can be drag reductants effective at concentrations as low as a few ppm, they lose their effectiveness permanently when exposed to extreme shear or extensional stresses which break

primary bonds predominantly near the molecules' midpoints [57]. Conventional WLMs have long been found to be superior to polymers as drag-reducing (DR) agents [58] because they reform after being broken-down by high shear stresses, and the long micellar chains may help to damp small turbulent eddies and reduce the dissipation of turbulent energy, and the alignment of threadlike micelles along the flow may cause anisotropic resistance to turbulent vortices, resulting in suppressed flow fluctuations in the direction normal to the flow [57].

However, these fluids suffer from poor heat-transfer capability [59] and are therefore limited to recirculating systems in which heat exchange is not important. SWLMs overcome this limitation by being able to switch on demand from a short aggregate structure (thus low-viscosity and high heat-transfer capacity), to a long structure (thus high viscoelasticity and high DR state). The DR capability could thus be switched “off” at the inlet of the heat exchanger in a recirculating system and switched back on at its exit. Light represents a convenient trigger for such applications, being easily spatially confined, as recently demonstrated by the work of Zakin et al. [60]. They studied mixtures of the cationic surfactant oleyl bis(2-hydroxyethyl)methyl ammonium chloride and the sodium salt of OMCA, which form a highly viscoelastic fluid, very effective at reducing drag (up to 75 % DR). Upon exposure to light, the *trans*-to-*cis* transition of OMCA leads to a shortening of the micelles, thus lower viscoelasticity and DR properties, considerably enhancing heat-transfer properties. This constitutes a very promising approach to developing effective drag-reducing systems for use in cooling and heating installations.

7.7 Templating

The last promising area of SWLMs to mention is in templating. While the “sol/gel” transition and network structure of WLMs solutions has been exploited by several workers to build-up nanofibers [61], silica nanoparticles [62, 63], and porous nanostructured materials [64], it is expected that SWLMs would be advantageous in bringing more control on the sol–gel transition, rather than relying on temperature alone to bring the transition [65].

While the examples discussed above represent promising areas of application of SWLMs, many others can be envisaged and have been pointed out all along this review. In particular, responsive WLMs could be envisioned as optical sensors, by mixing with solvatochromic species or aggregachromic dyes [66]. These materials are based on colour changes in absorption or in emission associated with structural modification of the molecular assemblies of the dyes dispersed in a matrix. These dyes could be incorporated in SWLMs and react to modifications of the geometry of the aggregates. Other areas of applications of SWLMs include heterogenous catalysts [67], recyclable catalysis [68], and separation [69].

Due to their versatility but simple design principles, stimuli-responsive WLMs have captured interest over recent years and a range of smart WLMs systems have been reported, which react and change their properties in response to temperature,

light, pH, CO₂, redox reaction, and hydrocarbon. The fabrication of smart WLMs usually relies on the introduction of a stimulus-sensitive unit, either by attachment of a responsive chemical group to the WLM-forming amphiphiles, or, more simply, by introducing a “responder” in the surfactant solutions. The responsive surfactant or additive acts by modifying the critical packing parameter when stimulated by the appropriate trigger, therefore inducing spontaneous morphological transition. The change in aggregate geometry translates into a modification of the rheological behaviour, from viscoelastic solutions of entangled WLMs to low-viscosity solutions of globular aggregates or vesicles. Not all WLM systems display the typical Maxwell behaviour, and some display remarkably high viscoelastic properties, with elastic and viscous moduli nearly independent of shear frequency over a wide region, thus very similar to polymeric gels. These intelligent “gels” show real promise for a very diverse range of applications, as sensors, in microfluidics, drug delivery, biomedical applications, nanostructured materials, and in the oil industry.

Future trends in this field may see an expansion towards multi-stimuli-responsive WLMs, multi-sensitive hydrogels, or a departure from the traditional triggers to ultrasounds, microwaves, and magnetism. The hybridization of stimuli-responsive WLMs with polymers, colloids, nanoparticles, biomaterials, and any other functional materials could also open a facile way to fabricate stimuli-responsive hybrid materials. Reverse worms, which respond to either a single stimulus or multiple stimuli, have thus far been largely unexplored and may become the focus of further interest, given the biological relevance of most of them.

Overall, small amphiphiles offer a rich toolbox of building units to design customisable, responsive structures. Fundamental studies are paramount to establish relationships between the macroscopic and dynamic behaviour and the morphology at the nanoscale, in order to rationalize the forces driving self-assembly and help direct formulation rationales and future developments.

While still an emergent area of research, current advances augur well for the future development of multi-purpose WLM-based smart fluids.

References

1. Cohen Stuart MA, Huck WTS, Genzer J, Müller M, Ober C, Stamm M, Sukhorukov GB, Szleifer I, Tsukruk VV, Urban M, Winnik F, Zauscher S, Luzinov I, Minko S (2010) Emerging applications of stimuli-responsive polymer materials. *Nat Mater* 9:101–113
2. Löwik DWPM, Leunissen EHP, van den Heuvel M, Hansen MB, van Hest JCM (2010) Stimulus responsive peptide based materials. *Chem Soc Rev* 39:3394–3412
3. Ehrbar M, Schoenmakers R, Christen EH, Fussenegger M, Weber W (2008) Drug-sensing hydrogels for the inducible release of biopharmaceuticals. *Nat Mat* 7:800–804
4. Chu Z, Feng Y (2011) Thermo-switchable surfactant gel. *Chem Commun* 47:7191–7193
5. Raghavan SR, Kaler EW (2001) Highly viscoelastic wormlike micellar solutions formed by cationic surfactants with long unsaturated tails. *Langmuir* 17:300–306
6. Chu Z, Feng Y (2010) Amidosulfobetaine surfactant gels with shear banding transitions. *Soft Matter* 6:6065–6067

7. Kumar R, Kalur GC, Ziserman L, Danino D, Raghavan SR (2007) Wormlike micelles of a C22-tailed zwitterionic betaine surfactant: From viscoelastic solutions to elastic gels. *Langmuir* 23:12849–12856
8. Kefi S, Lee J, Pope TL, Sullivan P, Nelson E, Hernandez AN, Olsen T, Parlar M, Powers B, Roy A, Wilson A, Twynam A (2004) Expanding applications for viscoelastic surfactants. *Oilfield Rev* 16:10–23
9. Mano JF (2008) Stimuli-responsive polymeric systems for biomedical applications. *Adv Eng Mat* 10:515–527
10. Hirst AR, Escuder B, Miravet JF, Smith DK (2008) High-tech applications of self-assembling supramolecular nanostructured gel-phase materials: from regenerative medicine to electronic devices. *Angew Chem Int Ed* 47:8002–8018
11. Messing R, Schmidt AM (2011) Perspectives for the mechanical manipulation of hybrid hydrogels. *Polym Chem* 2:18–32
12. Lee KY, Mooney DJ (2001) Hydrogels for tissue engineering. *Chem Rev* 101:1869–1879
13. Afifi H, Karlsson G, Heenan RK, Dreiss CA (2011) Solubilization of oils or addition of monoglycerides drives the formation of wormlike micelles with an elliptical cross-section in cholesterol-based surfactants: a study by rheology, SANS, and Cryo-TEM. *Langmuir* 27:7480–7492
14. Afifi H, Karlsson G, Heenan RK, Dreiss CA (2012) Structural transitions in cholesterol-based wormlike micelles induced by encapsulating alkyl ester oils with varying architecture. *J Colloid Interface Sci* 378:125–134
15. Kretlow JD, Klouda L, Mikos AG (2007) Injectable matrices and scaffolds for drug delivery in tissue engineering. *Adv Drug Delivery Rev* 59:263–273
16. Ganta S, Devalapally H, Shahiwala A, Amiji M (2008) A review of stimuli-responsive nano-carriers for drug and gene delivery. *J Controlled Release* 126:187–204
17. You Y-Z, Zhou Q-H, Manickam DS, Wan L, Mao G-Z, Oupický D (2007) Dually responsive multiblock copolymers via reversible addition-fragmentation chain transfer polymerization: synthesis of temperature- and redox-responsive copolymers of poly(*N*-isopropylacrylamide) and poly(2-(dimethylamino)ethyl methacrylate). *Macromolecules* 40:8617–8624
18. Vaupel P, Kallinowski F, Okunieff P (1989) Blood-flow, oxygen and nutrient supply, and metabolic microenvironment of human tumors—a review. *Cancer Res* 49:6449–6465
19. Wang J, Jiang J, Liu Y, Li Z, Liu M (2010) Hierarchical self-assembly of bolaamphiphiles with a hybrid spacer and L-glutamic acid headgroup: pH- and surface-triggered hydrogels, vesicles, nanofibers, and nanotubes. *Langmuir* 26:18694–18700
20. Wu Q, Wang L, Yu H, Wang J, Chen Z (2011) Organization of glucose-responsive systems and their properties. *Chem Rev* 111:7855–7875
21. El-Hamed F, Dave N, Liu J (2011) Stimuli-responsive releasing of gold nanoparticles and liposomes from aptamer-functionalized hydrogels. *Nanotechnology* 22:494011
22. Yu H, Shi X, Yu P, Zhou J, Zhang Z, Wu H, Li Y (2013) pH-Responsive wormlike micelles for intracellular delivery of hydrophobic drugs. *J Controlled Release* 172:E33–E34
23. Yu HJ, Zou YL, Wang YG, Huang XN, Huang G, Sumer BD, Boothman DA, Gao JM (2011) Overcoming endosomal barrier by amphotericin B-loaded dual pH-responsive PDMA-b-PDPA micelleplexes for siRNA delivery. *ACS Nano* 5:9246–9255
24. Chase B, Chmilowski W, Marciniw R, Mitchell C, Dang Y, Krauss D, Nelson E, Lantz T, Parham C, Plummer J (1997) Clear fracturing fluids for increased well productivity. *Oilfield Rev* 9:20–33
25. Sullivan P, Nelson EB, Anderson V, Hughes T (2007) Oilfield applications of giant micelles. In: Zana R, Kaler EW (eds) *Giant micelles: properties and applications*. CRC Press, Boca Raton, pp 453–472
26. Al-Anzi E, Al-Mutawa M, Al-Habib N, Al-Mumen A, Nasr-El-Din H, Alvarado O, Brady M, Davies S, Fredd C, Fu D, Lungwitz B, Chang F, Huidobro E, Jemmali M, Samuel M, Sandhu D (2003) Positive reactions in carbonate reservoir stimulation. *Oilfield Rev* 15:28–45
27. Li XP, Yu L, Ji YQ, Wu B, Li GZ, Zheng LQ (2009) New type flooding systems in enhanced oil recovery. *Chin Chem Lett* 20:1251–1254

28. Lakatos I, Toth J, Bodi T, Lakatos-Szabo J, Berger P, Lee C (2007) Application of viscoelastic surfactants as mobility control agents in low-tension surfactant floods. Paper SPE 106005 presented at the 2007 Society of Petroleum Engineers (SPE) international symposium on oil-field chemistry held in Houston, USA, 28 Feb–2 Mar
29. Morvan M, Degré G, Leng J, Masselon C, Moreau P, Bouillot J, Zaitoun A (2009) New viscoelastic fluid for chemical EOR. Paper SPE 121675 presented at the 2009 Society of Petroleum Engineers (SPE) international symposium on oilfield chemistry held in The Woodlands, Texas, USA, 20–22 April
30. Morvan M, Degré G, Beaumont J, Dupuis G, Zaitoun A, Almaamari RS, Al-hashmi AR, Al-Sharji HH (2012) Optimization of viscosifying surfactant technology for chemical EOR. Paper SPE 154053 presented at the 8th Society of Petroleum Engineers (SPE) improved oil recovery symposium held in Tulsa, USA, 14–18 April
31. Degré G, Morvan M, Beaumont J, Colin A, Dupuis G, Zaitoun A, Almaamari RS, Al-hashmi AR, Al-Sharji HH (2012) Viscosifying surfactant technology for chemical EOR: a reservoir case. Paper SPE 154675 presented at the Society of Petroleum Engineers (SPE) EOR conference at oil and gas West Asia held in Muscat, Oman, 16–18 April
32. Morvan M, Degré G, Beaumont J, Colin A, Dupuis G, Zaitoun A, Almaamari RS, Al-hashmi AR, Al-Sharji HH (2012) Viscosifying surfactant technology for heavy oil reservoirs. Paper SPE 157729 presented at the Society of Petroleum Engineers (SPE) heavy oil Canada held in Calgary, Canada, 12–14 June
33. Zhu DW, Zhang JC, Han YG, Wang HY, Feng YJ (2013) Laboratory study on the potential EOR use of HPAM/VES hybrid in high-temperature and high-salinity oil reservoirs. *J Chem (CEOR Special Issue)*: No. 927519. doi:[10.1155/2013/927519](https://doi.org/10.1155/2013/927519)
34. Luo M, Jia Z, Sun H, Liao L, Wen Q (2012) Rheological behavior and microstructure of an anionic surfactant micelle solution with pyroelectric nanoparticle. *Colloid Surf A Physicochem Eng Asp* 395:267–275
35. Watkins C (2009) Chemically enhanced oil recovery stages a come back. *Inform* 20:682–685
36. Maitland GC (2000) Oil and gas production. *Curr Opin Colloid Interface Sci* 5:301–311
37. Shibaev AV, Tamm MV, Molchanov VS, Rogachev AV, Kuklin AI, Dormidontova EE, Philippova OE (2014) How a viscoelastic solution of wormlike micelles transforms into a microemulsion upon absorption of hydrocarbon: new insight. *Langmuir* 30:3705–3714
38. Stukan MR, Boek ES, Padding JT, Briels WJ, Crawshaw JP (2008) Flow of wormlike micelles in an expansion-contraction geometry. *Soft Matter* 4:870–879
39. Boek ES, Jusufi A, Löwen H, Maitland GC (2002) Molecular design of responsive fluids: molecular dynamics studies of viscoelastic surfactant solutions. *J Phys-Condens Matter* 14:9413–9430
40. Molchanov VS, Philippova OE, Khokhlov AR, Kovalev YA, Kuklin AI (2007) Self-assembled networks highly responsive to hydrocarbons. *Langmuir* 23:105–111
41. Philippova OE, Khokhlov AR (2010) Smart polymers for oil production. *Pet Chem* 50:266–270
42. Yu M, Mahmoud MA, Nasr-El-Din HA (2010) Propagation and retention of viscoelastic surfactants following matrix acidizing treatments in carbonate cores. Paper SPE 128047 presented at 2010 Society of Petroleum Engineers (SPE) international symposium and exhibition on formation damage control held in Lafayette held in Louisiana, USA, 10–12 February
43. Zhao Z, Lü G, Zhang Y, Lian S, Tian N (2014) Performance of EDAB-HCl acid blended system as fracturing fluids in oil fields. *Chin J Chem Eng* 22:202–207
44. Chen I-C, Yegin C, Zhang M, Akbulut M (2014) Use of pH-responsive amphiphilic systems as displacement fluids in enhanced oil recovery. *SPE J*, 19:1035–1046
45. Chu Z, Feng Y (2010) pH-Switchable wormlike micelles. *Chem Commun* 46:9028–9030
46. Ezrahi S, Tuval E, Aserin A, Garti N (2007) Daily applications of systems with wormlike micelles. In: Zana R, Kaler EW (eds) *Giant micelles: properties and applications*. CRC Press, Boca Raton, pp 515–544
47. Nicolas-Morgantini L (2007) Giant micelles and shampoos. In: Zana R, Kaler EW (eds) *Giant micelles: properties and applications*. CRC Press, Boca Raton, pp 494–514

48. Stanway R, Sproston JL, El-Wahed AK (1996) Applications of electro-rheological fluids in vibration control: a survey. *Smart Mater Struct* 5:464–482
49. Tsuchiya K, Orihara Y, Kondo Y, Yoshino N, Ohkubo T, Sakai H, Abe M (2004) Control of viscoelasticity using redox reaction. *J Am Chem Soc* 126:12282–12283
50. Ketner AM, Kumar R, Davies TS, Elder PW, Raghavan SR (2007) A simple class of photorheological fluids: surfactant solutions with viscosity tunable by light. *J Am Chem Soc* 129:1553–1559
51. Kumar R, Raghavan SR (2009) Photogelling fluids based on light-activated growth of zwitterionic wormlike micelles. *Soft Matter* 5:797–803
52. Kumar R, Ketner AM, Raghavan SR (2010) Nonaqueous photorheological fluids based on light-responsive reverse wormlike micelles. *Langmuir* 26:5405–5411
53. Ferri V, Elbing M, Pace G, Dickey MD, Zharnikov M, Samori P, Mayor M, Rampi MA (2008) Light-powered electrical switch based on cargo-lifting azobenzene monolayers. *Angew Chem Int Ed* 47:3407–3409
54. Wolff T, Klaussner B (1995) Overlap of colloid chemistry and photochemistry in surfactant systems. *Adv Colloid Interface Sci* 59:31–94
55. Baglioni P, Braccalenti E, Carretti E, Germani R, Goracci L, Savelli G, Tiecco M (2009) Surfactant-based photorheological fluids: effect of the surfactant structure. *Langmuir* 25:5467–5475
56. Pereira M, Leal CR, Parola AJ, Scheven UM (2010) Reversible photorheology in solutions of cetyltrimethylammonium bromide, salicylic acid, and trans-2,4,4'-trihydroxychalcone. *Langmuir* 26:16715–16721
57. Zakin JL, Zhang Y, Ge W (2007) Drag reduction by surfactant giant micelles. In: Zana R, Kaler EW (eds) *Giant micelles: properties and applications*. CRC Press, Boca Raton, pp 473–492
58. Dreiss CA (2007) Wormlike micelles: where do we stand? Recent developments, linear rheology and scattering techniques. *Soft Matter* 3:956–970
59. Zakin JL, Lu B, Bewersdorff H (1998) Surfactant drag reduction. *Rev Chem Eng* 14:253–320
60. Shi HF, Wang Y, Fang B, Talmon Y, Ge W, Raghavan SR, Zakin JL (2011) Light-responsive threadlike micelles as drag reducing fluids with enhanced heat-transfer capabilities. *Langmuir* 27:5806–5813
61. Li G, Zhang Z (2004) Synthesis of dendritic polyaniline nanofibers in a surfactant gel. *Macromolecules* 37:2683–2685
62. Tan B, Dozier A, Lehmler H-J, Knutson BL, Rankin SE (2004) Elongated silica nanoparticles with a mesh phase mesopore structure by fluorosurfactant templating. *Langmuir* 20:6981–6984
63. Nagamine S, Kurumada K-I, Tanigaki M (2001) Growth of silica particles in surfactant gel. *Adv Powder Technol* 12:145–156
64. Choi D, Kumta PN (2007) Surfactant based sol-gel approach to nanostructured LiFePO₄ for high rate Li-ion batteries. *J Power Sources* 163:1064–1069
65. Raghavan SR (2009) Distinct character of surfactant gels: a smooth progression from micelles to fibrillar networks. *Langmuir* 25:8382–8385
66. Pucci A, Bizzarri R, Ruggeri G (2011) Polymer composites with smart optical properties. *Soft Matter* 7:3689–3700
67. Díaz DD, Kühbeck D, Koopmans RJ (2011) Stimuli-responsive gels as reaction vessels and reusable catalysts. *Chem Soc Rev* 40:427–448
68. Komori K, Matsui H, Tatsuma T (2005) Control of heme peptide activity by using phase transition polymers modified with inhibitors. *Bioelectrochemistry* 65:129–134
69. Li J-L, Bai R, Chen B-H (2004) Preconcentration of phenanthrene from aqueous solution by a slightly hydrophobic nonionic surfactant. *Langmuir* 20:6068–6070